VETENSKAP
OCH
KONST

KTH

Fibre Optic Magnetic Field Sensors Utilizing Iron Garnet Materials

by
Hans Sohlström

**ROYAL INSTITUTE
OF TECHNOLOGY**
**Department of
Signals, Sensors & Systems
Instrumentation Laboratory
S-100 44 STOCKHOLM**

KUNGL TEKNISKA HÖGSKOLAN
**Institutionen för
Signaler, Sensorer & System
Elektrisk mätteknik
100 44 STOCKHOLM**

Fibre Optic Magnetic Field Sensors Utilizing Iron Garnet Materials

Thesis by
Hans Sohlström

VETENSKAP
OCH
KONST

KTH

Abstract

This thesis deals with the subject of fibre optic magnetic field sensors utilizing iron garnet materials. Such materials exhibit a large Faraday rotation which make them advantageous for application in compact magnetic field sensors.

After an introduction, in which fibre optic sensors and optical methods to measure electric current are reviewed, the original research work is summarized.

A system for the measurement of the magneto-optic properties of transparent materials is described. Measurement results, showing the influence of temperature, magnetic field direction and sample treatment on the magneto-optical properties of YIG-crystals, are presented. The properties of thin magneto-optical waveguiding films have also been studied using different light coupling methods. Measurement results obtained for holographic grating, prism and edge (end-fire) light coupling to different substituted YIG films are presented. It is shown that the launching method may affect the properties to be measured.

The design and performance of several versions of extrinsic guided wave fibre optic magnetic field sensors are then reported. The sensors employ substituted YIG (Yttrium Iron Garnet, $Y_3Fe_5O_{12}$) thin film waveguides as sensing elements. Polarization maintaining fibres were used as feed and return to provide two signal channels. The signals were combined in a balanced measurement system, providing insensitivity to both fluctuations in optical power and loss. Sensors have been made both with separate fibres to guide the light to and from the sensing element and with a single fibre for both functions. The two fibre version, although less "elegant", is found to have a better performance. This version also makes it possible to determine both the magnitude and sign of the magnetic field. Measurement results indicate a usable measurement range of at least several mT with a noise equivalent magnetic field level of less than $8 \text{ nT}/\sqrt{\text{Hz}}$.

The design and performance of multimode fibre optic magnetic field sensors utilizing the Faraday effect in an epitaxially grown thick (YbTbBi)IG film is also described. This type of sensor is found to be linear over a range from 27 mT to less than 270 nT. Sensor prototypes suitable for current monitoring in high voltage transmission lines have also been developed.

Descriptors

YIG, iron garnets, rare earth garnets, magneto-optics, optical waveguide, fibre optic sensors, magnetic field measurement, current measurement.

List of publications

This thesis is based on the work contained in the following papers:

A: U. Holm, H. Sohlström and T. Brogårdh, "Measurement system for magneto-optic sensor materials", *J. Phys. E: Sci. Instrum.*, vol. 17, p. 885–889, 1984.

B: U. Holm, H. Sohlström and T. Brogårdh, "YIG-sensor design for fibre optical magnetic field measurement", *OFS 84*, R. Th. Kersten and R. Kist, p. 333–336, VDE-Verlag, Berlin, 1984.

C: U. Holm and H. Sohlström, *Measurement of YIG crystal characteristics for the design of optical magnetic field sensors*, TR 84.01, Instrumentation Laboratory; Royal Institute of Technology, Stockholm, 1984.

D: H. Sohlström, U. Holm and K. Svantesson, "A Polarization Based Fibre Optical Sensor System Using a YIG Optical Waveguide for Magnetic Field Sensing", *Springer proceedings in Physics 44: Optical Fiber Sensors*, H. J. Arditty, J. P. Dakin, and R. Th. Kersten, p. 273–278, Springer-Verlag, Berlin, 1989.

E: H. Sohlström, U. Holm and K. G. Svantesson, "Characterization of Magnetooptical Thin Films for Sensor Use", *SPIE Proc Electro-Optic and Magneto-Optic Materials and Applications*, J. P. Castera, vol. 1126, p. 77–84, 1989.

F: K. Svantesson, H. Sohlström and U. Holm, "Magneto-optical garnet materials in fibre optic sensor systems for magnetic field sensing", *SPIE Proc Electro-Optic and Magneto-Optic Materials and Applications II*, H. Dammann, vol. 1274, p. 260–269, 1990.

G: H. Sohlström and K. Svantesson, "A waveguide based fibre optic magnetic field sensor with directional sensitivity", *SPIE Proc Fiber Optic Sensors: Engineering and Applications*, A. J. Bruinsma and B. Culshaw, vol. 1511, p. 142–148, 1991.

H: H. Sohlström and K. Svantesson, "The performance of a fibre optic magnetic field sensor utilizing a magneto-optical garnet", *Fiber and Integrated Optics*, vol. 11, p. 137–141, 1992, also presented at the OFS 8 conference in Monterey, Jan. 92.

VIII

Contents

x

1. The aim and organization of the thesis

The industrial development has created a growing demand for new types of measurement and therefore new types of sensors, to enhance the quality of different processes. The physical environment for the sensors has, at the same time, become tougher and more electromagnetically polluted.

To overcome the electromagnetic pollution and also to achieve other advantages, there has, starting in the mid seventies, been a steadily growing interest in fibre optic sensors. Optical methods have long been used for measurement purposes, but the technological base developed for fibre optic communication applications has widened the scope considerably. Fibre optic remote sensing systems, providing immunity to electromagnetic interference, electrical isolation and a number of other advantages, could now be developed.

The measurement of magnetic field or current in electrical power systems are applications in which these advantages are very significant.

This thesis is to a large extent based on work made as part of the "Single Mode Sensor Project" that was started in 1981 as a co-operative effort by the *Instrumentation Laboratory of the Royal Institute of Technology*, the *Institute of Microelectronics (IM)* and the *Institute of Optical Research (IOF)*. The project was financed by the *National Swedish Board for Technical Development (STU)*.

The aim of the project was to study the applicability of single mode optical fibre technology for sensor use. *ASEA AB* (now ABB), one of the proponents of the project, had at that time developed a number of multimode fibre optic sensors. Partly because of their interest the development of a magnetic field or electric current sensor was chosen as the working goal.

Most of the electric current sensors developed at that time utilized the Faraday effect in long lengths of fibre, coiled around the conductor. The difficulties encountered with such sensors led us to study sensors based on localized sensing elements made from materials having a large Faraday rotation, e. g. YIG ($Y_3Fe_5O_{12}$).

During the early stages of the project work, polarization maintaining fibres became available. We then recognized the possibility of a system in which polarisation maintaining fibres were used to carry the light to and from a sensing element in the form of a YIG waveguide.

Studies of multimode sensors using bulk YIG or thick films of substituted YIG , were also carried out. A number of such sensors were developed for different applications.

The aim of this thesis is to study the feasibility of magnetic field sensors based on iron garnet materials. As both single-mode and multimode sensors
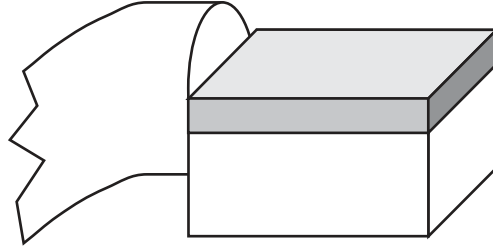
Fig. 1. A magnetic field sensor in the form of a waveguiding "chip" – the idea as envisioned during the initial stages of the project.

are treated, the thesis can also be said to form a comparison of the two types.

Measurement technology is an application oriented research area, and the stress in this thesis is on the sensor development and the material characterization. The papers on which the thesis is based describe different aspects of the sensor development work, from the initial ideas to working sensor prototypes. In this summary I will primarily motivate and discuss the work in order to give a context to the different papers. For this purpose the summary includes an introduction in which the theory is outlined and also some illustrative results, that were omitted in the papers due to the limitations of the conference contribution format. The introduction also contains an overview of fibre optic sensors and current measurement in general. In section 3, I then outline the sensor development and the role of the material characterization. The summary of my work is given in sections 4 and 5. At the end of each of these two sections references are given to the different papers. Finally, in the conclusion, I summarize and speculate somewhat about the implications of the results.

2. Introduction

Fibre optic sensors

Definitions

A *fibre optic sensor* consists of an optical sensing element which under the influence of the quantity to be measured modulates light, and optical fibres to guide the light to and from the sensing element. When also the sensing element consists of optical fibres, the sensor is *intrinsic*, and when the fibres are only utilized to guide the light to and from the sensing element, which is itself external to the fibre, the sensor is *extrinsic*. In literature, the term fibre optic sensor is sometimes reserved for the intrinsic sensors only.

This definition does not include pyrometers that use an optical fibre between the collecting optics and the detector. Formally it also excludes the pyrometric devices that measure the temperature of a metallic film on the fibre end and similar devices where the sensing element "emits light", although they are often considered to be fibre optic sensors.

Another class of sensors that should be mentioned in this context are the optically powered electronic sensors or *hybrid* sensors. As all their connections with the outside world are optical, they share many of the advantages of the fibre optic sensors, while at the same time they allow the use of established electronic sensing principles. They may also provide a way for conventional sensors to be integrated into optical sensor networks.

Historical notes

Optical measurement methods have long been used: optical telephone transmission was patented in 1880, and patents from 1927 (Marconi Co.) and 1934 (American Telephone & Telegraph Co.) [1] show the principles of optical fibres, wavelength multiplexing, etc. Without usable optical fibres and laser light sources, however, little progress was made. In the 1960's the laser was invented and optical fibres became available, figure 2. The rapid development in the optical communications field has since then made optical and electro-optical components available at reasonable prices also for measurement applications.

In the first fibre optic sensors that were developed, bundles of optical fibres were used [2], but similar sensors with single fibres soon appeared [3]. During the early 70's many of the commonly used sensing principles where developed [4,5,6,7,8]. Since then, the technological advances of the fibre optic communications research and development have immediately been taken advantage of in the sensor community.
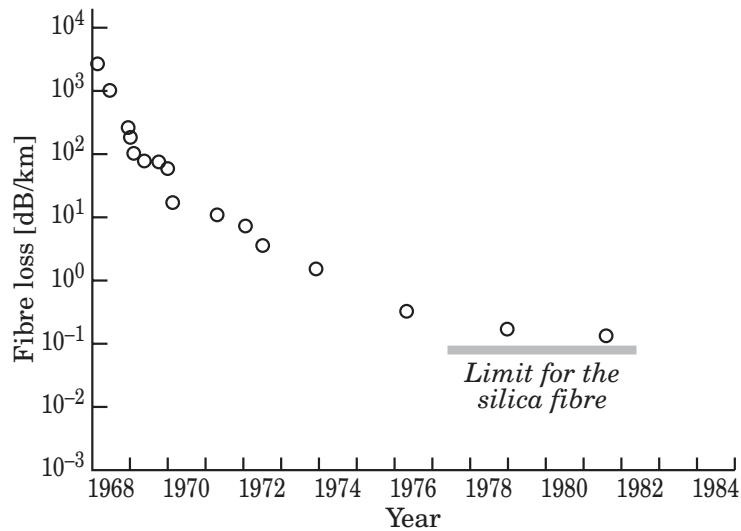
Fig. 2. The minimum losses of fibres developed for optical communications.

The truly unique features of the fibre optic sensors, their immunity to electromagnetic interference and their electrical isolation, were recognized from the very start, and scenarios from the seventies indicated a complete switch to optical measurement technologies. What was not, however, thoroughly recognized was that industry really needed reliable standardized equipment with proven performance, not laboratory prototypes. After a general disappointment at the end of the 80's, there is now in the 90's a renewed optimism, though on a more realistic scale, as the first industrial prototypes of fibre optic sensors are being introduced. One of the leading application areas for this is the electrical power industry, one of the areas where the original interest first stirred, indicating the important role of time and a pioneering application in the acceptance of new technologies.

Principles

Just as with the conventional electric sensors the number of combinations of measurement quantity, sensing principle and output parameter is large. The output parameter, the type of modulation that carries the information from the sensing element is a possible principle of classification.

The optical power or the *intensity* of the returned light is a fundamental parameter. In fact, intensity is the only quantity we can measure. All other quantities must in some way be converted to intensities at one or more detectors and possibly with a variation with time.

The use of the term *intensity* here is somewhat unclear. *Intensity* or *radiant intensity* is, according to international standards, defined as power per solid angle. Although this quantity is modulated when the total power is modulated, it would in principle be more correct to speak of *optical power* and *power modulation*. The use of the term *intensity* as a relative measure of power is, however, established in literature and will also be followed in this text.

In an extrinsic intensity sensor the modulation can take place in an optical system with moving parts [9], a piece of material with an environmentally dependent optical loss [10], etc. In an intrinsic sensor the modulation is caused by a variation in the optical properties of the fibre itself. Several loss mechanisms can be exploited, microbending [11,12], reflections from gratings in the fibre [13], temperature dependent scattering in the fibre [14], losses caused by dopants in the fibre and light decoupling from the fibre [15] are some examples.

Several of these are loss mechanisms that are always present in a fibre optic system. This indicates a major weakness of an intensity based sensor: there is in principle always a loss variation in the optical system and this could not directly be discriminated from variations in the measurand. Often however, some known properties of the measurand signal can be used to separate it from the loss variation.

To completely remove the uncertainty that is created by the loss variation, a system with a reference channel can be used. In such a system two light intensities are measured. If the relation between the influence of the loss and the influence of the measurand is different for the two channels, the influence of the loss can be removed. One realization of this is the *balanced* system in which the sum of the two detected intensities is affected by the system loss and the distribution between them only by the measurand. A similar approach is to use the intensity variations with time to achieve a system that is independent of the absolute intensity. The use of fluorescence decay for temperature sensing has been studied [16].

The *wavelength* of the light can be used to carry information in several ways. The sensing element can cause a wavelength dependent loss and transmit only certain wavelengths of those emitted from a broadband light source [17]. The sensing element can also receive light with one wavelength and emit light with another. The information can then lie in the spectral content of the emitted light [18], in which case it is a true wavelength modulation, or in the intensity of the converted light, in which case it is better described as an intensity based system, perhaps with a reference channel.

The *phase* of the light is used in the very sensitive interferometric sensors [19]. In such a sensor the free-path arms of a conventional interferometer are replaced by optical fibres that make the interferometer much more rugged and at the same time very sensitive to any change in the effective refractive indices or lengths of the fibres. The changes can for example be caused by an absolute rotation, making the device a rotation sensor; the environmental pressure, making it a very sensitive hydrophone or a magnetostrictive perturbation, making it a very sensitive magnetometer.

The *polarization state* of the light can also be utilized in the sensing element. The most usual examples of this are sensors using the Faraday effect, as will be further discussed below, but extrinsic electro-optic electric field sensors [20] and pressure sensors based on photoelastic effects in extrinsic sensors [21] or in fibres [22,23] can also be found in literature. The

polarization state can, however, not be used as the information carrying parameter in the fibre.

Most of the sensors that use polarization modulation in the sensing element internally convert it to an intensity modulation. Alternatively, it could be converted to two different intensities creating a balanced system, cf. above. The use of a polarization maintaining optical fibre makes it possible to transmit these two channels in one fibre core.

Single-mode or multimode

Out of the above mentioned parameters, only the wavelength and the intensity can be maintained when the light propagates along a *multimode* fibre. The optical loss variation always present in a practical system, however, limits the applicability of intensity as the information carrier. The many different propagation modes allowed in the multimode fibre, give rise to a dispersion that destroys the phase information and causes a bandwidth limitation for the intensity information.

The core of a *single-mode* fibre is so thin, normally 5–10 µm, that only one mode is allowed. For monochromatic light it has no dispersion. The small dispersion associated with the spectral width of the light can, in many instances, be ignored. The phase information is retained in the single-mode fibre. The phase drift associated with changes of the optical length of the fibre must, however, be taken into account. The polarisation state cannot be maintained for any longer lengths of fibre because the almost perfect circular symmetry of the fibre makes the two orthogonal polarization modes degenerate, allowing the polarization state to change under the influence of the fibre birefringence.

The *polarization maintaining (p. preserving)* fibre is a special type of single-mode fibre with a core that is elliptical or has an anisotropic index of refraction. This removes the degeneracy of the fibre polarization modes, allowing them to exist independently of each other. Polarized light coupled into the fibre will, thus, be distributed into the two polarization modes and will then travel along the fibre without mode coupling. The polarization state is in fact *not* generally maintained as the phase relation between the two orthogonal components present at the input is lost due to the difference in propagation constant for the two modes. The intensity ratio between the light in the two modes is however maintained. Only for the special case where only one polarization mode is excited the fibre is really polarization maintaining.

Planar waveguides

Just as light can be guided in an optical fibre which is a circular waveguide, it can be guided in a planar waveguide. The simplest structure is the *planar slab guide*, figure 3, where a planar film of refractive index n_f is sandwiched between a *substrate* and a *cover* material with lower refractive indices ($n_f > n_s$, n_c). Often the cover material is air ($n_c = 1$). In the slab guide there is no confinement of the light in the plane of the film.
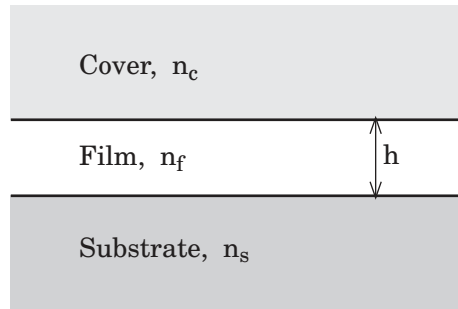
Fig. 3. The planar slab waveguide.

The light is guided in the same way as in an optical fibre, though confined only in one dimension. Just as with the fibre, there are single-mode and multimode guides. Some of the material combinations used for planar guides have much larger index differences than normally used in fibres. Because of this, waveguide thicknesses, h, of $1\,\mu m$ or less are often necessary to achieve strict single-mode guiding.

In analyzing the guide one has to treat the case of *TE (Electric field transverse to the propagation direction) and TM (Magnetic field transverse to the propagation direction)* state of polarization separately. Due to the different phase shifts on total reflection, the propagation constants will be different for the two cases. For small index differences and with thick guides, the difference in propagation constant between the TE and the TM mode, $\Delta\beta$, is small,

$$\Delta\beta = \beta_{TE} - \beta_{TM}$$

In many practical cases however, the magnitude of $\Delta\beta$ is noticeable.

Below, I will describe how the Faraday effect in a planar waveguide can be treated as a coupling between the TE and TM modes of the same order. This coupling cannot effectively take place if the two modes do not run in synchronism, i. e. if $\Delta\beta$ is far from zero.

As in a slab waveguide there is no confinement of the light in the plane of the waveguide, one must use the planar equivalent of conventional "bulk optical" methods to control the light in the transverse direction. The alternative is to confine the light in both dimensions with a *channel waveguide*.

Magnetic field measurement

Before dealing with the optical magnetic field measurement methods, a short description of magnetic field measurement in general is relevant.

Magnetic field measurements are not only made to measure the magnetic field itself, but also to provide indirect information about other quantities. Measurement of electric current, rotation speed measurement using a permanent magnet and a pick-up coil, acoustic pressure sensing using
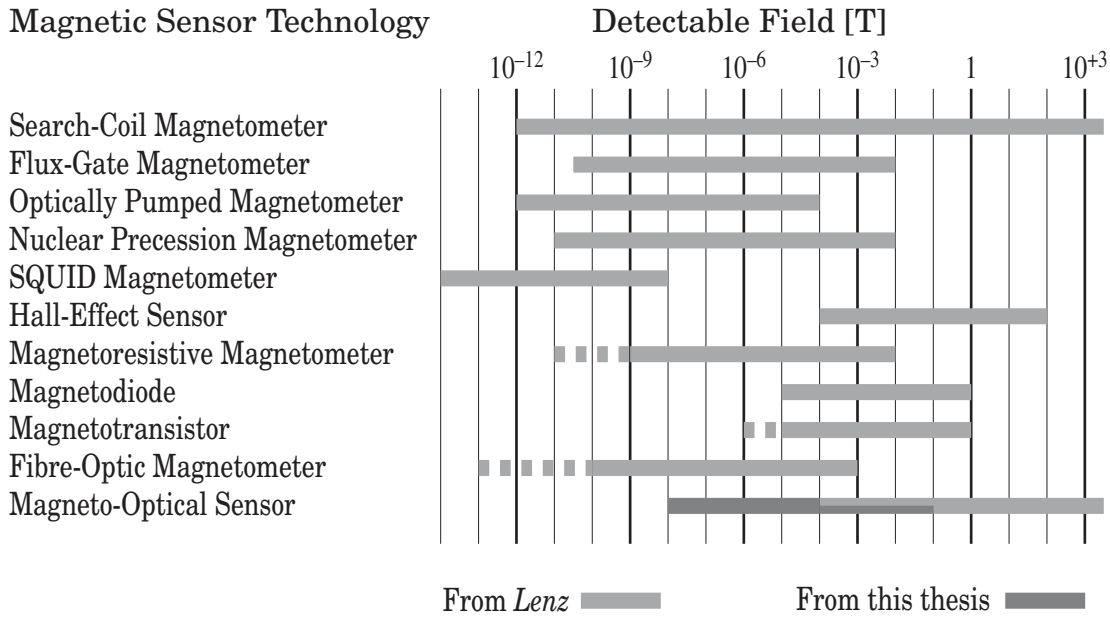
Magnetic Sensor Technology   Detectable Field [T]

Fig. 4. Magnetic field sensor comparison, adapted from [26]. In addition to the data taken from the reference, the magnetic field range for the sensors demonstrated in this thesis is given.

dynamic microphones, and submarine detection using SQUID:s (Superconducting Quantum Interference Device) to detect perturbations of the earth's magnetic field are some examples. In addition to the large practical differences, the ranges of magnetic field encountered are very different. The measurement of electric current may involve fields exceeding 1 T, while submarine detection demands a noise level around 10^{-11} T [24,25]. The required bandwidths range from about 1 Hz for submarine detection to GHz for EMC measurements.

An overview of some different measurement technologies is given in figure 4. The magnetic field range for the fibre optic sensors demonstrated in this thesis is indicated in addition to the data from the reference. Evidently, sensors utilizing magneto-optical effects cover a large field range. Together with the "Fibre-Optic Magnetometer", they cover the entire range given in figure 4 except the very low fields that can only be detected by SQUID Magnetometers.

Measurement of electric current has been the main application considered in this work. It is, therefore, appropriate to widen the view and also have a brief look at current measurement in general.

Measurement of electric current

Current and perhaps voltage are the only quantities that can really be measured with conventional electrical methods. All other quantities are converted to a current or a voltage that can in turn be measured, e. g., by an

indicating instrument. It may therefore seem somewhat surprising to find that there is a considerable interest in unconventional methods to measure current in high voltage power systems. A cause for this is that even though the measurement is in principle a simple one, it is in practice complicated for two reasons: the power dissipation in the measurement circuit and the need to keep the display unit at ground potential.

The conventional way to solve this is to use a *current transformer* that transforms the current down to a reasonable level and provides an isolation barrier between the primary winding at line potential and the secondary winding at ground potential. The size and cost of such a current transformer, however, increase with the line voltage. Also, current transformers can only be used for AC measurements. For DC measurements, more complex devices with Hall elements are often used.

The increasingly complex control systems used in the power transmission networks also creates a need for more points of measurement and a wider range of measurement situations. Current metering for billing purposes is usually done with equipment having an accuracy in the order of 0.2% and with a relatively low bandwidth, typically less than 1 kHz. For control and protection purposes, however, errors of 1% or even more are usually accepted. There is even a need for on/off devices that indicate the presence of current over a certain level.

Current transformers with optical downlinks as well as systems using the Faraday effect at microwave frequencies have been investigated [27]. In recent years the interest has, however, been focused on fibre optic systems.

Optical methods for magnetic field and electric current measurement

Two main methods

Most of the work that has been published on optical methods to measure magnetic fields concern either the *Faraday effect* or *magnetostrictive perturbation of optical fibres*. The Faraday effect, which is a change of the polarization state of propagating light under the influence of a magnetic field, is the phenomenon utilized in this work.

Before we further describe the Faraday effect, a short description of the other principle is appropriate. In contrast to the Faraday effect, which can be utilized in both bulk optical elements, planar waveguides and in fibres, the magnetostrictive principle requires the use of fibres. The magnetostrictive principle was first suggested in 1980 [28]. It uses a magnetostrictive material which is mechanically linked to the fibre, for example in the form of a magnetostrictive jacket on the fibre or a bulk magnetostrictive element onto which the fibre is wound. When subjected to a magnetic field the magnetostrictive element will change its form, thereby causing a strain and a change of the length of the fibre. This change of the optical length can be detected if the fibre is placed in one arm of a *Mach-Zehnder* interferometer.

The fibre can be long and as the phase sensitivity of the interferometer is high, this device can potentially be very sensitive [29]. However, it is unfortunately also sensitive to all other parameters that influence the optical length of the fibre, e. g. temperature [30]. Although the measurement of electric current was mentioned as a possible application [31], the driving force of the development was the potential possibility of detecting the small changes in the earth's magnetic field caused by passing submarines. At first nickel was used for the magnetostrictive element, and later *metallic glasses* [32,33]. Different biasing [34] and feedback [35,36] arrangements have been investigated.

Many of the problems with temperature and vibration sensitivity have been overcome with proper jacketing of the fibre and with the use of all fibre optical systems. This type of sensor offers extremely high sensitivity, with noise levels down to 10^{-15} T/$\sqrt{\text{Hz}}$ [37], but it is not suited for electric current measurement and other large-signal applications.

Other sensing principles that have been studied are: interferometric detection of the movement of a metal coated fibre in a magnetic field when a current is sent through the coating [38,39,40], surface plasmon resonance [41], liquid crystals [42] and resistor heating [43]. The use of a current transformer that is in turn interrogated by a fibre optic interferometer has also been tried [44].

In this context, the possibilities to use conventional current transformers together with an optical data link for current measurements in high voltage systems should be mentioned. The equipment at high potential could then be powered by pick-off from the power line [45], or be a hybrid sensor, optically powered through the fibre [46].

The Faraday effect

When a material exhibiting the *Faraday effect* is placed in a magnetic field and a beam of linearly polarized light is sent through it in the direction of the field, a rotation of the plane of polarization of the light will occur, figure 5.

The phenomenon was discovered in 1845 by Michael Faraday. Other names for the same effect are the *magneto-optical rotation (MOR)*, *magnetic circular birefringence (MCB)* or the *magneto-optical effect*. The last term is, however, more general and may also include other effects.

The effect is non-reciprocal in nature. This means that when the direction of light propagation is reversed, the direction of rotation as seen from a fixed reference system, is not reversed. A light beam that passes twice through the medium in opposite directions will thus acquire a net rotation which is twice that of a single pass.

The Faraday rotation is proportional to the magnetization of the material,

$$\theta = \int_L k\mathbf{M}\cdot\mathbf{dl}$$

Fig. 5. The Faraday effect
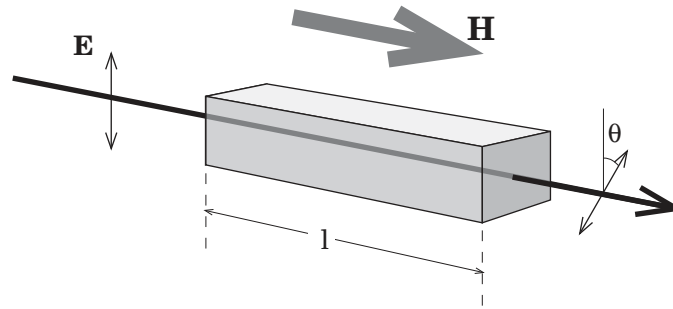
where θ is the polarization rotation, **M** is the magnetization, L is the light path and k is a constant that is dependent on the material in question, the wavelength and the temperature. (Bold letters denote vector quantities.)

In paramagnetic and diamagnetic materials the magnetization and, thus, also the polarization rotation is practically proportional to the magnetic field strength, **H**. One can then describe the rotation in terms of the *Verdet constant, V,*

$$\theta = \int_L V \cdot \mathbf{H} \cdot \mathbf{dl} = \{\text{according to the geometry of figure 5}\} = V \cdot H \cdot l$$

where H is the component of the magnetic field strength parallel to the light propagation direction. (The Verdet constant is sometimes expressed in terms of the magnetic flux density, **B**, which for these materials is linearly related to the magnetic field strength, **B=μH.**)

In ferri- and ferro-magnetic materials the magnetization is not linearly related to the magnetic field strength, and a Verdet constant cannot be used.

In addition to the magnetic circular birefringence, a linear birefringence can be induced by a magnetization perpendicular to the light propagation direction. This is called *MLB (magnetic linear birefringence)*, *Voigt* or *Cotton-Mouton* effect, though the last name originally denoted a similar effect in fluids due to molecule orientation in the magnetic field. There may also be a magnetic field dependent difference in optical absorption between the linear or the circular polarization states, *MLD (magnetic linear dichroism)* and *MCD (magnetic circular dichroism)* [47,48]. One should, however, keep in mind that there seems to be a considerable confusion concerning the names for these effects in literature.

Besides magnetic field sensing, the main application of the Faraday effect is in isolators and circulators for microwave or optical frequencies though in these applications, the effect is used in a static rather than dynamic manner.

The isolator is a device that allows power to flow in one direction, while the other direction is blocked. The basic design consists of a polarizer followed by a 45° Faraday rotator and a second polarizer with its polarization direction 45° from that of the first one. The 45° angle, however, makes

the basic isolator design unsuitable for optical waveguide implementation, and a number of variations of the principle have been tried [49].

A circulator is a similar device but with three ports, in which power incident on one port will emerge at the next port.

The origin of the Faraday effect

The Faraday effect arises from the interaction of the electron orbit and spin with a magnetic field. The electron orbit forms a magnetic dipole that tends to align in an applied constant field. As it, from a classical viewpoint, is a spinning particle, it will react to a perturbing momentum at right angles to the spin axis by *precessing* about the original spin axis, just as a spinning top would do. The electron spin behaves similarly, though this is not obvious from a classical viewpoint. The perturbing momentum can be caused by an electromagnetic wave of "optical" or microwave frequency. The closer this frequency is to the precessional frequency the more marked is the interaction. If they coincide there is a resonance, called paramagnetic resonance or ferromagnetic resonance, depending on the actual material properties.

Macroscopically, the precession has the effect of creating a magnetization at right angles to both the applied constant magnetic field and to the perturbation, cf. figure 6.

The magnetic susceptibility of the material will, under the influence of the steady magnetic field (in the z-direction), become a tensor with off-diagonal components of the form,
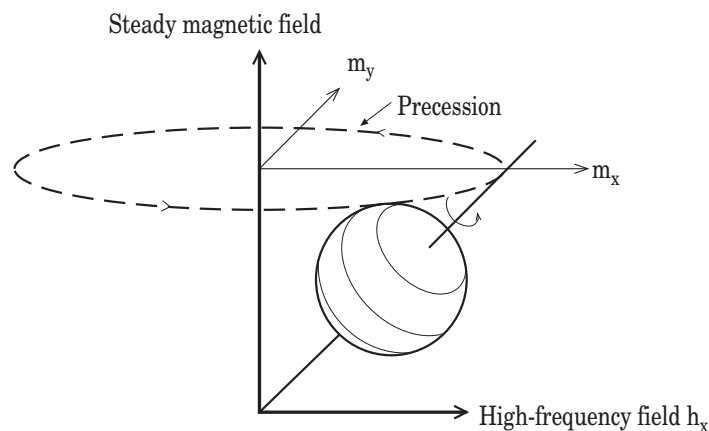
Fig. 6. Electron precession: The high-frequency field h_x creates magnetization both in the x- and the y-direction. After [50].

$$\chi_{yx} = -i \frac{\omega_M \, \omega}{\omega_0^2 - \omega^2}$$

$$\chi_{xy} = +i \frac{\omega_M \, \omega}{\omega_0^2 - \omega^2}$$

where ω is the angular frequency of the applied high-frequency field, ω_0 is the precession angular frequency and ω_M is a factor that depends on the material and the magnetization. The expressions become somewhat simpler if we consider instead the magnetic susceptibility for a left or right circularly polarized perturbing high frequency field,

$$\chi_R = \frac{\omega_M}{\omega_0 - \omega}$$

$$\chi_L = \frac{\omega_M}{\omega_0 + \omega}$$

$$\mu_R = \mu_0 \left(1 + \frac{\omega_M}{\omega_0 - \omega} \right)$$

$$\mu_L = \mu_0 \left(1 + \frac{\omega_M}{\omega_0 + \omega} \right)$$

In these expressions we recognize the resonances discussed above. If loss terms are included, the resonances will be damped and the permeabilities will have imaginary parts, causing loss and dichroism.

The strong interaction between neighbouring atoms in ferri- and ferromagnetic materials causes these materials to have several resonances at different frequencies and with different strengths, creating rather complicated frequency (wavelength) dependencies for both the real and the imaginary terms.

Light propagation in magneto-optical materials

To understand how the Faraday effect influences the light propagation, the wave equation is a suitable starting point. For an infinite medium with no external electrical polarization, the wave equation can be written,

$$\nabla^2 \mathbf{E}(\mathbf{r}, t) = \mu\varepsilon \frac{\partial^2 \mathbf{E}(\mathbf{r}, t)}{\partial t^2}$$

The solution to this is a plane wave with the phase velocity given by,

$$u = \frac{1}{\sqrt{\mu\varepsilon}}$$

Waves with different circular polarization states will have different μ:s, and thus travel with different speeds.

A linearly polarized wave can be seen as the sum of two circularly polarized waves with equal amplitude but opposite directions of rotation. As these two waves propagate with different speeds, they will acquire a phase difference proportional to the travelled distance. In terms of their sum, the

phase difference has the effect of rotating the linear state of polarization by an angle which is equal to half the phase change.

If we want to study the influence of the Faraday effect on the light propagation in a waveguide with different propagation constants for the TE and TM modes, this simple reasoning is not applicable. Instead one can use the *coupled-mode formalism* [51]. In this formalism one studies how a small perturbation causes a coupling between the orthogonal eigenmodes of the unperturbed medium. In the literature this perturbation is normally in the electrical permittivity ε, causing an electric polarization **P**. As only the product of μ and ε appear in the wave equation, the Faraday effect can be treated as a perturbation in ε of the following form,

$$\Delta\varepsilon = \begin{bmatrix} 0 & -i\delta & 0 \\ i\delta & 0 & 0 \\ 0 & 0 & 0 \end{bmatrix} \cdot \varepsilon_0$$

$$\delta = \frac{\omega\omega_M}{\omega_0^2 - \omega^2}$$

With this approach, one finds for the case with only one of the modes exited, that the power in the other mode can be represented by,

$$F = \frac{1}{\left(1 + \left(\frac{\Delta\beta}{2\theta}\right)^2\right)} \sin^2\left[\sqrt{\theta^2 + \left(\frac{\Delta\beta}{2}\right)^2} \cdot z\right]$$

where $\Delta\beta$ is the difference between the propagation constants of the two modes, θ is the polarization rotation per unit length in a homogeneous medium, and z is the distance along the propagation direction. If $\Delta\beta=0$ this simplifies to,

$$F = \sin^2(\theta \cdot z)$$

From the above, it is evident that $\Delta\beta$ should be smaller than θ if any appreciable amount of power is to be coupled between the modes.

Electric current sensing using the Faraday effect

Glass sensing elements

The first optical current transducers utilizing the Faraday effect used bulk optical glass elements interrogated by an open path light beam, figure 7.

Using two detectors, and a polarization separating prism, a system which is not affected by variations in the optical loss, can be achieved, figure 8 [52].
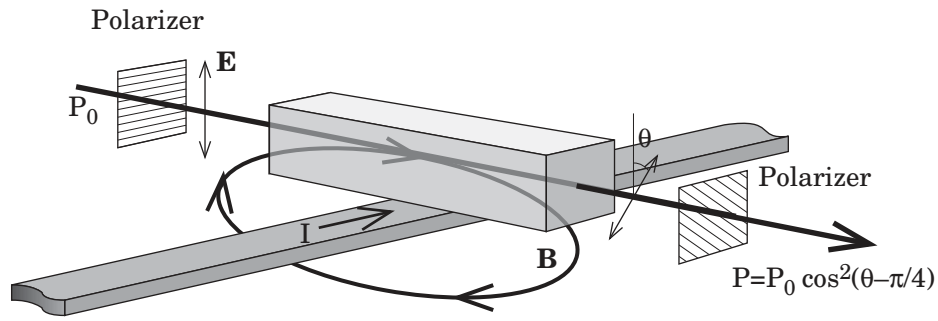
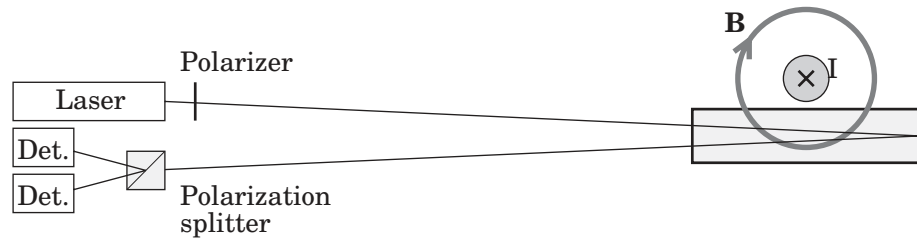*Fig. 7. The simplest form of an optical current sensor utilizing the Faraday effect.*

Fig. 8. A bulk optic current measurement system with polarization state detection. As the Faraday effect is non-reciprocal the two-way pass through the sensing element effectively doubles the rotation.

The sensor is sensitive to the total magnetic field, thus, also to the contributions from other conductors nearby. Also, the distance between the conductor and the sensing element will influence the scale factor. With two sensing elements, one on each side of the conductor, a differential system is achieved, reducing the influence from conductors at large distances. [53]

An *iron core* reduces the position dependence and the influence of external fields, but as the iron core must have a relatively large gap to accommodate the glass sensing element, some sensitivity to the conductor position and to external fields will remain.

A more fundamental approach is to use a basic property of the magnetic field encircling the conductor,

$$\oint_L \mathbf{H} \cdot \mathbf{dl} = \iint_S \mathbf{i} \cdot \mathbf{ds} = \mathrm{I}$$

where **i** is the current density through the surface S, with the contour L, and I is the total current through S.

This means that if the sensing light path completely encircles the conductor, fig 9, the sensor becomes insensitive to external fields and independent of the conductor position in the sensing element. This can be approximated with a bulk sensing element with a central hole for the conductor or sensing element assembled from several pieces of glass. The reflections at the corners must be suitably arranged not to influence the polarization state of the light. [54]
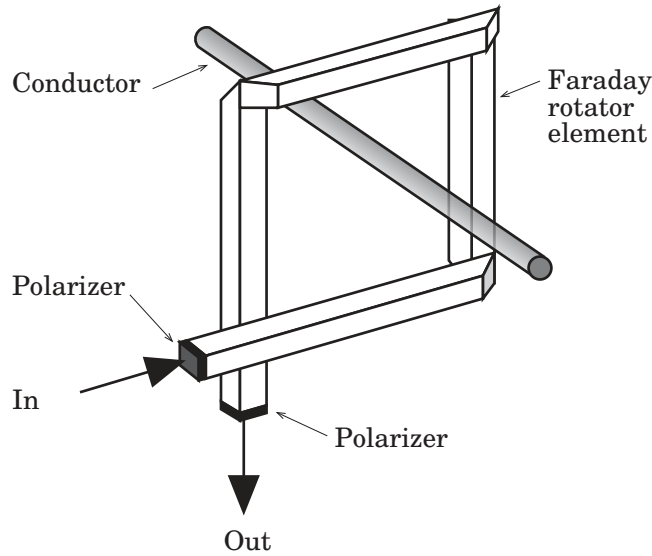
Fig. 9. A glass sensing element that encircles the conductor, after [55]

The early experiments were made with glass sensing elements having relatively small Verdet constants, typically about 10^{-5} rad/A, requiring long sensing elements for good sensitivity. Although YIG ($Y_3Fe_5O_{12}$) and other materials with much larger polarization rotation were studied [56], no transducers using such materials were presented. Multiple reflections were, however, tried to reduce the physical size of the sensing element without sacrificing optical path length [57,58].

Devices to measure both the current and the voltage simultaneously were also presented. [59,60]

With optical fibres many of the problems associated with the open optical path could be eliminated [61]. The possibilities with optical fibres, however, go further than that. The sensing element can be made from an optical fibre. Although the Verdet constant of the fibre material is not high, about $4 \cdot 10^{-6}$ rad/A, a measurable rotation can be achieved with a long fibre, and with the fibre wound round the conductor, a good approximation of the closed line integral of the field is achieved.

There was a considerable interest in this type of device at the end of the 70's and the results were promising [62]. The bending of the fibre in the coil, however, causes a temperature dependent linear birefringence that quenches the circular birefringence caused by the Faraday effect. Several methods have been tried to overcome this problem.

If the fibre is twisted, a circular birefringence "bias" is introduced, which is magnetic field independent and large enough to quench the linear birefringence. This bias birefringence is, however, temperature dependent [63]. With the sensing fibre divided into sections with opposite twists, the bias rotation and the temperature dependence can be cancelled and with the use of polarization maintaining fibre for the downlead, the vibration sensitivity is reduced [64]. A similar approach is to use a fibre with a strong birefringence which is almost circular [65]. This circular birefringence is strongly

16

temperature dependent. Techniques to compensate for this have, however, been studied [66].

The fibre can be wound into a coil in such a way that the beat length (the fibre length that causes a phase difference of 2π between the two orthogonal linear polarization modes) is equal to the circumference of the fibre coil. When an external field is then applied to the fibre coil, the periodic magnetic field that is in this way applied to the fibre will cause a net polarization rotation. [67,68,69]. A principally similar scheme is to use a polarization maintaining fibre with a very short beat length and arrange a periodic magnetic field with the same period [70].

A more fundamental approach is to anneal the coiled fibre to remove the temperature dependent linear birefringence [71].

Also, the Faraday effect is temperature dependent. The use of a temperature dependent linearly birefringent optical element has been suggested as a way to introduce a temperature dependent partial quenching of the Faraday effect, thereby reducing the effective temperature dependence [72].

In addition to the simple polarization detection system described above, a number of interferometric systems to detect the polarization rotation has been presented [73]. Closed-loop systems [74] and heterodyne detection systems [75] have been studied. A system for simultaneous measurement of two currents has also been presented [76]. To eliminate the influence of reciprocal effects in the fibre, some of these systems utilize *Sagnac* interferometers [77,78]. The non-reciprocity of the Faraday effect also makes it possible to use a *Fabry-Perot* resonator to increase the effective polarization rotation [79].

Experiments with techniques to make the sensor output independent of variations in the Verdet constant [80], or to convert the polarization rotation to a spectral modulation [81], have been made.

The *measurement bandwidth* of Faraday sensors with bulk glass or fibre coil sensing elements is limited by the transit time of the light in the sensing element [82],

$$B_{3\,dB} = \frac{0.44}{\tau} = 0.44 \cdot \frac{c}{n} \cdot \frac{1}{2\pi r} \cdot \frac{1}{N}$$

where c/n is the speed of light in the fibre, N the number of turns in the fibre coil and r is the radius of the fibre coil. With N=100, r=0.1 and n=1.5 a bandwidth of 1.4 MHz is achieved. Obviously, there is a trade-off between sensitivity and bandwidth. With high pulsed currents the sensing element can be made short, giving very large bandwidths. A number of systems with bulk glass [83] or fibre sensing elements [84,85] for measurement of transient currents in the 10^6 A range have been presented. Other specialized applications such as aerospace [86] current measuring and space plasma current measurements [87] have been studied. There is also a potential for distributed magnetic field sensing [88].

Although the use of an optical fibre coil for current measurements may in principle seem straightforward, the practical application of the technology

is, however, complicated by the linear birefringence of the fibre and many optical current metering devices that are installed in the high voltage power lines are of the bulk optical type [89,90].

Other materials

Optical fibres with high Verdet constants may increase the applicability of current sensing using fibre sensing elements. Terbium doped silica fibre [91], with a Verdet constant of $1.2 \cdot 10^{-5}$ rad/A, and doped plastic fibre [92], with a Verdet constant of $2 \cdot 10^{-5}$ rad/A, have been developed.

The alternative solution is to use a compact sensing element made from a material with a Faraday rotation larger than that of the glasses. A small sensor head is an advantage in many applications, including current measurement using an iron core.

BGO ($Bi_{12}GeO_{20}$) [93], BSO ($Bi_{12}SiO_{20}$) [94,95] and ZnSe [96] offer Verdet constants of about $7 \cdot 10^{-5}$ rad/A, which is about an order of magnitude higher than that of the silica fibre material. Certain glasses also have Verdet constants that are almost as high. A considerably higher Verdet constant, about $2 \cdot 10^{-3}$ rad/A, is achieved with $Cd_{1-x}Mn_xTe$ [97,98,99,100,101,102].

YIG and substituted YIG offer polarization rotations which, for many applications, is larger than that of $Cd_{1-x}Mn_xTe$ by about an order of magnitude. As YIG is a ferrimagnetic material, it can, however, not be directly compared to the paramagnetic and diamagnetic materials mentioned. Since YIG is the material chosen in this work, it will be further described below.

YIG

YIG, *Yttrium iron garnet* is a *ferrimagnetic* garnet crystal with the composition $Y_3Fe_5O_{12}$. It is transparent for light with a wavelength longer than about 1.1 µm. At 1.3 µm and 1.5 µm, wavelengths at which reliable light sources and detectors are readily available, the optical loss is very low. YIG has a substantial Faraday rotation in large parts of the optical and microwave spectrum. Crystals of optical quality can be grown from flux melts or grown epitaxially on substrates. Epitaxially grown films can be used as high quality optical waveguides exhibiting the Faraday effect [103]. YIG crystal material, often in the form of polished spheres, are used in microwave components.

The crystal lattice of YIG is rhombohedral, almost cubic, with the iron atoms occupying two different kinds of sites in the lattice, figure 10. For this reason the formula is sometimes written $Y_3^{3+}Fe_2^{3+}Fe_3^{3+}O_{12}^{2-}$.

The magnetic properties of the crystal are mainly determined by the iron atoms. The iron atoms in the two kinds of sites interact antiferromagnetically with each other, giving a net magnetic moment equal to that of one atom. The Yttrium is magnetically polarized by the field from the iron atoms, but it has little influence on the strength of the magnetic interaction.
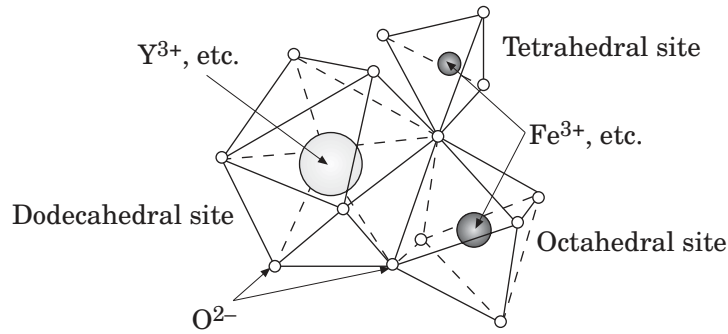
Fig. 10. The different kinds of atomic sites in YIG, after [106].

This is evident from the fact that all *rare-earth iron garnets* (RIG, $R_3Fe_5O_{12}$ where R is a rare earth) have a Curie temperature of about 550 K [104]. The Curie temperature is the temperature at which the thermal agitation breaks down the magnetic ordering of the atoms and the material ceases to be ferromagnetic. The Curie temperature can therefore be used as a measure of the strength of the magnetic interaction. The Curie temperature for pure YIG is 559 K [105]. The net magnetic moment for the rare earth garnets is, however, influenced by the rare earth, in several cases giving *compensation points*, where the temperature dependent magnetic moments of the different kinds of atoms cancel each other at a specific temperature, figure 11. YIG, however, does not have any compensation point.

It is possible to substitute part of the yttrium with other rare earths, giving mixed rare earth garnets. Also, other substitutions can be made, but this normally has little effect on the magnetic interaction. Bismuth substitution is an exception as it increases the strength of the magnetic interaction, thereby increasing the Curie temperature.

If the iron is substituted, the magnetic interaction is weakened, giving a lower Curie temperature.
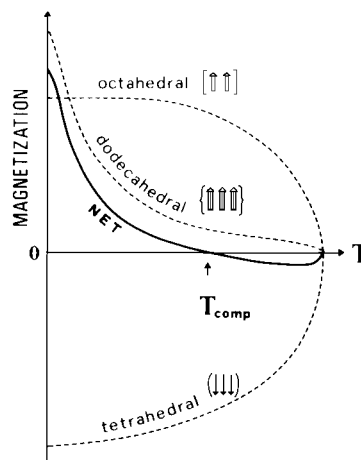

Fig. 11. Qualitative behaviour of the different contributions to the net magnetization of rare earth garnets having a compensation point. From [107].

The *lattice constant* of pure YIG is such that it can be epitaxially grown on substrates of GGG, Gadolinium gallium garnet ($Gd_3Ga_5O_{12}$). Such substrates of high quality are readily available. For substituted films, the substitutions of the film and substrate must be combined to give the proper lattice constants.

The *magnetic anisotropy* in pure YIG is mainly cubic and not so strong. Strain, however, strongly affects the magnetic anisotropy [108]. Epitaxially grown YIG films can, therefore, have easy directions of magnetization in the plane of the film, or perpendicularly to it, depending on the film strain caused by the lattice mismatch. In addition to the strain anisotropy, there can also be a growth-induced anisotropy, arising from a certain ordering of the magnetic ions in the growth process.

Because of the ferrimagnetic properties of the material, volumes of equal direction of magnetization, so called *magnetic domains* will form. The domains are separated by thin *Bloch walls* where the magnetization direction is changed. The domain size is determined by a magnetostatic energy balance that depends on the material properties and the sample geometry.

With thin bulk samples and epitaxially grown films with suitable anisotropy, the domains can form two-dimensional patterns extending through the entire thickness of the film, figure 12. Under certain conditions this pattern degenerates to small circular domains, *bubbles*. These bubbles can be moved around in the film, created and annihilated by small perturbations in the field. This is the phenomenon that was used in the bubble memories, in which more than 1 Mbit of information could be stored in the form of a bubble pattern in 1 cm^2 of iron garnet film [109].

For a large sample with many domains, the actual form of the individual domains and their movement when an external field is applied seems to be stochastic. For the entire sample or a large part of the sample the behaviour of the domains, however, averages out and the net magnetization reflects the variations in the applied magnetic field. There is however a tendency for the domain walls to stick to imperfections in the material, such as lattice dislocations, causing discontinuities in the magnetization change.

The direction of magnetization of the individual domains will also change
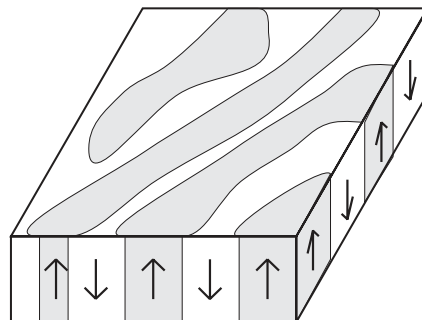
Fig. 12. Two-dimensional domain pattern in thin sample with an out of plane anisotropy.

under the influence of an applied field. The magnetic anisotropy will, however, keep the magnetization approximately along the easy directions. When the net magnetization of the sample cannot be adjusted to the external field through redistribution of the domains between the easy directions only, a rotation of the magnetization direction within the domains will occur. For a very strong applied field, the magnetization will be completely aligned with the field.

The rapidity with which the magnetization of the material can be changed is limited by the dynamic properties of the domain wall movements. This gives an upper frequency limit somewhere in the 10 MHz to GHz range [110]. Very little work has however been done in measuring the frequency response of YIG material based devices [111].

The contribution to the magneto-optical rotation per unit length from the different atoms can be described by a formula from [112],

$$\theta = (A_m + A_e)M_{Fe}^o + (B_m + B_e)M_{Fe}^t + (C_m + C_e)M_R$$

The indices "m" and "e" indicate contributions from different kinds of resonances and the superscripts "o" and "t" indicate octahedric and tetrahedric positions for the iron atoms. Apparently, the contributions from the iron atoms in the two kinds of sites are different. In the reference, $A_e/B_e = 1.72$ is given.

The magneto-optical rotation increases with decreasing wavelength from 3 µm to 0.5 µm [113]. At 1.15 µm, the saturation rotation is about 200°/cm ($3.5 \cdot 10^2$ rad/m) for pure YIG. Bismuth substitution can increase this value by a factor of more than 10 depending on the composition; 7400°/cm ($13 \cdot 10^3$ rad/m) has been reported at 1.15 µm [114]. The magneto-optical rotation is temperature dependent, but it has been shown that substitutions can reduce this dependence substantially [115,116].

It is important to remember that the magneto-optical rotation of ferrimagnetic materials, just as the magnetization, microscopically always has the saturation value. When measurements show other values, it is either because the magnetization is not parallel to the measuring light beam or because the light path goes through several domains with different magnetization directions.

The rare earth garnets also possess a magnetic linear birefringence in the order of 100°/cm ($1.7 \cdot 10^2$ rad/m) [117,118]. For bismuth substituted YIG, literature data also indicate a magnitude which is about half that of the magneto-optical rotation [119].

The index of refraction for pure YIG is 2.15. As the index for GGG is 1.95, a YIG film on a GGG substrate can form a high quality optical waveguide.

Using ion beam etching, or wet etching and multilayer growth, it is possible to make *strip* or *channel* waveguides in YIG film [120]. The technologies used to define the channel are, however, not so well developed. Furthermore, all changes made in the magneto-optical film will change not only the optical properties, but also the magnetic properties such as the anisotropy, etc.

3. Starting points for the sensor development work

A conclusion from the above description of YIG and other rare earth garnets is that they, compared to other magneto-optical materials, have many favourable features such as a large magneto-optic rotation, well-defined magnetic properties and good optical quality in the near IR. Furthermore, particularly with the epitaxially grown films, many of these properties can be altered at will through a number of substitutions. Unfortunately however, some of the properties are interlinked, mainly through the mechanical strain, in such a way that they cannot easily be independently optimized. We have, therefore, not considered it fruitful to design any devices based on a "perfect" magneto-optical material that has not yet been developed. Instead, our approach has been to find device structures that are useful for a *demonstration* with existing materials or with relatively simple modifications of known compositions. For similar reasons, no experiments have specifically been made to measure the bandwidths of the experimental sensors. No evidence of bandwidth limitations has, however, been found in measurements of magnetic fields at frequencies up to about 1 MHz.

The most striking feature of this type of material for sensors, is the large Faraday rotation. To achieve a polarization rotation of 90° (or a complete TE to TM conversion in the waveguide case) at 1.3 μm, from less than 1 mm to about 6 mm of optical path length is needed, depending on the material in question. The volume of the sensing element can, thus, be made very small, in the order of $1\,mm^3$. With a sensing volume of this size, the spatial variations of the magnetic field can be resolved. This is in contrast to the sensors using glass sensing elements. They often require a large sensing element and/or a closed measurement path.

In the design of a measurement system that utilizes a YIG or substituted YIG sensing element either in the form of a bulk crystal or a waveguide, there are a number of system design options. To be able to choose between these, we had to acquire a thorough knowledge of the properties of the material. As the available literature data, relevant for this application, were insufficient, this knowledge had to be gained through measurements.

For the single mode sensors we have, in order to avoid alignment problems, decided to work with waveguiding sensing elements only. The relatively large index difference between GGG and YIG, however, poses some problems. Guides that are single mode in the near infrared region are very thin, less than 1 μm. A slab guide of this kind will have a large linear birefringence that prevents the TM–TE conversion.

A number of techniques have been used to solve this problem. Multilayer structures with a layer between the GGG and the iron garnet film have been investigated [121]. A magnetic field that shifts its direction with a period that is equal to the beat length between the TE and TM modes can also be

used. In this way, a net conversion can be obtained even with a relatively large $\Delta\beta$ [122].

At an early stage of our project a periodic cover structure in GGG on top of the YIG waveguide was suggested as a means to achieve a net conversion with a single mode YIG waveguide [123].

We have, however, used another approach. Because of the high optical quality of the YIG waveguides, the coupling between the different modes in a multimode guide is negligible for the propagation distances in question. As it is also possible to achieve a fibre to waveguide coupling that only excites the fundamental mode of the waveguide, a relatively thick guide can effectively be used for single mode use [124]. For the fundamental mode, this kind of guide has a relatively small $\Delta\beta$ that can be cancelled by a moderate strain-induced $\Delta\beta$ introduced during the film growth [125]. The magnetic properties of the film are also influenced by the strain necessary to achieve a small net $\Delta\beta$ but it is possible to achieve a usable device with this approach.

Some of the critical design decisions then were:

- To use or not to use a magnetic bias field.
- One fibre for sending light to the sensing element and for receiving the signal, or separate fibres for the two functions.
- The selection of a suitable optical configuration that allows a measurable polarization modulation and an acceptable optical loss. A channel waveguide structure or a slab guide combined with some other means of controlling the light propagation are two of the options for this purpose.

The available selection of film types for waveguiding sensors was quite small. The YIG films were originally developed for bubble memory use and have later been modified for use in display units, printers [126,127], waveguiding optical isolators [128] and sensors.

For the multimode sensors, which are of a more immediate interest from the application point of view, a design which is suitable for production must be selected.

In the multimode case a larger selection of useful materials was available. The bulk YIG material that we initially used for the multimode sensors was originally produced for microwave applications and had to be cut and polished to optical quality. Later when the thick ($\approx$100 μm) epitaxially grown films with large magneto-optical rotation were developed, mainly for optical isolator use, we could use this type of material for the multimode sensors.

As the material characterization measurements went on, we were gradually able to transform the original sensor ideas envisioned at the start of the project, into practical sensor designs. In reality, of course, the influence also went the other way: The sensor design ideas made further measurements necessary. Below, however, the material characterization measurements and the sensor prototype experiments are presented in separate sections.

4. Material characterization measurements

Bulk materials

Measurement options

The magnetic and magneto-optical measurements that can be made on bulk YIG crystals can be divided into two categories, those made on *homogeneously magnetically saturated* samples and those made on *non-saturated* samples. Microscopically, the saturated state is the only one that exists and macroscopically, it is the only well-defined state. Examples of phenomena that are studied are the influence of material composition, temperature, wavelength, etc. on the saturation rotation. Such measurements are of interest not only from an application point of view, but also for material science, as they provide information about the nature of the magnetic interactions. Results from these types of measurements are, however, relatively well covered in literature, and will not be further described here.

For sensor applications, the properties of YIG also at low applied fields are of interest. These include the domain structure and how it is influenced by the crystal orientation, sample geometry, sample treatment and temperature.

Some measurements such as the measurement of the net magnetization of the sample and its dependence on external factors, can be made using magnetic methods [129]. Most of these results can, however, also be indirectly obtained from magneto-optical measurements and as our main interest is in the magneto-optical properties, this is the approach we have taken. The optical methods also facilitate changes of the measurement volume, which is a key measurement parameter.

If the sample is thin and the domains are large enough, a *focused light beam*, figure 13 a, allows the behaviour of a single domain or domain wall to be studied. Ideally, with a beam passing through only one domain, one should obtain the same results as those obtained for a homogeneously saturated material. One can then study changes in the domain magnetization direction and the effect on the magnetization and magneto-optical rotation caused by, for example, temperature.

With a *large diameter beam*, figure 13 b, the contributions from the different domains will be averaged. The exact nature of the averaging process is rather complicated as the pattern of the domains will act as a phase grating. For a thin sample with a two-dimensional domain pattern as in figure 13, the resulting polarization rotation can often be approximated using the area ratio between the two kinds of domains.
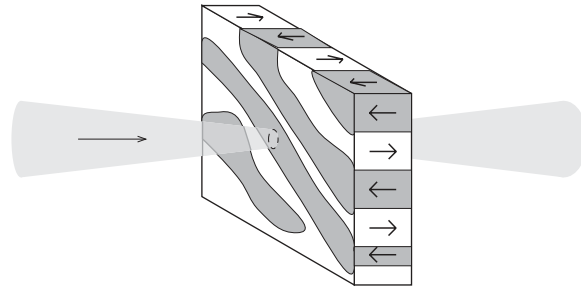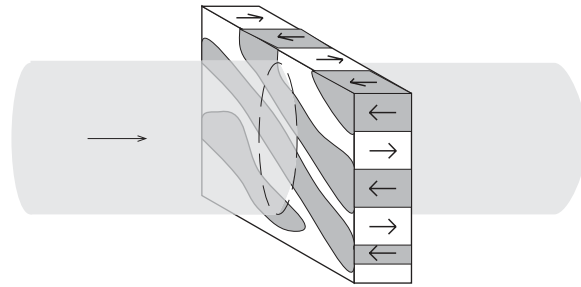
Fig. 13 a. Small measurement volume.

Fig. 13 b. Large measurement volume.

Measurement set-up

To study the magneto-optical properties of bulk materials, a measurement system according to the principle shown in figure 14 has been used. Linearly polarized light is sent through the measurement object. The beam transmitted by the measurement object has its plane of polarisation rotated by an angle θ. In a polarization splitting Wollaston prism, the beam is split into two orthogonal polarization components with the intensities I_1 and I_2. From these two values, and the input intensity I_0, the polarization rotation and the optical loss of the material can be calculated.

Other polarization detection principles such as the use of polarization modulation or rotating analysers are also possible [130]. The simple two-detector system was chosen mainly because it was also adaptable for evaluation of sensor prototypes.

The holder for the measurement object was temperature controlled and surrounded by coils allowing a magnetic field of arbitrary direction to be
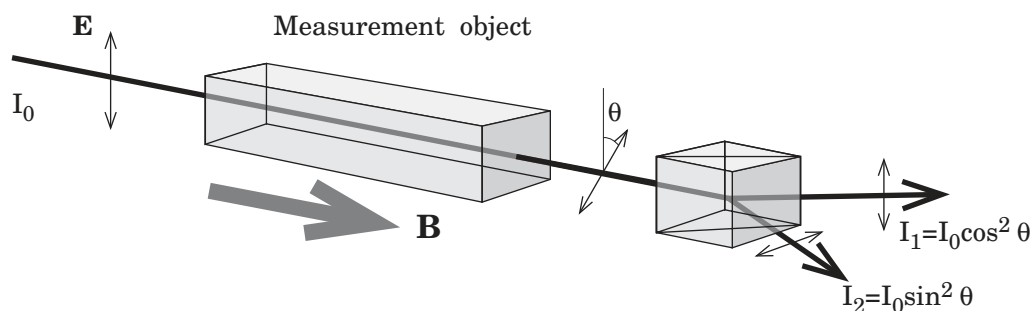
Fig. 14. Measurement system principle.
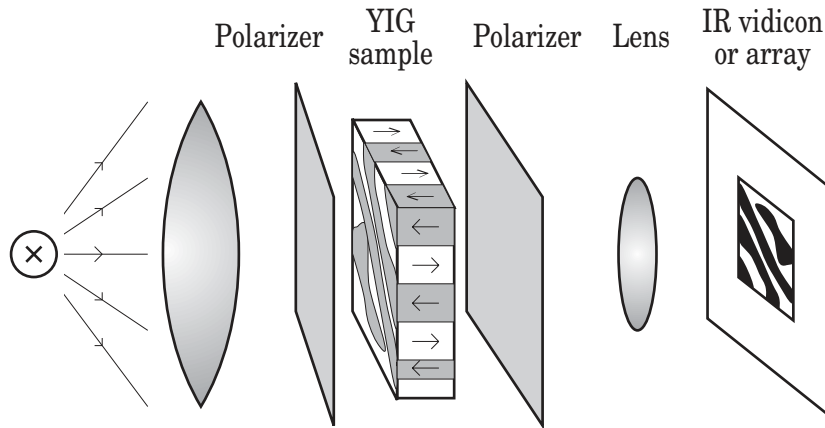
Fig. 15. Domain visualizing set-up.

generated. To allow automatic calibration and measurement routines, the system was designed with computerized control and data acquisition.

For a qualitative display of domain patterns, a set-up according to figure 15 was used.

Measurement results

Large measurement volume

Our first measurements of the magneto-optical rotation versus the applied field were made with a 200 µm diameter light beam through a cube 2×2×2 mm of YIG, figure 16. This rather discouraging result was, however soon supplemented with other results indicating that a larger light beam diameter and sample annealing improved the results, cf. the prototype sensor results below.
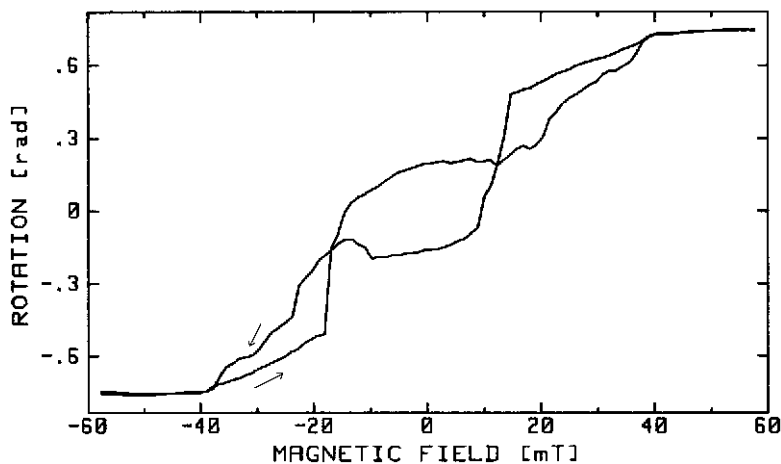
Fig. 16. Magneto-optical rotation versus the applied magnetic field for a 2×2×2 mm YIG cube as measured with a 200 µm diameter light beam with λ=1.15 µm.

We also found that a thinner sample with a two-dimensional domain structure gave a more reproducible result, though at the cost of a lower rotation, about 5° for a single pass through a 0.3 mm YIG slice.

Later, however, epitaxially grown Bi-substituted thick YIG films giving 22.5° rotation in a 0.13 mm film became available. The domains in this type of film are also smaller, giving a more efficient averaging effect. The well-controlled growth conditions for these films should also give a smaller number of defects which should allow the domain walls to move more freely.

Small measurement volume

When a 0.13 mm thick (YbTbBi)IG film on a GGG substrate is observed in the IR through suitably arranged polarizers in a set-up according to figure 15, a two-dimensional domain pattern is observed. The average domain width is in the order of 12 µm. The application of an external magnetic field changes the area ratio between the two kinds of domains, figure 17a,b. At high field levels, close to saturation, the majority of the small domains disappear, leaving a pattern with a lower spatial periodicity, figure 17c. For this specific material, the remaining domains shrink to bubble-like form just before saturation, figure 17d.

When measurements on materials of this kind are to be interpreted, one should remember that the periodic domain structure will work as a phase grating for the light component with a polarization state that is perpendicular to that of the input beam. Fig 17e,f,g show examples of diffraction patterns obtained with the (YbTbBi)IG film for similar conditions as those used for 17a,c,d. The diffraction patterns have been recorded with a set-up similar to the one in figure 15, though with the camera focused on infinity, i.e. the light source. The second polarizer is set to block the central beam when no field is applied. The central beam is, however, not completely extinguished in 17e. With field applied, the central beam will have its polarisation rotated, and it will thus pass the second polarizer and saturate the CCD array. The polarization of the diffracted light is always perpendicular to that of the input beam.
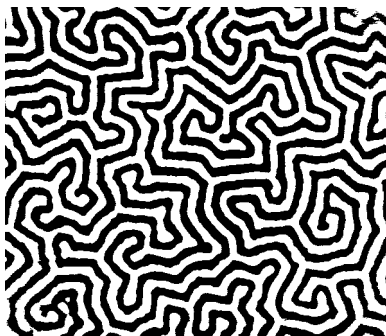
Fig. 17a. Domains in 0.13 mm (YbTbBi)IG film with no external field applied. Picture height corresponds to 0.54 mm.
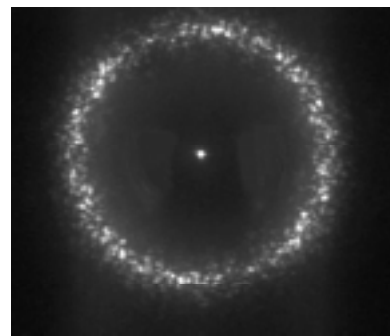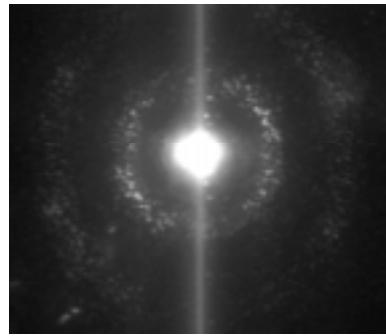

Fig. 17e. Diffraction from a domain pattern like the one in 17a. The diffraction angle is approximately 2.6°, corresponding to a domain width of 12 µm.
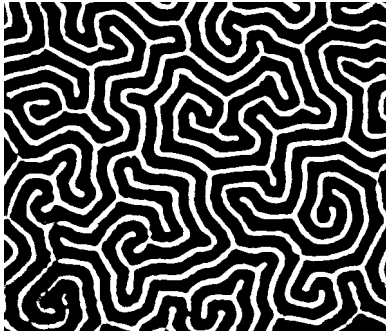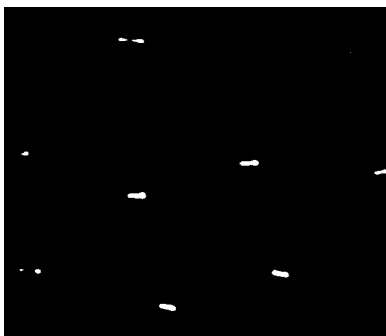
Fig. 17b. Domains in 0.13 mm (YbTbBi)IG film with 50 mT applied perpendicularly to the film. The domain pattern is nearly unchanged. Only the width ratio has changed.


Fig. 17c. Domains in 0.13 mm (YbTbBi)IG film with slightly less than 100 mT applied perpendicularly to the film. Some of the domains from a and b are still visible.

Fig. 17f. Diffraction from domain pattern similar to the one in 17c. First order diffraction at 1.6°, indicating a domain width of 20 μm. Second order diffraction just visible.

Fig. 17d. Domains in 0.13 mm (YbTbBi)IG film with about 100 mT applied perpendicularly to the film.
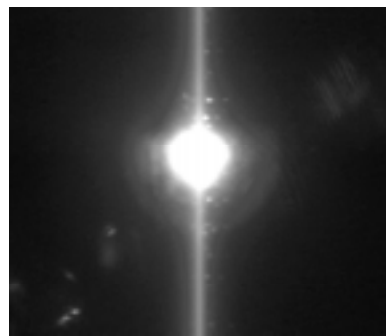
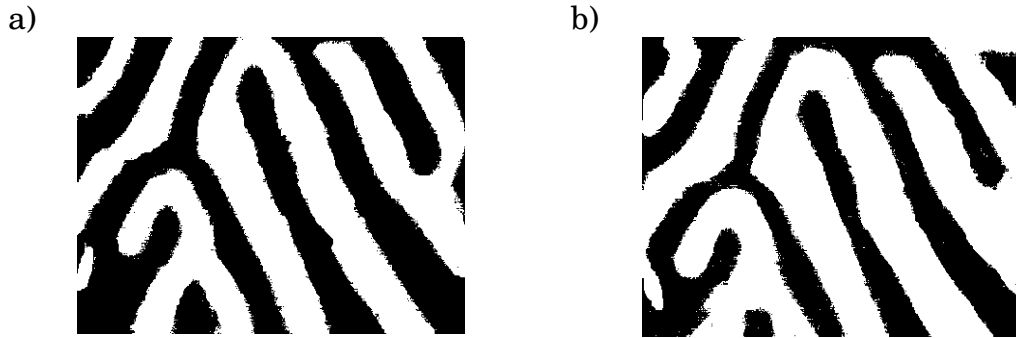*Fig. 17g. No diffraction is observed when all domains have disappeared.*

a) b)

Fig. 18. Domain patterns in 0.3 mm slice of pure YIG.
a) with no external field applied.
b) with a magnetic field applied perpendicularly to the plane of the sample.

Similar results obtained with a 0.3 mm YIG slice are shown in figure 18. The average domain width is, in this case, in the order of 0.1 mm.

To get more quantitative results we used the above mentioned measurement system with the beam focused down to a diameter smaller than the domain width. Results as the one in figure 19 were then obtained.

In this figure, the domain structure at two different temperatures is shown. It can be seen that both the rotation within the domains and the domain pattern differ. The polarization rotation in each domain is smaller at the higher temperature. Our measurements of polarization rotation versus magnetic field over a larger volume, however, show an increase in the sensitivity ($d\phi/dB$) with temperature. This can be explained by a saturation field H_S that decreases with increasing temperature. These results, that are both in agreement with work published by others, indicate a way to reduce the temperature dependence of sensors made from YIG and substituted YIG material [131].
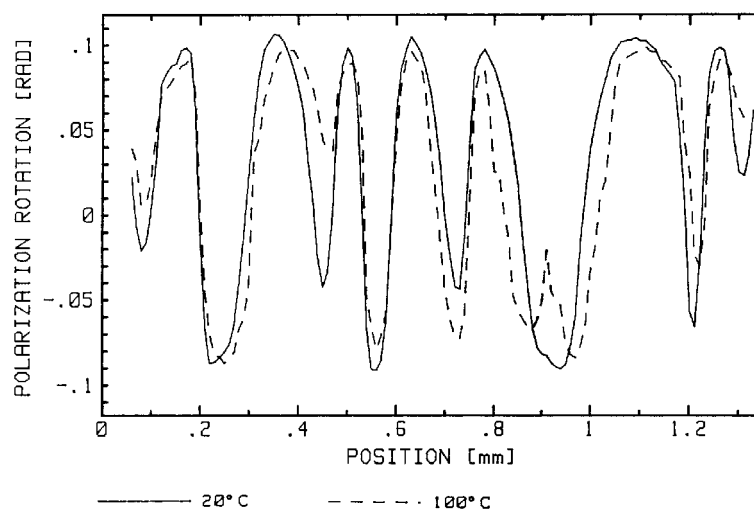

Fig. 19. Polarization rotation as measured with a 30 μm diameter beam scanned across a 0.3 mm thick YIG sample. Applied field perpendicular to slice plane 33 mT. Measured at 20°C and 100°C.

Sensor design considerations

From the measurement results, we were able to draw some conclusions concerning how to design sensors based on bulk YIG crystals:

- A thin crystal with a one-layered domain pattern , simplified the analysis and gave good results, though at the cost of a reduced rotation.
- A probing light beam much wider than the domain size, and preferably covering a large part of the crystal surface, reduced the effect of single domain behaviour.
- Annealing the crystal after sawing and polishing improved the results.

Waveguides

Measurement options

Most of the magneto-optical measurements on waveguiding samples are, principally, similar to those made on bulk samples. The situation is, however, complicated by the role of the linear birefringence. Furthermore, the cases differ in the means by which the light is coupled into and out of the material. For the waveguide characterization measurements, methods based on holographic grating, prism and end-fire light coupling, have been used.

The grating based method was used to determine accurately the linear birefringence and the saturation value of the magneto-optical rotation. In these measurements a grating, which is formed in photoresist on top of the waveguide, works as a distributed light coupler. A sketch of the measurement set-up is shown in figure 20.

The sample is turned to the coupling angle corresponding to the mode to be studied. As the coupling angle is, within the divergence of the laser beam, the same for the TE and TM modes of the same order, a polarizer and a retarder can be used to excite an arbitrary state of polarization at the input point. As the light propagates along the guide, a small fraction will continuously be coupled out, allowing the evolution of the intensity and the polarization state to be studied.

To determine the linear birefringence and the magneto-optical rotation,
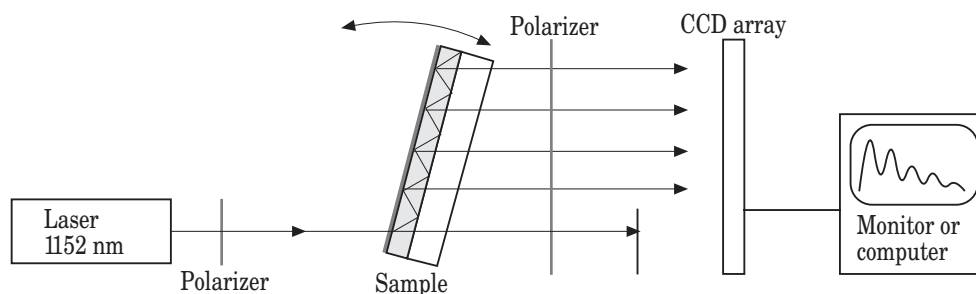
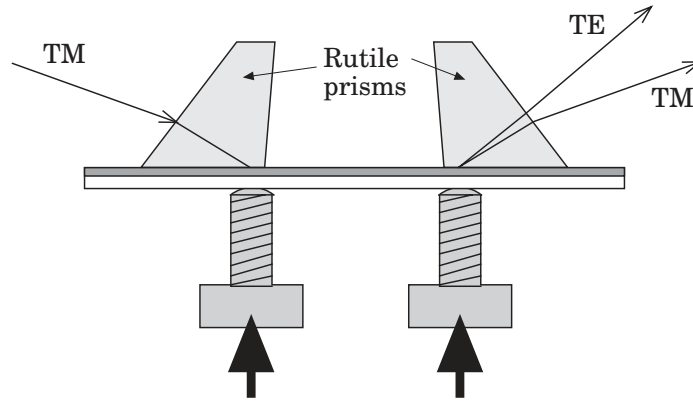*Fig. 20. Experimental set-up for the grating based measurements*

Fig. 21. Prism coupling method.

the spatial distributions of the outcoupled light under different magnetic field and input polarization conditions is recorded [132].

Even though the grating method can be used to measure the polarization rotation under different magnetic field conditions, it is more convenient to use the prism coupling method to study the variations in the rotation once the saturation value is determined.

A prism with an index of refraction equal to or higher than that of the guide is brought into contact with the guide by mechanical pressure, figure 21. Light impinging on the prism–guide interface with a suitable angle can then couple to a waveguide mode. Similarly, light can be coupled out through a second prism. For YIG waveguides, rutile is a suitable prism material. As rutile is birefringent, the TE and TM modes will have different coupling angles. With only one of the polarization modes excited at the input, the fraction of light converted can easily be monitored under different magnetic field conditions. Just as in the bulk measurement case, we have used a computer controlled measurement set-up to provide relevant magnetic field variations.

A number of experiments were also made with the fibre end coupled directly to the waveguide edge (butt-coupled). This method, in contrast to the prism method, does not involve any mechanical perturbation of the sample during the measurement. On the other hand, the samples must be specially prepared with polished edges.

Results of the waveguide measurements

The grating based method was used in an early stage of the project to select samples with sufficiently small linear birefringence to allow a large TE–TM mode conversion in the fundamental mode. Most of the samples we have used allowed a conversion of 90% or more. The results shown in this summary, except where is otherwise indicated, are obtained with 6.4 μm thick samples of Gd,Ga substituted YIG film on GGG substrate with a saturation polarization rotation of 150°/cm ($2.6 \cdot 10^2$ rad/m) at λ=1.15 μm. This material was known to be "easy in plane", i. e. the magnetization of the
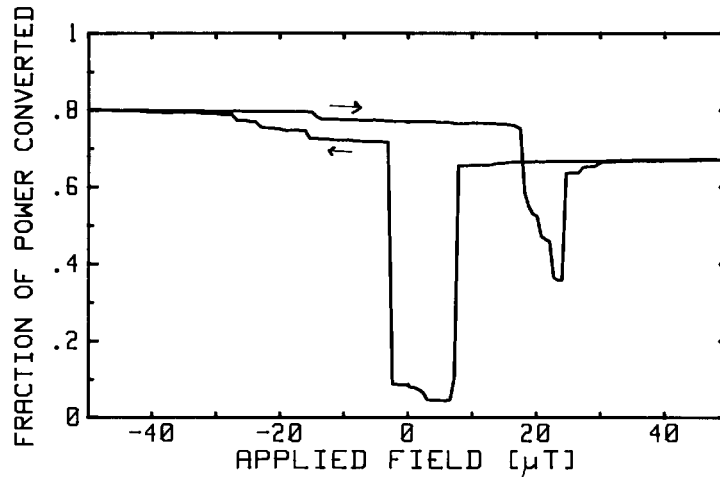
Fig. 22. TM to TE mode conversion versus a magnetic field applied in the plane of the film and parallel to the light propagation direction. The interaction length was 4 mm.

film could move relatively easily in the plane of the film but could not easily be turned from the plane of the film [133,134].

Our first results with prism coupling seemed, just as in the bulk measurement case, somewhat discouraging, figure 22. With a 50 μT field applied parallel or anti-parallel to the light propagation direction, the conversion is rather high and between those two extremes, the conversion goes down. There is, however, a large hysteresis, and the magnetization apparently changes in steps.

We found that the mechanical waveguide strain induced by the pressure applied to the prisms was responsible for part of the hysteresis. This is
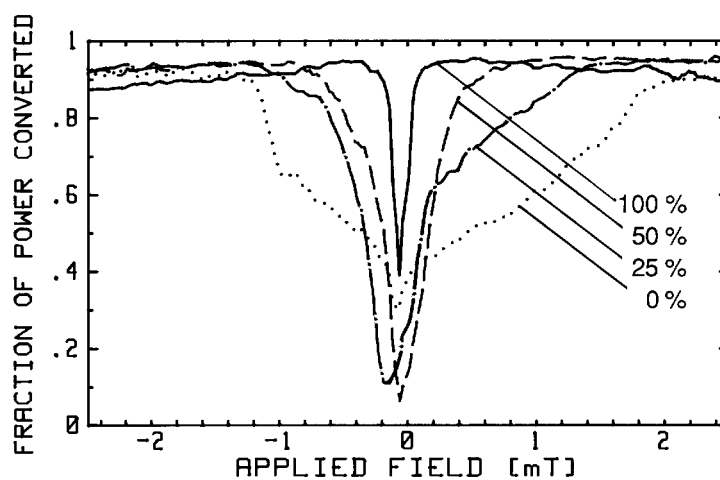

Fig. 23. TM to TE conversion, measured through a butt-couple fibre, versus the magnetic field applied in the plane of the film and parallel to the light propagation direction. The parameter is the pressure applied to the coupling prism.

demonstrated by the results shown in figure 23. Here, the conversion is measured through a fibre, butt-coupled to the edge of the waveguide sample. A coupling prism was also applied to the sample using different amounts of pressure. Evidently the pressure applied to the prism influenced the magnetic behaviour.

With the material used a "bias" field, in the plane of the film and perpendicular to the field to be measured, was found to be necessary to obtain an unambiguous and smooth result even with the prism removed. To select an appropriate magnitude for this bias field, we applied a field of constant amplitude but with variable angle in the plane of the guide. The conversion was then plotted versus the angle of the applied field. One could then observe the variation in conversion and, thus, also how the magnetization followed the direction of the applied field. Starting with a very weak field, figure 24a, we noticed that even though the magnetization followed the applied field there was a strong anisotropy. With higher field magnitude,
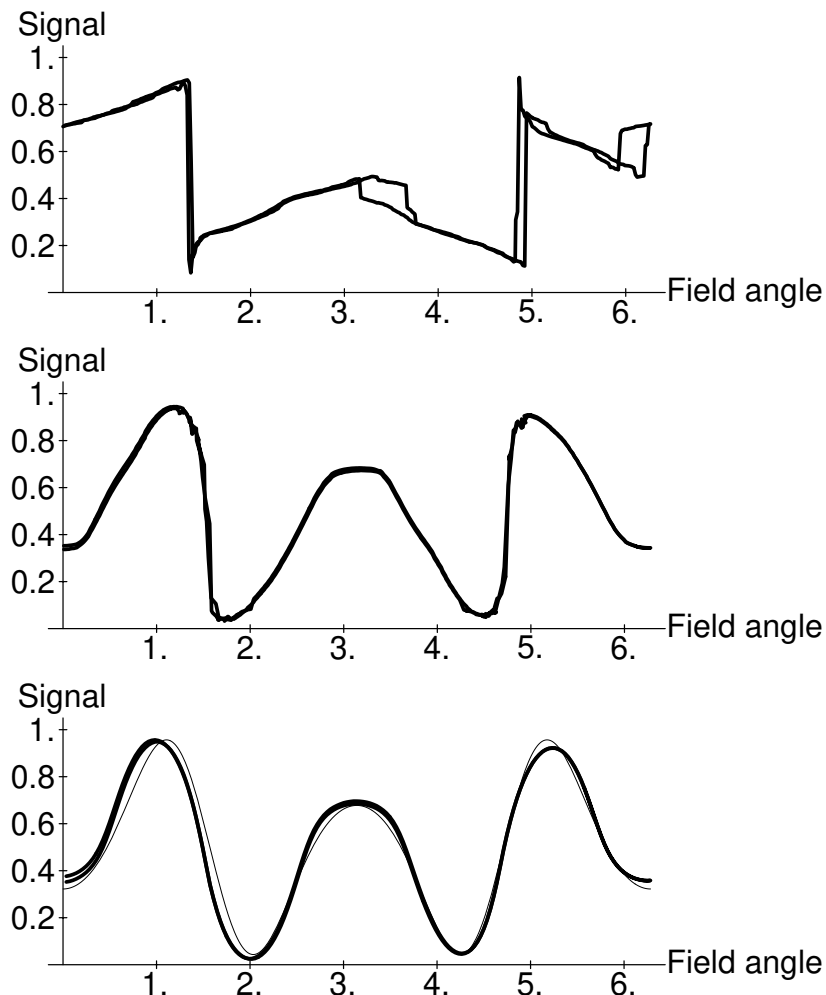

Fig. 24. The conversion versus the direction [rad] of an applied field for a two-way light pass in a 7.6 mm long sample. a) 100 μT field magnitude, b) 1 mT field magnitude c) 5 mT field magnitude (thick line) and theoretical calculation (thin line)

figure 24b, we could observe how the magnetization direction more and more closely followed the direction of the field. In figure 24c, with a 5 mT field, the magnetization almost completely follows the direction of the applied field. Although there are some deviations from the theoretical curve, the measured curve is smooth and free from hysteresis. This indicates that the 5 mT field was strong enough to create a single domain with a magnetization which could then be rotated by the field to be measured.

In order to study the magnetic behaviour of a channel structure in the film, experiments were made with strip waveguides delimited by parallel slits sawn through the waveguiding film. The hysteresis problems were, however, found to increase. A probable explanation is that the "channel structure", and the rough sawn edges, affected the domain structure. Some experiments with etching of YIG were also made [135].

Sensor design considerations

From measurements such as those described above, we drew the conclusion that with this type of material, which was known to have a relatively small anisotropy, a bias field of about 5 mT was needed to achieve a reproducible sensor behaviour.

The use of a bias field, however, limits the applicability of the sensor in several ways. The bias field may disturb the measurement situation in an unacceptable way. If the bias field is to be supplied by a permanent magnet, the effects of strong overload fields on this magnet must be considered. It may also prove difficult to find a magnet material that maintains the bias field constant over the temperature range required. On the other hand, there is in principle also a possibility to use a temperature dependent bias field to partly compensate the temperature dependence of the sensor material.

An alternative approach is, as will be shown below, to use a material with a strong anisotropy.

Partly because of the results that were obtained in the channel waveguide experiments, and partly because of the extent of process development work necessary to make channel waveguide structures, we also decided to use slab guides only.

Paper reference

The design and performance of the measurement system for bulk samples are discussed in paper A. In this paper, some examples of results are also given. The results are more fully described in paper C, and the sensor design rules are given in paper B.

The different waveguide characterization methods and the role played by the pressure applied to the prisms are covered in paper E.

The use of a variable in-plane field to select a suitable bias field, is described in paper G.

5. Sensors.

Single-mode systems

The sensing element of a measurement system with polarization maintaining single-mode fibres could, in principle, be either waveguiding or bulk optical. To avoid alignment problems, we have decided to work only with waveguiding sensing elements in our single mode systems. With a thickness of 5–10 μm, the sensing elements have been capable of carrying several modes, but we have shown that it is possible to use them effectively as single mode guides, butt-coupled to fibres.

The other two coupling methods that we have used in the characterization work can also be used in sensor configurations. The prism coupling method, however, lacks the ruggedness and potentially low cost that the butt-coupling and grating methods have. While we have preferred the simple butt-coupling in our sensors, grating coupling is a good alternative, particularly for thinner guides which cannot be effectively butt-coupled to fibres.

The basic principle of a waveguiding sensing element in combination with polarization preserving fibres is demonstrated in figure 25. One of the polarization modes of the fibre is used to carry linearly polarized light (white arrow) to the sensing element, where it is launched into the fundamental TE mode of the planar waveguide. In the waveguide, part of the optical power is converted to the TM mode (graded arrows). The light is then coupled into the return fibre, which is oriented in such a way that each of the modes of the planar guide matches one of the fibre polarization modes. At the output end of the fibre, the light from the two fibre modes is separated and detected. The detector outputs are then combined to give an intensity independent signal that is a measure of the magnetic field.

With this configuration it is not possible to detect the sign of the
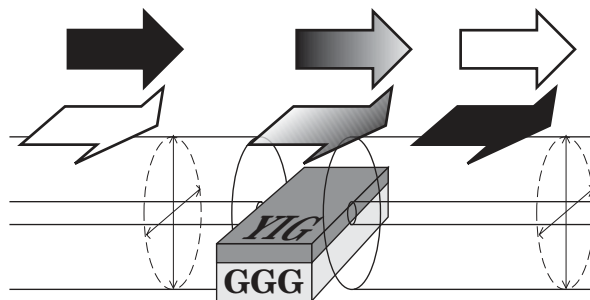
Fig. 25. Basic sensing principle

magnetic field. Fields that are parallel to, or anti-parallel to the light propagation direction, cause TE to TM coupling factors that are equal in magnitude and, consequently, they cause equal amounts of light to be coupled into the TM mode. However, if the return fibre is mounted with its birefringence axes at ±45° to those of the waveguide, the amplitude in each of the fibre modes will be a linear combination of the amplitudes of the TE and TM waveguide mode fields leaving the waveguide, giving a suitable anti-symmetric sensor behaviour. This is in analogy with a conventional bulk optic polarization rotation measurement set-up with the analyzer rotated 45° or –45° from the input polarizer orientation.

The absence of a lateral light confinement leads to a severe light loss when a configuration as the one in figure 25 is used. The loss can be of acceptable size only if the sensor is very short. Consequently, there is then a trade-off between polarization rotation and loss, but with materials having a very large Faraday rotation, it is possible to find a useful compromise. This is demonstrated by the results obtained with a sensor using a short bismuth-substituted YIG waveguide having a saturation magneto-optic rotation of about 1000°/cm ($1.7 \cdot 10^3$ rad/m) at 1.15 µm, figure 26. This waveguide had a strong out-of-plane anisotropy.

The idea was that this anisotropy should replace the bias field necessary with the other waveguiding sensors. The sensor output versus the applied field is shown in figure 27. A hysteresis effect appears for field magnitudes less than 1 mT. For such field levels, the magnetization direction is almost perpendicular to the film plane. For larger field levels, the performance is as expected, i.e. a smooth field versus conversion relationship. It is also evident from the non-symmetry of the curve that the return fibre was not correctly mounted, but was rotated slightly off the intended angular position with its birefringence axes at 45° from those of the input fibre. The imperfections of this experimental prototype should, however, not conceal the fact that the design principle is working. With another material having a stronger anisotropy it may be a viable concept.
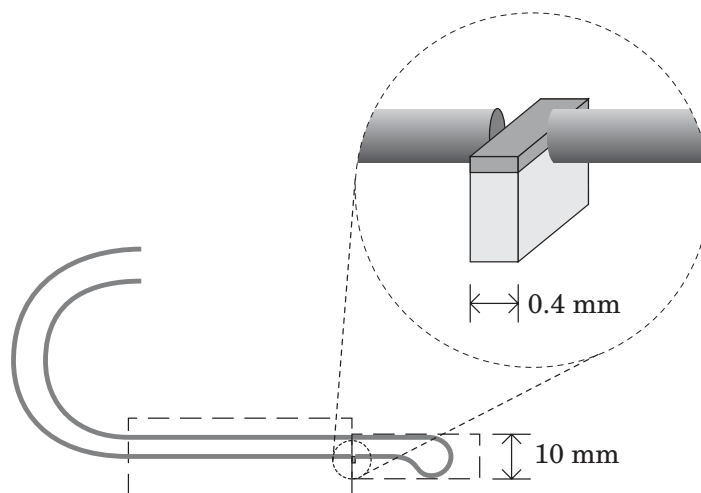

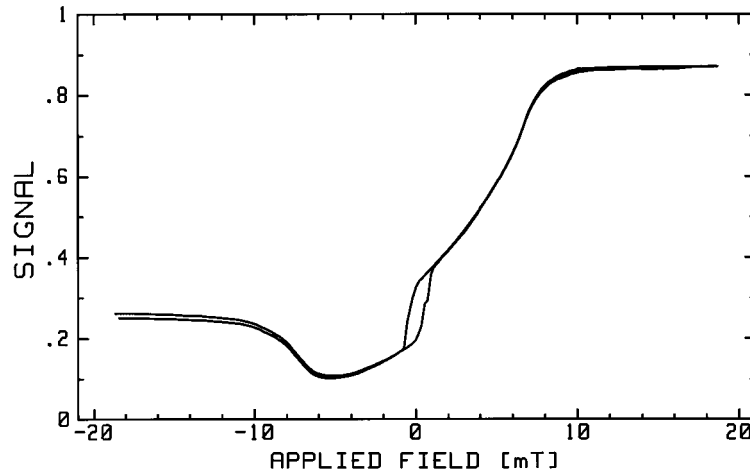*Fig. 26. Two-fibre sensor with 3.7 µm Bi-substituted waveguide.*

Fig. 27. Sensor output versus the applied field for a sensor according to figure 26.

An approach that in addition to solving the loss problems also allows the input and output fibres to be mounted side by side instead of in line on opposite edges of the waveguide, is to make a focusing reflector on the waveguide, figure 28a. In the experimental sensors, this reflector was made by polishing the rear edge into a semicircular form. A thin gold coating was then applied. Etched waveguide mirrors or grating reflectors are alternatives that could be taken into consideration. An experimental prototype is shown in figure 29.

As the Faraday effect is nonreciprocal in nature, the mode conversion of the forward and backward trip will add, making the effective interaction length twice the sensing element length.

This is the single-mode sensor design for which we have recorded the largest amount of test data. Results obtained with a sensor prototype with a 7.6 mm long Gd,Ga substituted YIG waveguide of the kind previously mentioned, are shown in figure 29. A bias field of 5 mT was used according to the sensor design considerations in the previous section of the summary.
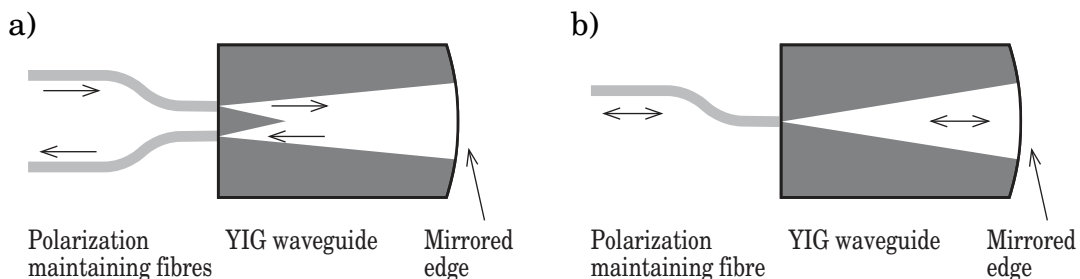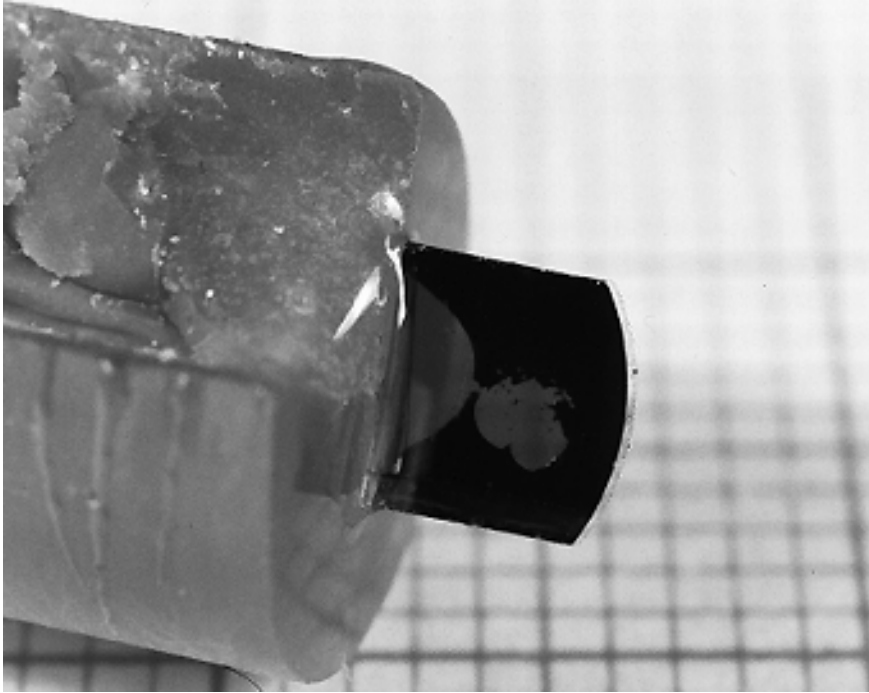

Fig. 28. Configurations for waveguiding sensors with focusing reflectors. a) With two fibres. b) With one fibre.

Fig. 29. Experimental sensor according to fig 28a.

The results show the expected sensor function with a central smooth sensing range and a slope reversal at approximately ±2 mT, figure 30. This indicates that the optical power couples back into the mode which it was originally launched into, equivalent to a polarization rotation of more than 45°. A sensor with a shorter interaction length would give a monotonous relationship.

Tests made with a spectrum analyzer, confirm the good signal quality and indicate a detector and amplifier noise level equivalent to about 8 nT in a 1 Hz bandwidth with a 5 mT bias field. The detection limit of the sensing
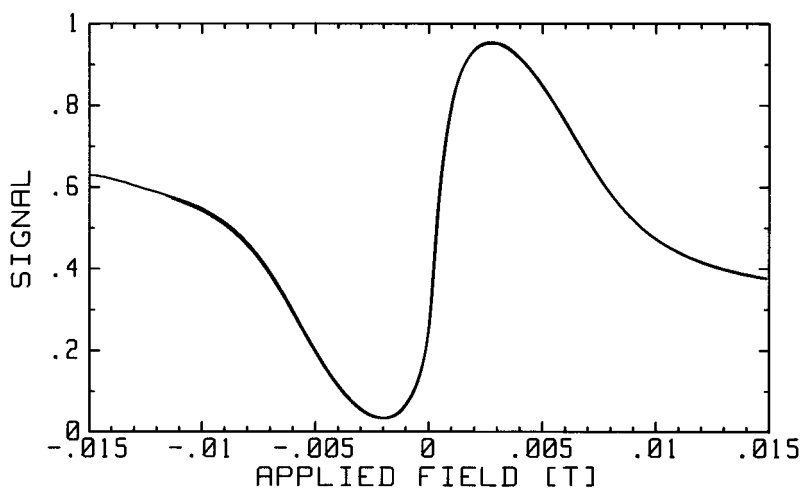

Fig. 30. Sensor output versus the applied field for the folded two-fibre design. Bias field 5 mT perpendicular to the axis of the sensing element.

element is, thus, lower than this value. By increasing the bias field, the measurement range can, of course, also be scaled to higher values.

We have also made a sensor where the same polarization maintaining fibre is used to guide the light both to and from the sensing element, figures 28b and 31. In such a configuration, the 45° displacement of the return fibre needed to achieve directional discrimination, is obviously not possible. For systems covering large distances, it is an advantage with only one fibre. Typically, however, such systems will include discontinuities in the fibre, e.g. removable connectors without index matching. Reflections from such discontinuities will be a problem in a one-fibre system. The reflected power will interfere with the light returning from the sensing element. As the phase angle between the unwanted reflection and the signal is determined by the length of the optical path to the sensing element, which will vary with the environment, rapid amplitude variations will take place. Although only one of the channels is affected, the performance of the balanced sensing system can be severely degraded.

The optoelectronic unit needed in a one-fibre system is also much more complex than the one in a two-fibre system. In addition to the polarization splitter, an extra beamsplitter, to couple the laser light into the fibre, is needed, figure 32. As the light has to pass this extra beamsplitter twice, the loss introduced is large. Furthermore, the risk of stray light from the laser falling on the detectors is substantial.
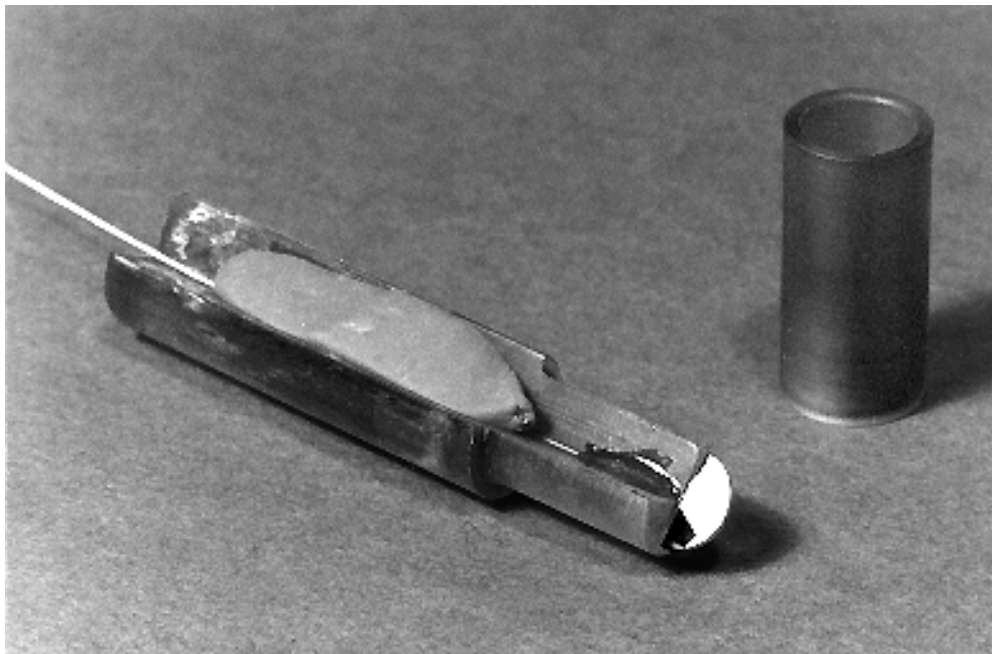
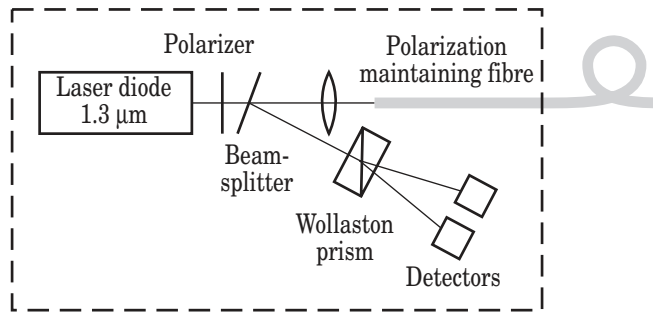*Fig. 31. Experimental one-fibre sensor according to figure 28b.*

Fig. 32. Optoelectronic unit for one-fibre sensing system.

Using a 1.3 μm laser with short coherence length we have, however, obtained good results with a one fibre system with no removable connectors and with the fibre ends obliquely cut to avoid reflections, figure 33. The sensing element is similar to the one used in the two-fibre sensor. The non-symmetry of the curve is, at least partly, due to the non-symmetry of the sensing element caused by the oblique mounting of the fibre.

The systems described here are balanced, i.e., the sum of the optical power from the two channels is independent of the measurand and only dependent on the system loss, while the distribution of power between the two channels is ideally only dependent on the measurand. This is completely true for the light path to the sensing element but only approximately so for the path from the sensing element to the detectors. Loss mechanisms that unequally affect the two fibre polarization modes in the return fibre, will influence the output signal.
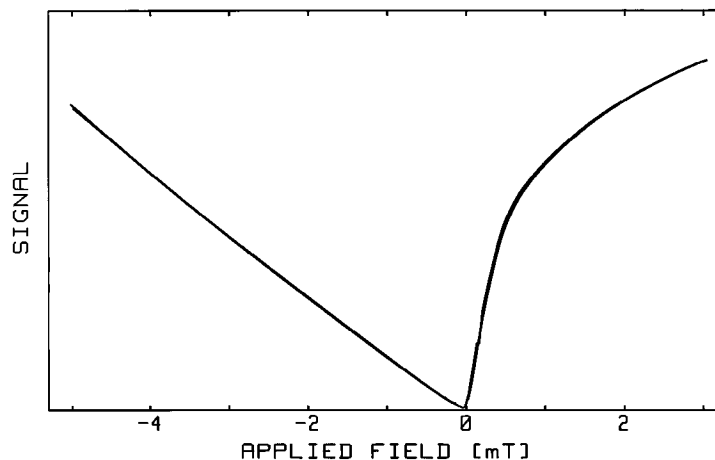

Fig. 33. Output signal from one-fibre sensor according to figure 28 b with an optoelectronic unit according to figure 32. A bias field of 3 mT in the plane of the waveguide is used.

Multimode systems

Iron garnet materials can also be utilized in multimode fibre optic magnetic field sensors. Such sensors provide a technologically simpler approach that may be more appropriate for many applications. Figure 34 shows the basic principle. Light is launched into and returns from the sensing element through multimode optical fibres. Polarizers are placed on both sides of the crystal. The intensity of the light transmitted through the second polarizer depends on the polarization rotation in the crystal.
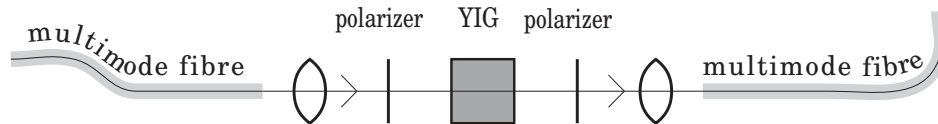

Fig. 34. Basic principle for the intensity based multimode sensors.

Different relative orientations of the transmission axes of the two sensor polarizers will produce very different sensor characteristics. To achieve a sensitivity to the direction of the applied magnetic field, a maximum unambiguous range and a maximum sensitivity to small fields, an angle of 45° between the polarizer axes can be chosen. In this case, the polarization rotation in the sensing element should not exceed 45°. For certain applications, other polarizer orientations are more favourable.

In most applications, it is unpractical to have the fibres on opposite sides of the sensing element. Thanks to the non-reciprocity of the Faraday effect it is, just as in the single-mode case, possible to use a folded design, figure 35. In this illustration, I have also indicated the use of a thick YIG film rather than a bulk crystal.

The DC field characteristics of such a sensor is shown in figure 36. The sensor was realized with an epitaxially grown 0.13 mm thick (YbTbBi)IG layer on a GGG substrate. The thickness of the layer was chosen to give a single pass maximum rotation of 22.5° at 1.3 µm.

The saturation points fall at approximately ±100 mT. Using a spectrum analyzer the output signal was measured for different levels of applied 1 kHz field from 27 mT (1% distortion) down to 270 nT.

The measurement results are summarized in figure 37, where the signal amplitude is plotted versus the applied 1 kHz field amplitude. Apparently the sensor is, within the experimental accuracy, linear over a range of at least 100 dB. The experimental data show a 1 Hz noise equivalent magnetic field of 1 µT. By decreasing the optical loss of the sensor and by improving
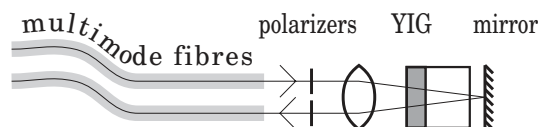

Fig. 35. Folded multimode sensor design

the amplifier, a reduction of this value to 100 nT should be within reach.

The accuracy of this type of sensor is, in most cases, limited by the loss variations in the system and by the temperature dependence of the sensor material. In some applications, e.g. AC measurement, the average value of the mesurand is known. One can then compensate for the slow loss variation. By optimizing the sensor material composition and thickness the temperature dependence of the material can be reduced considerably, less than 1% between –20°C and 80°C has been reported [136].

A recent prototype version of the multimode sensor is shown in fig 38. Other versions are shown in fig 39.
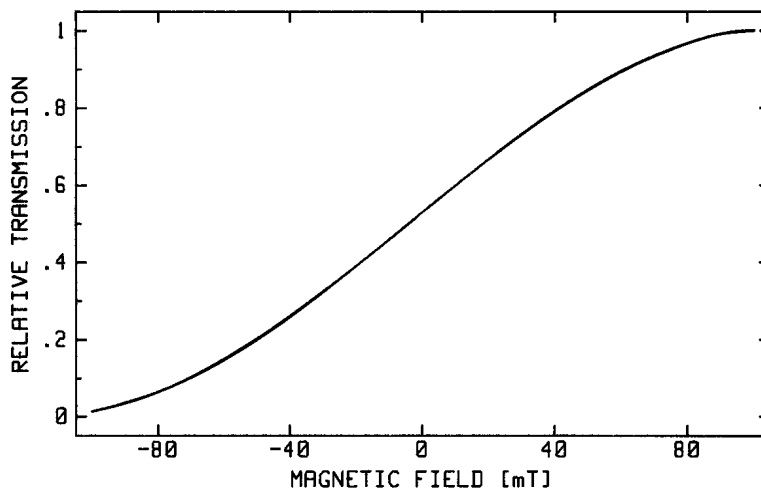

Fig. 36. The magnetic field characteristics of a multimode sensor with an epitaxially grown 0.13 mm thick (YbTbBi)IG layer on a GGG substrate.
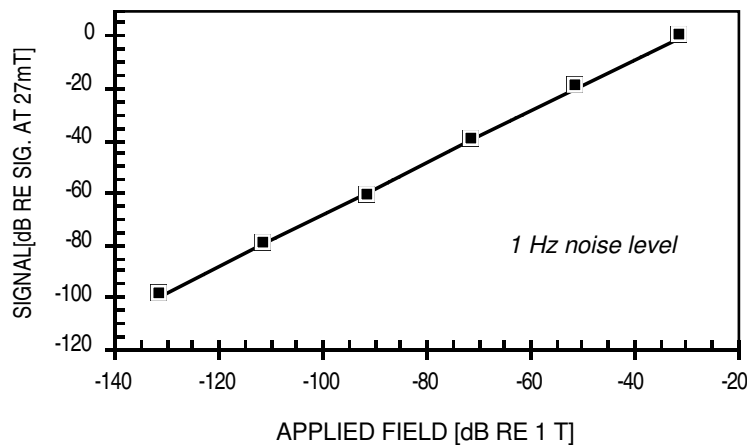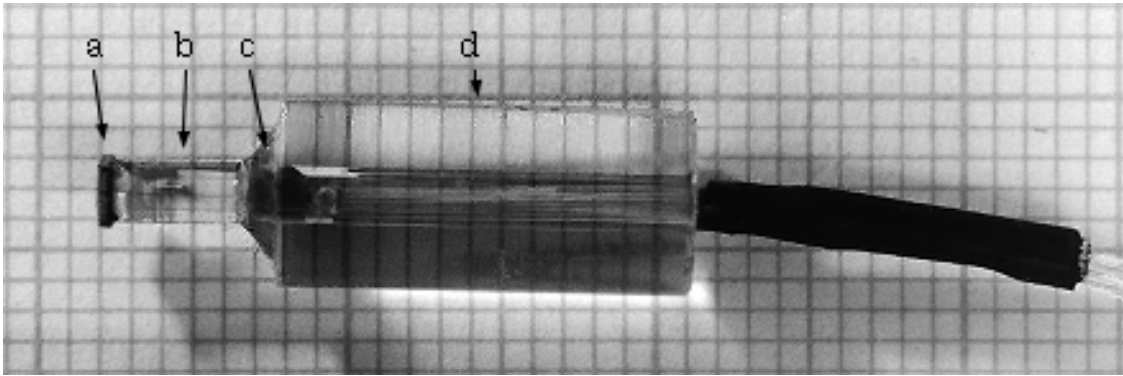

Fig. 37. The signal amplitude versus the applied field.

Fig 38. Prototype sensor developed for a field trial in co-operation with ABB Power Systems, with protective cover removed, lying on a piece of paper with mm rulings. a: YIG/GGG sensing element with gold coating, b: gradient index lens, c: polarizers, d: fibre holder made from a piece of glass tube.

Fig 39. Three versions of multimode sensors with folded design

Paper reference

The waveguiding sensors are first introduced in paper D. Results from an experiment with a two-fibre unfolded system are shown, but the paper is mainly about the one-fibre folded design according to figure 27b in this summary. Different techniques to avoid interference effects are also described.

In paper F, a similar folded sensor is used but with an 1.3 µm semiconductor laser diode light source to reduce the interference problems. A sensor utilizing a very short piece of highly magnetically anisotropic Bi-YIG wave-

guide is also described. In the same paper there is also a description of a number of multimode sensors.

The two-fibre folded design sensor and its performance is treated in paper G.

The performance of the folded multimode sensor is treated in paper H.

6. Conclusions

Fibre optic magnetic field sensors based on iron garnet material have a number of favourable features. They can be made very compact, have large measurement ranges and resolutions in the nT region. The small size is an advantage not only for the point sensing of magnetic fields, but also for current measurement together with an iron core.

Both single-mode and multimode systems are demonstrated in this thesis. The two types of systems differ both in their measurement possibilities and in more practical handling aspects.

Using polarization maintaining single-mode fibre and sensing elements made from few-mode YIG waveguide, several versions of balanced measurement system have been built. The output signal from such a system is approximately independent of the system loss. Sensors have been made both with separate fibres to guide the light to and from the sensing element and with a single fibre for both functions. The two fibre version is, however, less complicated and has a better performance.

While the waveguiding single-mode sensors have some attractive features and perhaps potentially the best performance, the multimode sensors are less complicated to manufacture. As they can be produced at a low cost, they could replace Hall elements, not only in magnetic field sensors, but also for rotation speed sensing, etc. Also for electric current measurement they are a viable alternative. While an accuracy equal to that of precision current transformers has not yet been demonstrated, sensor prototypes suitable for other current monitoring applications in the electric power grid have been developed.

The temperature dependence of the Faraday rotation which at present limits the accuracy of the sensors can be substantially reduced with new sensor material compositions.

The renewed interest in magneto-optical materials may make suitable sensor materials more readily available in the near future.

7. Acknowledgements

There are a number of persons who have helped me during the work.

First I would like to express my gratitude to professor *Kjell G. Svantesson*, who has been my supervisor and friend during the major and last part of the work, for his constant support and encouragement. Also I would like to thank professor *Gunnar Brodin* and professor *Torgny Brogårdh* who have, for different periods of time, been my supervisors.

I would also like to thank my co-worker *Ulf Holm*, not only for his collaboration in the work and good advice, but also for the many almost endless, but indeed fruitful, discussions about work and life in general. *Bengt Molin* is not mentioned as a co-worker in the papers, but his help with the mechanical design and fabrication of the sensors and laboratory equipment has been very important, and I would like to thank him for this. In fact, I would like to thank the entire staff of the Instrumentation Laboratory and a number of other persons at KTH, who have all, in various ways, helped me. *Carolyn Kyrning*, who has helped me to remove a number of language mistakes in the summary, should also be mentioned. New errors have, however, undoubtedly been added afterwards.

Finally, I would like to thank my wife and children for their support and for making the thesis work possible by taking over a lot of responsibilities during the last months of intense work.

The thesis is based on work supported by the National Swedish Board for Technical Development (STU).

References

1   J. Hecht, "Victorian experiments and optical communications", *IEEE Spectrum*, p. 69–73, February 1985.

2   C. Menadier, C. Kissinger and H. Adkins, "The fotonic sensor", *Instruments & Control Systems*, vol. 40, p. 114–120, 1967.

3   J. A. Powell, "A simple two-fiber optical displacement sensor", *Rev. Sci. Instrum.*, vol. 45 no. 2, 1974.

4   D. E. N. Davies and S. Kingsley, "Method of phase-modulating signals in optical fibres: Application to optical-telemetry systems", *Electronics Letters*, vol. 10, p. 21–22, 1974.

5   J. A. Bucaro, H. D. Dardy, E. F. Carome, "Fiber-optic hydrophone", *Journal of the Acoustical Society of America*, vol. 62, p. 1302, 1977.

6   J. P. Dakin, D. A. Kahn, "A novel fibre-optic temperature probe", *Optical and Quantum Electronics*, vol. 9, p. 540, 1977.

7   C. D. Butter and G. B. Hocker, "Fiber optics strain gauge", *Applied Optics*, vol. 17, no. 18, p. 2867–2869, 1978.

8   K. A. James, W. H. Quick and V. H. Strahan, "Fiber optic sensors for military, industrial and commercial applications", *Proc. of the International Telemetering Conference*, p. 777–782, Instrument Society of America, 1978.

9   H. Sohlström and U. Holm, "A fibre optic displacement sensor", *Acta IMEKO*, p. 183–192, 1982.

10   I. Kajtano and A. T. Friberg, "A silicon-based fibre-optic temperature sensor", *J. Phys. E: Sci. Instrum.*, vol. 21. p. 652–656, 1988.

11   J. N. Fields, C. K. Asawa, O. G. Ramer and M. K. Baronski, "Fiber optic pressure sensor", *J. Accust. Soc. Am.*, vol. 67, no. 3, p. 816–818, 1980.

12   M. Krigh, O. Steijer, O. Pers, G. Edwall, "Fibre-optic dark-field micro-bend sensor", *SPIE Proc. Fiber Optic Sensors*, vol. 586, p. 216–222, 1985.

13   W. W. Morey, G. Meltz and W. H. Glenn, "Fiber optic Bragg grating sensors", *SPIE Proc. Fiber Optic and Laser Sensors VII*, vol. 1196, p. 98–107, 1989.

14   J. P. Dakin and D. J. Pratt, "Distributed optical fibre Raman temperature sensor using a semiconductor light source and detector", *Electronics Letters*, vol. 25, p. S56–S57, 1989.

15   G. P. Hancke, "A fiber-optic density sensor for monitoring the state-of-charge of a lead acid battery", IEEE Trans. on Instrumentation and Measurement, vol. 39, no. 1, p. 247–250, 1990.

16   K. A. James, V. H. Strahan and W. H. Quick, *Analysis and Preliminary Design of Optical Sensors for Propulsion Control*, NASA CR-159519, Rockwell International, Anaheim, USA, 1979. (Available NTIS.)

17   S. Stueflotten, T. Chrisensen, S Iversen, J. O. Hellvik, K. Almås and T. Wien, "An infrared fibre optic gas detection system", *Proc. Second Int. Conf. on Optical Fibre sensors (OFS'2),* p. 87–90, VDE-Verlag, Berlin, 1984.

18   B. Hök, Ch. Ovrén and L. Jonsson, "Faseroptische sensorfamilie zur messung von temperatur, vibration und druck" (Fibre-optic sensor family for the measurement of temperature, vibration and pressure), *Technisches Messen*, vol. 53, no. 9, p. 322–330, 1986.

19   D. A. Jackson and J. D. C. Jones, "Interferometers", *Optical Fiber Sensors: vol. 2; Systems and Applications*, B. Culshaw and J. Dakin, p. 329–380, Artech House, Norwood, 1989.

20   M. Kanoi, G. Takahashi, T. Sato, M. Higaki, E. Mori and K. Omura, "Optical voltage and current measuring system for electric power systems", *IEEE Trans. on Power Delivery*, vol. PWRD-1, no. 1, 1986.

21   P. Dario, D. Femi and F. Vivaldi, "Fiber-optic catheter-tip sensor based on the photoelastic effect", *Sensors and Actuators*, vol. 12, p. 35–47, 1987.

22   W. J. Bock, T. R. Wolinski and A. Barwicz, "Development of a polarimetric optical fiber sensor for electronic measurement of high pressure", *IEEE Trans. on Instrumentation and Measurement*, vol. 39, no. 5, p. 715–721, 1990.

23   M. N. Charasse, M. Turpin and J. P. Le Pesant, "Dynamic pressure sensing with a side hole birefringent optical fibre", *Optics Letters*, vol. 16, no. 13, p. 1043–1045, 1991.

24   D. A. Jackson and J. D. C. Jones, "Interferometers", Optical Fiber Sensors: vol. 2; Systems and Applications, B. Culshaw and J. Dakin, p. 329–380, Artech House, Norwood, 1989.

25   A. R. Davis, S. S. Patrick, A. Dandridge and F. Bucholtz; "Remote fibre-optic AC magnetometer", *Electronics Letters*, vol. 28, no. 3, p. 271–273, 1992.

26   J. E. Lenz, "A review of magnetic sensors", *Proc. of the IEEE*, vol. 78, no 6, p. 973–989, 1990.

27   M. N. Rzewuski and M. Z. Tarnawecky, "Unconventional methods of current detection and measurement in EHV and UHV transmission systems", *IEEE Trans. on Instrumentation and Measurement*, vol. IM-24, no. 1, 1975.

28   A. Yariv and H. V. Winsor, "Proposal for detection of magnetic fields through magnetostrictive perturbation of optical fibres", *Optics Letters*, vol. 5, no. 3, p. 87–89, 1980.

29   J. Jarzynski, J. H. Cole, J. A. Bucaro and C. M. Davis jr., "Magnetic field sensitivity of an optical fiber with magnetostrictive jacket", *Applied Optics*, vol. 19, no. 22, p. 3746–3748, 1980.

30   H. I. Heaton, "Thermal straining in a magnetostrictive optical fiber interferometer", *Applied Optics*, vol. 19, no. 22, p. 3719–3720, 1980.

31   A. Dandridge, A. B. Tveten and T. G. Giallorenzi, "Interferometric current sensor using optical fibres", *Electronics Letters*, vol. 17, no. 15, p. 523–524, 1981.

32   K. P. Koo and G. H. Sigel Jr, "Characteristics of fiber-optic magnetic field sensors employing metallic glasses", *Optics Letters*, vol. 7, no. 7, p. 334–336, 1982.

33   A. D. Kersey, M. Corke, D. A. Jackson and J. D. C. Jones, "Detection of DC and low-frequency AC magnetic fields using an all single-mode fibre magnetometer", *Electronics Letters*, vol. 19, no. 13, p. 469–471, 1983.

34   K: P. Koo and G. H. Sigel, "Detection scheme in a fiber-optic magnetic field sensor free from ambiguity due to material magnetic hysteresis", *Optics Letters*, vol. 9, no. 6, p. 257–259, 1984.

35   A. D. Kersey, M. Corke and D. A. Jackson, "Closed loop D. C. field fibre optic magnetometer", *Proc. Second Int. Conf. on Optical Fibre sensors (OFS'2),* p. 51–54, VDE-Verlag, Berlin, 1984.

36   C. J. Nielsen, "All fiber magnetometer with magnetic feedback compensation", *Proc. SPIE Fiber Optic and Laser Sensors III*, vol. 566, p. 286–293, 1985.

37   F. Bucholtz, D. M. Dagenais and K. P. Koo, "High-frequency fibre-optic magnetometer with 70 fT/$\sqrt{\text{Hz}}$ resolution", *Electronics Letters*, vol. 25, no. 25, p. 1719–1720, 1989.

38 K. A. Arunkumar, "An ultrasensitive fiber-optic magnetic field sensor", *Pre-prints Annual meeting of Optical Society of America*, 1985.

39 G. Tanogan, D. I. Persechini, R. J. Morrison and J. A. Wysocki, "Current sensing with metal-coated multimode optical fibres", *Electronics Letters*, vol. 16, no. 25, p. 958–959, 1980.

40 B. S. Ramprasad and T. S. Radha Bai, "Speckle-based fibre-optic current sensor", *Optics and Laser Technology*, June, p. 156–158, 1984.

41 B. Moslehi, M. W. Foster and P. Harwey, "Optical magnetic and electric field sensors based on surface plasmon polariton resonant coupling", *Electronics Letters*, vol. 27, no. 11, p. 951–953, 1991.

42 S. Sato and M. Kushima, "Liquid-crystal electric and magnetic field sensors", *Mol. Cryst. Liq. Cryst.*, vol. 141, p. 229–235, 1986.

43 G. L. Mitchell, E. W. Saaski and J. W. Pace, "Gigaherz RMS current sensors for electromagnetic compatibility testing", *Proc. SPIE Fiber Optic and Laser Sensors VIII*, vol. 1367, p. 266–272, 1990.

44 Y. N. Ning, B. C. B. Chu and D. A. Jackson, "Interrogation of a conventional current transformer by a fiber-optic interferometer", *Optics Letters*, vol. 16, no. 18, p. 1448–1450, 1991.

45 L. E. Berkebile, S. Nilsson and S. C. Sun, "Digital EHV current transducer", *IEEE Trans. on Power Apparatus and Systems*, vol. PAS-100, no. 4, p. 1498–1504, 1981.

46 M. Adolfsson, C.-H. Einvall, P Lindberg, J. Samuelsson, L. Ahlgren and H. Edlund, "EHV series capacitor banks. A new approach to platform to ground signalling, relay protection and supervision", IEEE Power Engineering Society Summer Meeting in Portland Oregon, 1988.

47 G. R. Fowles, *Introduction to Modern Optics*, Holt Rinehart and Winston, New York, 1975.

48 J. F. Dillon jr., "Magneto-optical properties of magnetic garnets", *Proc. of the Intern. School of Physics "Enrico Fermi"; Course LXX: Physics of Magnetic Garnets*, A. Paoletti, North-Holland, Amsterdam, 1978.

49 K. Ando, "Nonreciprocal devices for integrated optics", *SPIE Proc. Electro-Optic and Magneto-Optic Materials and Applications*, vol. 1126, p. 58–65, 1989.

50 H. W. Katz (editor), *Solid State Magnetic and Dielectric Devices*, John Wiley & Sons Inc., New York, 1959.

51 A. Yariv, "Coupled-mode theory for guided-wave optics", *IEEE J. of Quantum Electronics*, vol. QE-9, no. 9, p. 919–933. 1973.

52 T. Sasano, "Laser CT and laser PD for EHV power transmission lines", *Electrical Engineering in Japan*, vol. 93, no. 5, 1973.

53 A. J. Rogers, "Optical technique for measurement of current at high voltage", *Proc. IEE*, vol. 120. no. 2. p. 261–267, 1973.

54 T. Yoshinio and Y. Ohno, "Highly sensitive all-optical method for measuring magnetic fields", *Fiber and Integrated Optics*, vol. 3, no. 4, p. 391–399, 1981.

55 C. Carter and J. Stites, "A magneto optic current transducer", *InTech*, June 1987, p. 41–46.

56 G. Massey, D. C. Erickson and R. A. Kadlec, "Electromagnetic field components: their measurement using linear electrooptic and magnetooptic effects", *Applied Optics*, vol. 14, no. 11, p. 2712–2719, 1975.

57   Yu. A. Gamazov, S. F. Glagolev, V. P. Zubkov, T. P. Koroleva, A. D. Krastina, L. A. Kuznetsova and L. G. Revin, "8-kA Magnetooptical measuring DC transducer", *Measurement Techniques (USA)*, vol. 26, no. 12, p. 1024–1026, 1984.

58   Y. n. Ning, B. C. Chu and D. A. Jackson, "Miniature Faraday current sensor based on multiple critical angle reflections in a bulk-optic ring", *Optics Letters*, vol. 16, no. 24, p. 1996–1998, 1991.

59   A. J. Rogers, "Electrogyration effect in crystalline quartz", *Electronics Letters*, vol. 12, no. 4, p. 103–104.

60   A. J. Rogers, "Method for simultaneous measurement of current and voltage on high-voltage lines using optical techniques", *Proc. IEE*, vol. 123. no. 10. p. 957–960, 1976.

61   K. Kyuma, S. Tai, M. Nunoshita, T. Takioka and Y. Ida, "Fiber optic measuring system for electric current by using a magnetooptic sensor", *IEEE Journal of Quantum Electronics*, vol. QE-18, no. 10, p.1619–1623, 1982.

62   A. Papp and H. Harms, "Magnetooptical current transformer. 1: Principles", *Applied Optics*, vol. 19, no 22, p. 3729–3734. 1980.
H. Aulich, W. Beck, N. Douklias, H. Harms, A. Papp and H. Schneider, "Magnetooptical current transformer. 2: Components", *Applied Optics*, vol. 19, no 22, p. 3735–3740. 1980.
A. Papp and H. Harms, "Magnetooptical current transformer. 3: Measurements", *Applied Optics*, vol. 19, no 22, p. 3741–3745. 1980.

63   S. C. Rashleigh and R. Ulrich, "Magneto-optic current sensing with birefringent fibers", *Appl. Phys. Lett.*, vol. 34, no. 11, p. 768–770, 1979.

64   J. Lizet, S. Valette and D. Langeac, "Reduction of temperature and vibration sensitivity of a polarimetric current sensor", *Electronics Letters*, vol. 19, no. 15, p. 578–579, 1983.

65   L. Li, J.-R. Qian and D. N. Payne, "Current sensors using highly birefringent bow-tie fibres", *Electronics Letters*, vol. 22, no. 21, p. 1142–1144, 1986.

66   R. I. Laming, D. N. Payne and L. Li, "Current monitor using elliptical birefringent fibre and active temperature compensation", *Proc. SPIE Fiber Optic Sensors II*, vol. 798, p. 283–287, 1987.

67   S. Donati and V. Annovazzi Lodi, "A fiber sensor for current measurements in power lines", *Alta Frequenza*, vol. 53, no. 6, p. 310–314, 1984.

68   S. N. Antonov, "Sensitive fiber-optic magnetic field transducer", Sov. Phys. Tech. Phys., vol. 36, no. 3, p. 357–358, 1991.

69   G. W. Day, D. N. Payne, A. J. Barlow, and J. J. Ramskov-Hansen, "Faraday rotation in coiled, monomode optical fibers: isolators, filters, and magnetic sensors", *Optics Letters*, vol. 7, no. 5, 1982.

70   W. Chu, D. McStay and A. J. Rogers, "Current sensing by mode coupling in fibre via the Faraday effect", *Electronics Letters*, vol. 27, no. 3, p 207–208, 1991.

71   D. Tang, A. H. Rose, G. W. Day and S. M. Etzel, "Annealing of linear birefringence in single-mode fiber coils: Application to Optical Fiber Current Sensors", *Journal of Lightwave Technology*, vol. 9, no. 8, p. 1031–1037, 1991.

72   P. A. Williams, G. W. Day and A. H. Rose, "Compensation for the temperature dependence of Faraday effect in diamagnetic materials: Application to optical fibre sensors", *Electronics Letters*, vol. 27, no. 13, p. 1131–1132, 1991.

73   R. P. Tatam, M. Berwick, P. Akhvan Leilabady, J. D. C. Jones and D. A. Jackson, "Applications of Faraday rotation using monomode optical fibre", *Proc. SPIE Fibre Optics '87: Fifth Int Conf. on Fibre Optics and Opto-Electronics*, vol. 734, p. 178–192, 1987.

50

74   A. D. Kersey and A. Dandridge, "Optical fibre Faraday rotation current sensor with closed-loop operation", *Electronics Letters*, vol. 21, no. 11, p. 464–465.

75   A. D. Kersey and D. A. Jackson, "Current sensing utilizing heterodyne detection of the Faraday effect in single-mode optical fiber", *Journal of Lightwave Technology*, vol. LT-4, no. 6, p.640–644, 1986.

76   S. P. Bush and D. A. Jackson, "Dual channel Faraday-effect current sensor capable of simultaneous measurement of two independent currents", *Optics Letters*, vol. 16, no. 12, p. 955–957, 1991.

77   P. Akhavan Leilabady, A. P. Wayte, M. Berwick, J. D. Jones and D. A. Jackson, "A pseudo-reciprocal fibre-optic Faraday rotation sensor: current measurement and data communication applications", *Optics Communications*, vol. 59, no. 3, p. 173–176, 1986

78   H. Arditty, Y. Bourbin, M. Papuchon and C. Puech, "Un capteur ampèremétrique a fibre optique (A fibre optic current sensor)", *Revue technique Thomson-CSF*, vol. 13, no. 3, p. 521–539, 1981.

79   F. Maystre and A. Bertholds, "Magneto-optic current sensor using a helical-fiber Fabry-Perot resonator", *Optics Letters*, vol. 14, no. 11, p. 587–589, 1989.

80   M. Abe, M. Shimosato, Y. Kozuka and M. Imaeda, "Magnetooptic current field sensor with sensitivity independent of Verdet constant and light intensity", *IEEE Translation Journal on Magnetics in Japan*, vol. 6, no. 5, 1991.

81   M. Lequime and C. Meunier, "Fiber optic magnetic field sensor using spectral modulation encoding", *Proc. SPIE Fiber Optic and Laser Sensors VIII*, vol. 1367, p. 236–242, 1990.

82   A. Kersey, F. Bucholts and A. Dandridge, "Sensitivity-bandwidth limitations in optical-fibre Faraday-rotation current sensors", *Int. Journal of Optoelectronics*, vol. 3, no. 4, p. 323–332, 1988.

83   R. Malewski and J. Szukalski, "Measuring impulse currents magneto-optically", *Elteknik (Sweden)*, no. 11, p.22–23, 1970.

84   L. Veeser, D. Kania, B. Freeman, P. Kruse, and E. Zimmerman, "Measurement of megaampere currents with optical fibers", *Proc. SPIE: Proc. of the Los Alamos Conference on Optics '83*, vol. 380, p. 300–304, 1983.

85   H. S. Lassing, A. A. M. Oomens and R. Woltjer, "Development of a magneto-optic current sensor for high, pulsed currents", *Rev. Sci. Instrum (USA)*, vol. 57, no. 5, p. 851–854, 1986.

86   R. L. Patterson, A. H. Rose, D. Tang and G. W. Day, "A fiber-optic current sensor for aerospace applications", *IEEE AES systems Magazine*, Dec., 1990.

87   F. Primdahl, P. Høeg, C. J. Nielsen and J. E. Schrøder, *A New Method for Measuring Space Plasma Current Densities by the Faraday Rotation of Laser Light in Optical Monomode Fibers*, 1986.

88   A. J. Rogers, "Point and distributed polarimetric optic-fibre sensors", *Journal of Optical Sensors*, vol. 1, no. 6, p. 457–472, 1986.

89   S. J. Weikel, "Application of magneto optic current sensors", *Proc. of the ISA '90 Int. Conf and Exhib. 1990; Advances in Instrumentation and Control; Proc*, vol. 45 part 4, p. 1589–1596, 1990.

90   T. D. Maffetone, T. M. McClelland, "345 kV substation optical current measurement system for revenue metering and protective relaying", *IEEE Trans on Power Delivery*, vol. 6, no. 4, p. 1430–1437, 1991.

91   T. Yu, Q. Li, R. Chen and J. Yan, "Magnet-sensitive optical fiber and its application in current sensor system", SPIE Proc. Fiber Optic and Laser Sensors IX, vol. 1584, p. 135–137, 1991.

92   S. Muto, N. Seki, T. Suzuki, "Plastic fiber isolator and current sensor", *Japanese J. of Appl. Phys.*, vol. 31, no. 3B, part 2–letters, p. L346–348, 1992.

93   K. Kyuma, S. Tai, M. Nunoshita, N. Mikami and Y. Ida, "Fiber-optic current and voltage sensors using a $Bi_{12}GeO_{20}$ single crystal", *Journal of Lightwave Technology*, vol. LT-1, no. 1, p. 93–97, 1983.

94   A. B. Semenov, A. N. Rodinov, V. V. Kutsaenko, V. M. Vatutin, V. K. Gorchakov and V. T. Potapov, "Light-guide magnetooptical sensor for study of pulsed magnetic fields", *Instruments and Experimental Techniques*, vol. 34, no. 1, p. 209–211, 1991.

95   S. Ihara, T. Mitsui, K. Tada, H. Takimoto, K. Tsujii, Y. Kuhara, M. Tatsumi, Y. Murakami, A. Kawakami and S. Miyamoto, "The development of BSO/fiber-optic magnetic field and voltage sensors", *Sumitomo Electric Technical Review*, no. 23, p. 175–184, 1984.

96   K. Itaka, K. Fujieda and T. Hara, "Fault section detecting system for power cable using optical magnetic field sensor", APSCOM-91 (Hong Kong) IEE 348, p. 644–649, 1991.

97   N. Kullendorf and B. Hök, "Temperature independent Faraday rotation near the bandgap in $Cd_{1-x}Mn_xTe$", *Appl. Phys. Letters*, vol. 46, p. 1016–1018, 1985.

98   M. A. Butler and S. J. Martin, "Optical fiber magnetic field sensor with nanosecond response time", Int. Conf. on Solid-state sensors and actuators; Philadelphia, 1985.

99   Aksionov, V. I. Konov, P. I Nikitin, A. M. Prokhorov, A. I. Savchuk, a. V. Savitski and K. S. Ulyanitski, "New aspects of giant exiton Faraday rotation in $Cd_{1-x}Mn_xTe$ semimagnetic compound: Fundamentals and applications", *Sensors and Actuators A*, vol. A23, no. 1–3, p. 875–878, 1990.

100   N. Mikami, C. Nagao, T. Sawada, H. Takahashi, Y. Furukawa and E. Aikawa, "Temperature dependence of magnetic field sensors using $(Cd_{1-x}Mn_x)Te$ and a light-emitting-diode light source", *J Appl. Phys.*, vol. 96, no. 1, p. 433–438, 1991.

101   E. Aikawa, A. Ueda, M. Watanabe, H. Takahashi and M. Imataki, "Development of new concept optical zero-sequence current/voltage transducers for distribution network", *IEEE Trans. on Power Delivery*, vol. 6, no. 1, p. 414–420, 1991.

102   T. Sawada, Y. Takada and K. Sato, "Growth technique and optical characterization of (Cd,Mn)Te for fiber-optic magnetic field sensors", *J. of Crystal Growth*, vol. 117, p. 826–829, 1992.

103   P. K. Tien, R. J. Martin, S. L. Blank, S. H. Wemple and L. J. Varnerin, "Optical waveguides of single-crystal garnet films", *Appl. Phys. Lett.*, vol. 21, no. 5, p. 207–209, 1972.

104   S. Geller, "Crystal and static magnetic properties of garnets", *Proc. of the International School of Physics "Enrico Fermi", Course LXX*, A. Paoletti, 1–55, North-Holland, Amsterdam, 1978.

105   M. A. Gilleo, "Ferromagnetic insulators: Garnets", *Ferromagnetic Materials Vol. 2,* P Wohlfarth, North Holland, Amsterdam, 1980.

106   N. Ohta, Y. Hosoe and Y. Sugita, "Submicron magnetic bubble garnets", *Recent magnetics for electronics*, Y. Sakurai, North Holland, Amsterdam, 1983.

107   P. Paroli, "Magneto-optical devices based on garnet films", *Thin Solid Films,* vol. 114, p. 187–216, 1984.

108   P Hansen, "Magnetic anisotropy and magnetostriction in garnets" *Proc. of the International School of Physics "Enrico Fermi", Course LXX*, A. Paoletti, 56–133, North-Holland, Amsterdam, 1978.

109   N. Ohta, Y. Hosoe and Y. Sugita, "Submicron magnetic bubble garnets", *Recent magnetics for electronics*, Y. Sakurai, p. 15–28, North Holland, Amsterdam, 1983.

110   S. N. Barybin, A. N. Grigorenko, V. I. Konov and P. I. Nikitin, "Magnetic field fibre-optical sensors based on Faraday effect", *Sensors and Actuators A*, vol. 25–27, p. 767–774, 1991.

111   M. N. Deeter, A. H. Rose and G. W. Day, "Fast, sensitive magnetic-field sensors based on the Faraday effect in YIG", *Journal of Lightwave Technology*, vol. 8, no. 12, p. 1838–1842, 1990.

112   J. F. Dillon jr., "Magneto-optical properties of magnetic garnets", *Proc. of the Intern. School of Physics "Enrico Fermi"; Course LXX: Physics of Magnetic Garnets*, A. Paoletti, North-Holland, Amsterdam, 1978.

113   P. Hansen and J.-P. Krumme, "Magnetic and magneto-optical properties of garnet films", *Thin Solid Films*, vol. 114, no. 1/2, p. 69–107, 1984

114   K. Ando, "Nonriciprocal devices for integrated optics", *SPIE Proc. Electro-Optic and Magneto-Optic Materials and Applications*, vol. 1126, p. 58–65, 1989.

115   Y. Tsujimoto, O. Kamada, T. Taniuchi and S. Serizava, "Temperature stabilized magnetic-field sensors using mixed rare-earth garnet crystals", OFC 83 New Orleans.

116   Y. Asahara and N. Nakamura, "The rare-earth iron garnet film with small temperature dependence of sensitivity used in magnetic field sensors", from Electronic materials Laboratory, Sumitomo Metal Mining Co., Ltd., 1-6-1 Suehiro-cho, Ohme-shi, Tokyo 198, Japan.

117   P. Paroli, "Magneto-optical devices based on garnet films", *Thin Solid Films,* vol. 114, p. 187–216, 1984.

118   K. G. Svantesson, "Measurements on magnetooptical waveguides by means of a distributed grating coupler", *J. Magn. Soc. Jpn.*, vol. 11 Supplement No S1, p. 405–408, 1987.

119   K. Ando, "Waveguide optical isolator: a new design", *Applied Optics*, vol. 30, p. no. 9, p. 1080–1084, 1991.

120   K. Ando, "Nonriciprocal devices for integrated optics", *SPIE Proc. Electro-Optic and Magneto-Optic Materials and Applications*, vol. 1126, p. 58–65, 1989.

121   M. Monerie, A. Leclert, P. Anizan, G. Moisan and P. Auvray, "Dispositifs magnetooptiques en couches minces a accord de phase: utilization d'une double heteroepitaxie de grenats ferromagnetiques", *Opt. Commun.*, vol. 19, p. 143–146, 1976.

122   P. K. Tien, R. J. Martin, R. Wolfe, R. C. Le Craw and S. L. Blank, "Switching and modulation of light in magnetooptic waveguides of garnet films", *Appl. Phys. Lett.*, vol. 21, no. 8, p. 394–396, 1972.

123   E. Berglind, *Förslag på en ny periodisk optisk vågledare för magnetfältsmätning (A proposal for a new periodic optical waveguide for magnetic field measurement)*, Report I 83-4035, Institute of Microelectronics (IM), Stockholm, Sweden, 1983. (In Swedish.)

124   U. Holm and K. Svantesson, "Mode selective light coupling from a single-mode fibre to a few-mode planar waveguide", to be published.

125   K. G. Svantesson, to be published.

126   P. Paroli, "Magneto-optical devices based on garnet films", *Thin Solid Films,* vol. 114, p. 187–216, 1984.

127   B. Hill and K. P. Schmidt, "Speichernde lichtsteuer- und display-komponenten", *Funkshau*, no. 20, p. 57–60, 1981.

128   K. Ando, "Nonriciprocal devices for integrated optics", *SPIE Proc. Electro-Optic and Magneto-Optic Materials and Applications*, vol. 1126, p. 58–65, 1989.

129   R. M. Bozorth, Ferromagnetism, chap. 19, D. Van Nostrand Company Inc., New York, 1951.

130 P. S. Hague, "Techniques of measurement of the polarization-altering properties of linear optical systems", *SPIE Proc. Optical Polarimetry*, vol. 112, p. 2–11, 1977.

131 Y. Asahara and N. Nakamura, "The rare-earth iron garnet film with small temperature dependence of sensitivity used in magnetic field sensors", from Electronic materials Laboratory, Sumitomo Metal Mining Co., Ltd., 1-6-1 Suehiro-cho, Ohme-shi, Tokyo 198, Japan.

132 K. G. Svantesson, "Measurements on magnetooptical waveguides by means of a distributed grating coupler", *J. Magn. Soc. Jpn.*, vol. 11 Supplement No S1, p. 405–408, 1987.

133 G. Doriath, R. Gaudry, and P. Hartemann, "A sensitive and compact magnetometer using Faraday effect in YIG waveguide", *Journal of Applied Physics*, vol. 53, no. 11, p. 8263–8265, 1982.

134 Private communication by Dr. H. LeGall and Dr. J. M. Desvignes, CNRS, Meudon, France.

135 M. Strömberg, *Våtetsning av YIG samt deponering av dielektriska skikt med brytningsindex nära 2 (Wet etching of YIG and deposition of layers with indices of refraction close to 2)*, Report I 84-2002, Institute of Microelectronics (IM), Stockholm, Sweden, 1984. (In Swedish.)

136 Y. Asahara and N. Nakamura, "The rare-earth iron garnet film with small temperature dependence of sensitivity used in magnetic field sensors", from Electronic materials Laboratory, Sumitomo Metal Mining Co., Ltd., 1-6-1 Suehiro-cho, Ohme-shi, Tokyo 198, Japan.

Comments on the authorship of the papers

The papers upon which this thesis is based, are written by myself and one or more co-authors from the fibre optic sensor group at the Instrumentation Laboratory. Torgny Brogårdh and Kjell Svantesson have been my supervisors, and their contributions have primarily been to provide good ideas and guidance. Also, their help in the actual writing of the text has been important. It is, however, difficult to quantify these contributions.

Most of the actual research work has been carried out by Ulf Holm and myself. Below I will indicate our different contributions to the papers. In the cases where Kjell Svantesson has made more active contributions to the work, this will also be indicated.

Paper A

Ulf Holm and I have taken equal parts in the development of the measurement system. The mathematical analysis of the performance was however made by Ulf Holm alone.

Papers B and C

Ulf Holm and I have made equal contributions to this work.

Paper D

I have done a major part of this work. The use of a few-mode waveguide with selective excitation was, however, originally suggested by Kjell Svantesson and the basic concepts behind the sensor design were jointly devised by the project group. Ulf Holm's main contribution is in the application of phase modulation to reduce the influence of the reflected light.

Paper E

This paper gives an overview of different methods applied in our characterization measurements. The grating method was devised by Kjell Svantesson and the results shown in the paper were obtained by him and Ulf Holm. The work on prism coupling and edge coupling was mainly done by myself.

Paper F

This paper gives a summary of our sensor work up to that time. Most of the work on multimode sensors was done by Ulf Holm and the work on single-mode systems was done by myself.

Paper G

This is primarily my work. Although he is not mentioned as a co-author, Ulf Holm has assisted in developing the model used in fig 6c, 7 and 8.

Paper H

This is primarily my work.

Paper abstracts

A: Measurement system for magneto-optic sensor materials

U Holm, H Sohlström and T Brogårdh

A system for the measurement of magneto-optic properties of IR-transparent materials is described. The system is designed for the characterization of fibre optic magnetic field sensor materials. Measurement results on YIG-crystals are presented. The accuracy of Faraday rotation and light transmission measurements are ±2 mrad and ±2% respectively. Important features for the sensor characterization are light beam scanning, temperature control and flexible magnetic field generation. A desktop computer is used for system control and data acquisition. The system is expected to be of great importance for future sensor development.

B: YIG-sensor design for fibre optical magnetic field measurement

U. Holm, H. Sohlström and T. Brogårdh,

Aiming at the design of a magnetic field sensor utilizing the Faraday effect, we give in this paper a description of measurements of magneto-optical properties of YIG. We also give sensor design rules based upon these measurements.

C: Measurement of YIG crystal characteristics for the design of optical magnetic field sensors

U. Holm and H. Sohlström

Measurements of the magneto-optic properties of YIG crystals, aiming at the design of fiber optic magnetic field sensors are presented. The Faraday polarization in YIG samples of different shapes, in applied fields –60 mT to +60 mT is given. The effects of temperature, perpendicular fields and sample treatment is studied. With thin, 0.3 mm samples, the linearity of the relationship between applied field and polarization rotation is found to be good with deviations from linearity of less than 1%.

D: A Polarization Based Fibre Optical Sensor System Using a YIG Optical Waveguide for Magnetic Field Sensing

Hans Sohlström, Ulf Holm and Kjell Svantesson

A sensor system utilizing a polarization maintaining fibre for the optical signal transmission and a planar optical waveguide for magnetic field measurements is presented. The system is based on polarization modulation

originating from the TE to TM mode conversion in a magneto-optical thin film of Gd,Ga substituted YIG (Yttrium Iron Garnet).

E: Characterization of Magneto-optical Thin Films for Sensor Use

Hans Sohlström, Ulf Holm and Kjell G. Svantesson

As a part of a fibre optical sensor development project we have made an evaluation of different optical waveguiding techniques to study the properties of thin magneto-optical films. Because of the application the methods are focused on the determination of the Faraday rotation, the linear birefringence and the dynamics and anisotropy of the magnetic properties of the samples. Measurements using holographic grating, prism and edge (end-fire) light coupling to different substituted YIG films are presented. The advantages of the different methods are discussed and it is shown that the launching technique may affect the properties to be measured. Film stress caused by the prism coupling method is found to influence the magnetic anisotropy.

F: Magneto-Optical Garnet Materials in Fibre Optic Sensor Systems for Magnetic Field Sensing

Kjell Svantesson, Hans Sohlström and Ulf Holm

Magneto-optical garnet materials such as YIG, undoped as well as substituted, exhibit a large Faraday rotation. This fact makes them potentially suitable as sensing elements in fibre optic magnetic field sensor systems.

We describe both an intensity based multimode system using bulk materials and a singlemode polarization based system using waveguiding films. A number of different material compositions, such as undoped YIG, (Gd,Ga)- and different Bi- substituted YIG have been used for the sensor elements. Measurement results are presented and discussed. A detection limit in the µT range and a measurement range exceeding 10^4 have been achieved.

G: A waveguide based fibre optic magnetic field sensor with directional sensitivity.

Hans Sohlström, Kjell Svantesson

In this paper we report on the design and performance of an extrinsic guided wave fibre optic magnetic field sensor. The sensor utilizes a substituted YIG (Yttrium Iron Garnet, $Y_3Fe_5O_{12}$) thin film as the waveguiding sensing element. A polarization maintaining fibre downlead was used to provide insensitivity to both power and loss fluctuations. The design makes it possible to determine both the magnitude and the sign of the magnetic field.

Measurement results indicate a usable measurement range of at least several mT with a noise equivalent magnetic field level of less than $8\,\text{nT}/\sqrt{\text{Hz}}$.

H: The performance of a fibre optic magnetic field sensor utilizing a magneto-optical garnet

Hans Sohlström, Kjell Svantesson

The design and performance of a multimode fibre optic magnetic field sensor utilizing the Faraday effect in an epitaxially grown thick (YbTbBi)IG film is reported. The sensor is found to be linear over a range of more than 100 dB.

59

Paper reprints

Paper A

U Holm, H Sohlström and T Brogårdh
"Measurement system for magneto-optic sensor materials"
J. Phys. E: Sci. Instrum., vol. 17, p. 885–889, 1984.

Measurement system for magneto–optic sensor materials

U Holm, H Sohlström and T Brogårdh
Royal Institute of Technology, Instrumentation Laboratory, S-100 44 Stockholm, Sweden

Abstract. A system for the measurements of magneto-optic properties of IR-transparent materials is described. The system is designed for the characterisation of fibre optic magnetic field sensor materials. Measurement results on YIG-crystals are presented. The accuracy of Faraday rotation and light transmission measurements are ± 2 m rad and $\pm 2\%$ respectively. Important features for the sensor characterisation are light beam scanning, temperature control and flexible magnetic field generation. A desktop computer is used for system control and data acquisition. The system is expected to be of great importance for future sensor developments.

1. Introduction

This paper describes a system adapted to the measurements of magneto-optic properties of IR-transparent materials. Since we are primarily interested in materials exhibiting a large Faraday rotation, e.g. ferrimagnetic materials, the system has not been designed to measure extremely small values of rotation of polarised light. Instead the system was designed to make accurate measurements of unique phenomena in ferrimagnetic materials, such as nonlinearities, hysteresis and magnetic domain formation. These phenomena are very important for e.g. fibre optic magnetic field sensors and the main applications of the system will be characterisation of candidate sensors materials.

YIG (yttrium iron garnet) is a ferrimagnetic material suitable for magneto-optic sensors because of its significant Faraday rotation (Wettling 1975, Massey et al 1975, Holm and Sohlström 1982). However, this material has not been useful for fibre optic sensor applications until recently since no reliable optoelectronic components have earlier been available in the wavelength region where YIG is transparent. Now the long wave fibre optic systems (1.2–1.6 μm) for long distance and high speed communication have changed the prerequisites. YIG and other garnets are therefore expected to grow in importance for optical sensing as well as for optical isolation. For sensing purposes the relation between applied magnetic field and polarisation rotation is of fundamental interest, rather than the properties of a uniformly saturated material which has been the subject of most reports published (Pisarev et al 1977, Toda and Nahagawa 1980, Berdennikova and Pisarev 1976). Evidently, there is now a need for measurements of different magneto-optic properties in nonsaturated YIG in relation to crystal composition, crystal growth methods, crystal defects, sample geometry, sample temperature etc. Later on we will describe this characterisation work in connection with a presentation of our sensor developments.

In the measurement system, a linearly polarised light beam is passed through the sample and the change of the state of polarisation caused by the sample is measured using a Wollaston prism and two photodetectors. This basic method was adopted instead of one using polarisation modulation, e.g. by means of a rotating analyser or retarder or a photoelastic modulator (Hague 1977). The main reason for our choice was that the same principle could be used in fibre optic sensors. Also the system is relatively inexpensive and adaptable to wide bandwidth measurements.

The polarisation rotation and transmission of the sample can be measured as functions of magnetic field parallel with and perpendicular to the light beam, position on the sample and temperature.

A desktop computer is used for automatic control, data acquisition and data processing, including auto-calibration routine giving increased accuracy.

First the basic measurement principle is outlined, then the measurement system is described. After that the measurement features are summarised and the performance of the system is analysed. Finally, we will discuss experimental results.

2. Measurement principle

In the measurement system, a linearly polarised light beam is incident on a measurement object, e.g. a YIG crystal. The polarisation plane of the incident beam is carefully fixed at an angle θ_0 with reference to the horizontal plane, figure 1. The beam transmitted by the measurement object has its plane of polarisation rotated an angle $\Delta\theta$. This rotation is due to the Faraday effect and thus dependent on the surrounding magnetic field. The transmitted beam is split into two orthogonal polarisation components I_1 and I_2 at $0°$ and $90°$ respectively, with reference to the horizontal plane. I_1 and I_2 denote the intensity values. If the input beam is at $45°$, we can write:

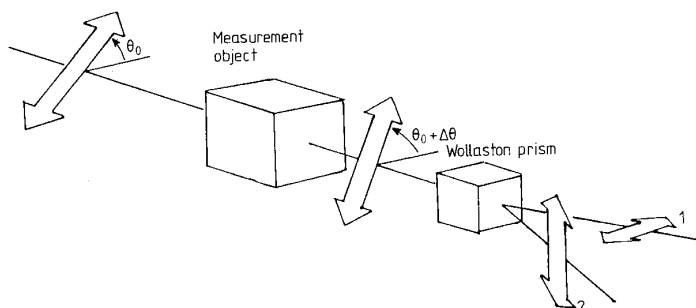$$Q = (I_1 - I_2)/(I_1 + I_2) = -\sin(2\Delta\theta).$$

Figure 1. Principle for polarisation rotation detection.

Thus Q gives a measure of the rotation of polarisation independent of the intensity I_0 of the incident beam.

To achieve a simultaneous measure of the transmittance of the measurement object, the sum of the signals I_1 and I_2 is divided by a signal from a reference channel.

3. Measurement system

Laser light (Spectra-Physics Stabilite model 120) of 1152 nm is used. To eliminate errors from beam position drift, a pinhole (0.3 mm dia) is mounted 250 mm from the laser output window. The pinhole gives the beam a divergence of about 5 mrad.

To achieve a reference beam a beam splitter with a transmittance of 90% is introduced. The reflected part $(c \cdot I_0)$ is focused onto a photodetector. All detectors used in the system are germanium photodetectors (Judson J-16-5, 2 mm), operating without bias.

The laser is oriented to have its plane of polarisation in an approximately correct direction (θ_0). To be able to control the polarisation more carefully, and to increase the degree of polarisation, a polarising prism is used. It is a calcite Glan–Focault prism (Oriel) with an extinction ratio $\leqslant 10^{-5}$.

To be able to make measurements with a small diameter beam at the measurement object, a convex lens with 200 mm focal length is used. At the surface of the measurement object this gives a beam diameter of 200 μm. A similar lens behind the crystal focuses the light on the detectors.

A Wollaston prism then splits the outcoming beam into two orthogonal directions of polarisation. The previously mentioned polarising prism is set to give incident polarisation at 45° with respect to the axes of the Wollaston prism when the measurement object is not present.

The measurement object is mounted in a holder consisting of a quartz block with a channel in which the object is placed, figure 3. The temperature is measured by a thermocouple moulded into the block. By means of micrometer controlled translation stages the block is accurately moveable in the plane perpendicular to the light beam.

Surrounding the quartz holder are two sets of electromagnets. One set is a pair of air coils to create a field (−60 mT, 60 mT) parallel to the light beam and the other set consists of
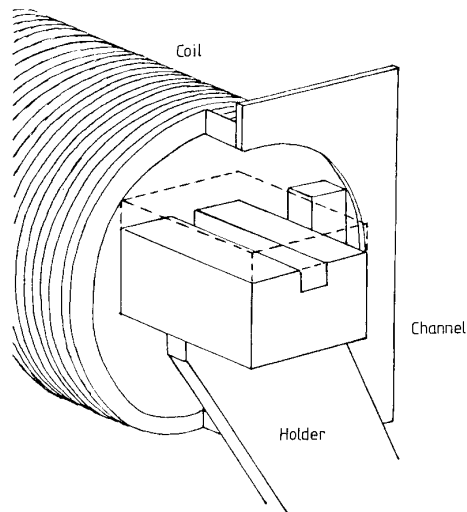
Figure 3. Measurement object holder.

two coils with an iron core, creating a transverse field (−50 mT, 50T). Also surrounding the holder is a resistance wire for the heating of the measurement object. The maximum attainable temperature is at present 100 °C limited by the maximum operating temperature of the electromagnet coils.

The measurements are controlled and logged by a HP 9826, which is a 16-bit desktop computer, with 320 kbyte primary memory and a floppy-disc mass storage. It is connected to peripheral units by the IEEE 488/IEC 625 bus.

The photodetector currents are transformed to convenient voltage levels by transimpedance coupled operational amplifiers (LF 356) and measured by digital voltmeters (Philips PM 2443).

The current producing the magnetic field parallel to the light beam is generated by a bus controlled DC power supply, (HP 6002 A) giving max. 200 W (max. voltage 50 V at 4 A and
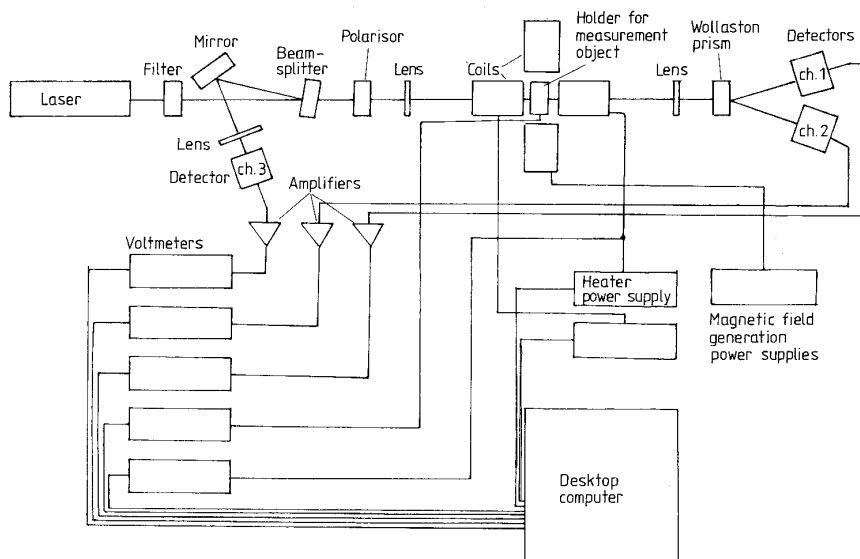
Figure 2. Measurement system.

max., current 10 A at 20 V). The direction of the current is altered by a bus controlled relay box. The transverse magnetic field is generated by a current supplied by a DC power supply, (Oltronix 628–20 R) giving max. 20 A at 30 V.

The computer controls the temperature by switching the current in the resistance wire on and off. The heating current is always off during sampling of the photodetectors.

4. Measurement features

At each measurement the following data are recorded:
(i) rotation of the plane of polarisation
(ii) transmission of the measurement object
(iii) current producing the magnetic field parallel to the light beam
(iv) temperature of the measurement object
(v) position of the measurement object relative to the light beam
(vi) time
Series of up to 400 measurements are made, though this number may easily be increased. Each recorded data is the mean value of a chosen number of readings (usually 10).

For the reliability and accuracy, a computerised calibration routine is included. By measuring detector outputs with the measurement object removed from the light path, and then with the light beam blocked, unequal detector sensitivities and offset signals are determined.

The current in the coils generating a magnetic field parallel to the light beam is set to a predetermined value by the computer at each measurement. The current is usually stepped from a negative value to an equal positive one and back.

The temperature can either automatically be held constant to $\pm 1\,°C$ or be swept up or down or be set to an arbitrary value at each measurement.

The system features obtained match the requirements of our present sensor development work. To meet future demands several changes will probably be made, as for example installation of a high frequency data collection system, motorised computer controlled micrometers for light beam scanning, monochromator light source together with phase locked amplifiers for spectral studies, coils for larger magnetic fields and optics for measurements on wave guiding structures.

5. Performance

The recorded data of the rotation of polarisation can be shown to be (Holm *et al* 1983)

$$M_{\text{rot}} = 0.5 \sin^{-1}[(1 - \Delta U_1 - \Delta U_2)\sin 2\Delta\theta + (\Delta_2 - \Delta_1)\sin^2 2\Delta\theta$$
$$+ 2\alpha(1 - \cos 2\Delta\theta - \sin^2 2\Delta\theta) + \Delta_1 - \Delta_2 + \Delta U_1 + \Delta U_2]$$

$\Delta\theta =$ rotation caused by the Faraday effect in the crystal
$\alpha =$ deviation of incident direction of polarisation from correct value (45° to Wollaston prism axes)

$$\Delta_i = \tfrac{1}{2}\left(\delta_{1_i} + \frac{\Delta\eta_i}{\eta_i^0} + \frac{\Delta F_i}{F_i^0}\right) \qquad i = 1, 2$$

($i = 1, 2$ corresponds to the two detector channels separated by the Wollaston prism)

$$\Delta U_i = \tfrac{1}{2}\Delta U_{i\,\text{offset}}/[0.6\,F_i^0\eta_i^0 T_C I'_L] \qquad i = 1, 2$$

$F_i =$ electrical amplification of detector output signal
$U_{i\,\text{offset}} =$ DC offset, electrical and due to stray light
$\eta_i =$ detector responsivity
$\delta_{1_i} =$ relative change in detector signal due to redistribution of energy within the beam
$T_C =$ crystal transmittance
$I'_L =$ power of the light passing through the pinhole
Superscript 0 denotes the values at time of calibration and prefix Δ denote the change since calibration (drift).

The transmission data is (Holm *et al* 1983)

$$M_{\text{trans}} = [1 + \alpha(1 + \sin 2\Delta\theta) + T_C\Delta_1(1 + \sin 2\Delta\theta)$$
$$+ \Delta_2(1 - \sin 2\Delta\theta) - \Delta_3 + \Delta U_1 + \Delta U_2 - \Delta U_3]$$

$$\Delta U_3 = \Delta U_{3\,\text{offset}} \frac{15}{\eta_3^0 F_3^0 I'_L}$$

(index 3 corresponds to the reference channel).

To estimate the maximum error in the measurement we assume that the errors are independent and all add. The errors in the detector channels (1 and 2) can also be assumed to be of equal magnitude, since the channels are equivalent. This gives:

$$M_{\text{rot}} = 0.5 \sin^{-1}[\sin 2\Delta\theta + 2\alpha(1 - \cos 2\Delta\theta - \sin^2 2\Delta\theta)$$
$$+ 2\Delta(1 - \sin^2 2\Delta\theta) + 2\Delta U].$$

$$M_{\text{trans}} = T_C[1 + 2\alpha(1 + \sin 2\Delta\theta) + 3\Delta + 2\Delta U + \Delta U']$$

where

$$\Delta = \tfrac{1}{2}\left(\delta_1 + \frac{\Delta\eta}{\eta^0} + \frac{\Delta F}{F^0}\right)$$

$$\Delta U = \tfrac{1}{2}U_{\text{offset}}/(0.6F^0\eta^0 T_C I'_L)$$

$$\Delta U' = 15\,\Delta U_{\text{offset}}/(F^0\eta^0 I'_L).$$

The different contributions to Δ are also assumed to be independent giving:

$$\Delta_{\text{max}} = \tfrac{1}{2}\left(|\delta_1| + \frac{|\Delta\eta|}{\eta^0} + \frac{|\Delta F|}{F^0}\right)$$

δ_1 is estimated to be less than 0.1%, which is based upon measurements of the sensitivity variations on the detector area, beam irradiance distribution at the pinhole and beam directional variation.

$\Delta\eta$ is mainly due to temperature dependence. The temperature coefficient of the detectivity of Judson J-16 detectors is given by Stock and Möstl (1982) as $0.3\%\,K^{-1}$. Since the temperature change during a measurement is $\leqslant 1\,°C$

$$\Delta\eta/\eta \leqslant 0.3\%$$

ΔF consists of three parts. (1) Thermal drift in amplifier resistances $\leqslant 5 \times 10^{-4}$. (2) Relative error in the voltmeter reading specified as $\leqslant 2 \times 10^{-4}$. (3) Error caused by a random trigger delay of max. 100 ms in the voltmeters. The fastest relative variations in laser intensity is measured to be $8 \times 10^{-3}\,s^{-1}$ (two hours after start). Resulting error $\leqslant 8 \times 10^{-4}$. Adding these contributions gives a maximum error of:

$$\Delta_{\text{max}} \leqslant \tfrac{1}{2}(1 \times 10^{-3} + 3 \times 10^{-3} + 5 \times 10^{-4}$$
$$+ 2 \times 10^{-4} + 8 \times 10^{-4}) \leqslant 3 \times 10^{-3}$$

ΔU_{offset} consists of amplifier offset drift $\Delta U_{\text{amp}} \leqslant 5 \times 10^{-3}$ V and the error due to stray light, which is estimated to $\leqslant 10^{-4}$ V.

The absolute error of the voltmeter is $\leqslant 10^{-4}$ V and thus

$$\Delta U_{\text{offset}} \leqslant 6 \times 10^{-3}\,V$$
$$\Delta U = \tfrac{1}{2}\Delta U_{\text{offset}}/(0.6\,F^0\eta^0 T_C I'_L) \leqslant 2.5 \times 10^{-4}/T_C$$
$$\Delta U' \leqslant 5 \times 10^{-3}$$

where

$$F_0 = 4 \times 10^6\,V\,A^{-1}$$
$$\eta^0 = 0.5\,A\,W^{-1}$$
$$I'_L = 1 \times 10^{-5}\,W.$$

The polariser is set at equal angular distance from a minimum value in each detector channel. The error α is then minimised by

minimising the influence of rotation $\Delta\theta$ on the transmission measurement. This calibration method is estimated to give $\alpha \leqslant 10^{-3}$.

Introducing these values into the expressions for M_{rot} and M_{trans} gives

$$M_{\text{rot}} = 0.5 \sin^{-1}[\sin 2\Delta\theta \pm 2 \times 10^{-3}(1 - \cos \Delta\theta)$$
$$\pm 6 \times 10^{-3}(1 - \sin^2 2\Delta\theta) \pm 5 \times 10^{-4}/T_{\text{C}}]$$

$$M_{\text{trans}} = T_{\text{C}}[1 \pm 2 \times 10^{-3}(1 - \cos 2\Delta\theta)$$
$$+ 9 \times 10^{-3} + 5 \times 10^{-4}/T_{\text{C}} \pm 5 \times 10^{-3}].$$

The magnitudes of the calculated worst case rotation and transmission error are shown in figures 4 and 5. Except for large angles of rotation, the calculated maximum rotation error with a typical 2 mm YIG sample is about 4 m rad. The calculated transmission error is in the same case 2%. These error values should be compared with the maximum observed system drift during long-time system tests, 0.5 m rad and 1% respectively. The main reason for this discrepancy is that the temperature drift errors of the three channels are not uncorrelated, which was assumed. In fact, there is a strong correlation between the temperatures of the detectors and detector amplifiers. It is reasonable to believe that the difference in temperature drift between the channels is about 10% of the total drift in one channel. This would bring the calculated system rotation error down to $\leqslant 2$ m rad.
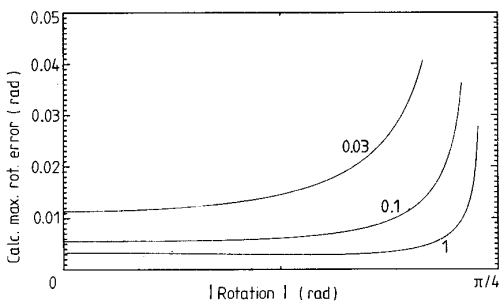
Figure 4. Calculated maximum rotation error. The parameter is the transmission of the measurement object.
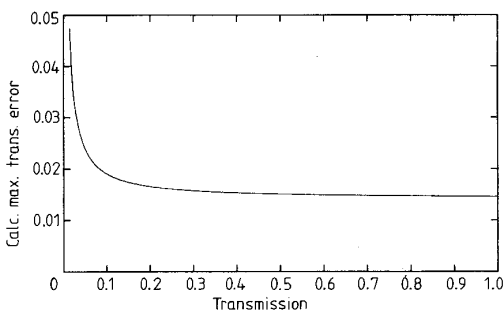
Figure 5. Calculated maximum relative transmission error.

6. Application examples

Figures 6–8 give some examples of how the measurement system can be used to study the magneto-optic properties of a YIG crystal. The crystal with the dimensions $2 \times 2 \times 2$ mm was inserted into the quartz holder depicted in figure 3 and a 200 μm
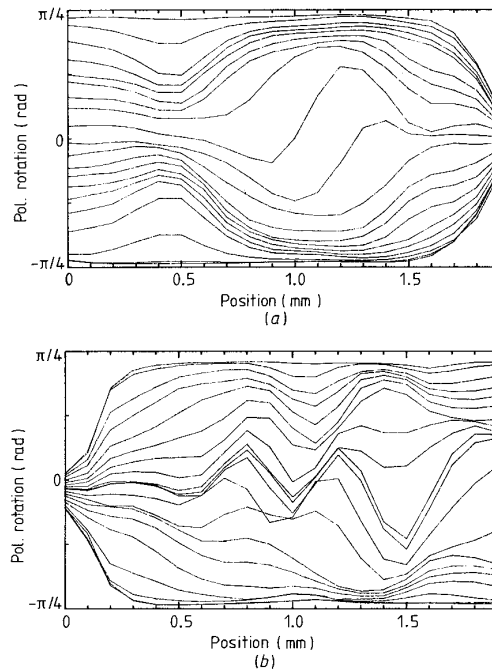
Figure 6. Line scan of rotation in 2 mm × 2 mm × 2 mm YIG cube. The parameter is the applied field which is varied from −50 mT to +50 mT in 20 steps. (a) and (b) are perpendicular scans on the same crystal side. Intersection point is at 1.15 mm in (a) and at 1.4 mm in (b). Polarisation fall off at end of scan is due to stray light not going through measurement object.
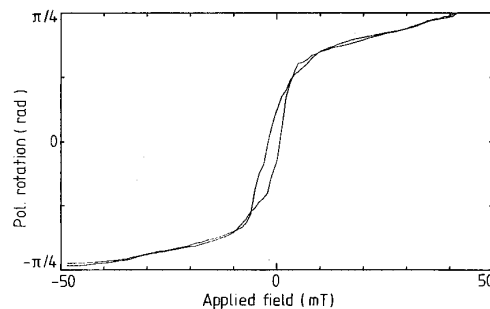
Figure 7. Rotation as function of applied field. Crystal as in figure 6.

diameter light beam is used to measure the Faraday rotation. In figures 6(a) and (b) the light beam makes line scans over one of the surfaces of the crystal. In figure 6(b) the scan direction is perpendicular to that in 6(a). Each curve in the two figures is the measured rotation of the polarisation plane ($\Delta\theta$) as a function of the light beam position, with 5 mT difference in applied magnetic field between adjacent curves.

From curves like those in figures 6(a) and (b) together with light transmission measurements and optical inspection the influence of inclusions, surface defects and edge effects on the magneto-optic behaviour can easily be found. For a more close study, curves describing the Faraday rotation as a function of the magnetic field can be plotted as in figure 7. Then hysteresis
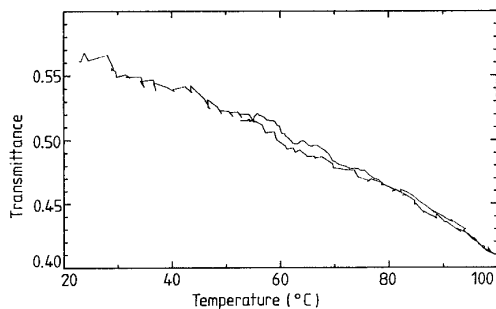
Figure 8. Transmission of YIG crystal in 17 mT applied field. Temperature ramp 30 °C → 100 °C → 50 °C. Crystal 2 mm × 2 mm × 2 mm.

effects and nonlinearities are easily identified. With the sample used in the examples, the maximum rotation unfortunately is near $\pi/4$, where the angle measurement error is great. Normally we are concerned with smaller rotations.

Finally, figure 8 shows the result of a light transmission measurement in one point when the crystal temperature is continuously increased from 30 °C to 100 °C. The decrease in transmission depends on the temperature shift of the absorption edge.

A more detailed description of the magneto-optic behaviour of YIG-crystals will be given in a later work on sensor material characterisation.

References

Berdennikova E V and Pisarev R V 1976 Sublattice contributions to the Faraday effect in rare earth garnets
Sov. Phys. Solid State **18** 45

Hague P S 1977 Techniques of measurement of the polarization-altering properties of linear optical systems
Proceedings of SPIE **112** *Optical Polarimetry* 2

Holm U and Sohlström H 1982 Magnetic field sensing using optical fibres
TRITA-ILA 82.04 (Stockholm: Instrumentation Laboratory, Royal Institute of Technology)

Holm U, Sohlström H and Brogårdh T 1983 Measurement system for magneto-optic sensor material characterization
TR 83.02 (Stockholm: Instrumentation Laboratory, Royal Institute of technology)

Massey G A, Erickson D C and Kadlec R A 1975 Electromagnetic field components: their measurement using linear electro-optic and magneto-optic effects
Appl. Opt. **14** 2712

Pisarev R V, Schoenes I and Wachter P 1977 High field magneto-optical study of yttrium iron garnet
Solid St. Commun. **23** 657

Stock K and Möstl K 1982 Einigung von Ge-Photoelementen für radiometrische Zwecke
Physikalisch Technische Bundesanstalt, Jahresbericht 1982, p 161 Braunschweig, West Germany

Toda H and Nahagawa Y 1980 Field dependence of the magneto-optical effect in YIG and GdIG
J. Phys. Soc. Japan **49** No 6 2191

Wettling W 1975 Magneto-optics of ferrites
J. Magn. Magn. Mater. **3** 147

Paper B

U. Holm, H. Sohlström and T. Brogårdh
"YIG-sensor design for fibre optical magnetic field measurement"
OFS 84, R. Th. Kersten and R. Kist, p. 333–336, VDE-Verlag, Berlin, 1984.

YIG-SENSOR DESIGN FOR FIBRE OPTICAL MAGNETIC FIELD MEASUREMENTS

Ulf Holm
Hans Sohlström
Torgny Brogårdh

Instrumentation Laboratory
Royal Institute of Technology, Stockholm

Abstract

Aiming at the design of a magnetic field sensor utilizing the Faraday effect, we give in this paper a description of measurements of magneto-optical properties of YIG. We also give sensor design rules based upon these measurements.

Introduction

Fiber optic sensors utilizing the Faraday effect for measuring current in high-voltage applications have been discussed for quite a long time [1,2]. One of many considerations is whether to use a sensor material which is magnetically linear but with low sensitivity, or a material with higher sensitivity but non-linear characteristics. As we are working towards a compact single-mode sensor system, with polarization-preserving optical fibers, and an integrated optic sensor element, we have chosen the latter alternative, with YIG ($Y_3Fe_5O_{12}$) as the sensor material.

To aquire knowledge of the influence of different parameters on the magneto-optical properties of YIG, and to optimize the sensor design, we have developed an equipment for measuring light polarization rotation and transmission as a function of magnetic field in two perpendicular directions and temperature under different conditions [3]. This paper gives a short description of this measurement system and a presentation of some of the most important experimental results, such as the influence of sensor dimensions, measuring beam size, sensor material treatment etc.

Measurement system

Polarized He-Ne laser light (1152 nm) is sent through a sample and is then split into two orthogonal polarization directions and focused onto two germanium photodetectors. The absolute accuracy in polarization angle determination is better than 0.5 mrad. Surrounding the sample are two sets of electromagnet coils and equipment to vary sample temperature. The sample is accurately moveable in the plane perpendicular to the laser beam. By varying the beam diameter, either the entire sample or selected spots down to 30 μm can be measured. All the instruments and actuators are connected to a desktop computer, which is controlling and logging the experiments.

Measurement results

YIG crystals grown by BTRL in England were used for all the experiments. Figure 1 shows the relationship between applied

field along the light beam and polarization rotation in a 2 mm
x 2 mm x 2 mm YIG cube as measured with a 0.2 mm diameter light
beam. The measurement was made on a cube cut from an inclusion
free part of the YIG crystal. Measurements made at different
locations on the sample and on other samples give similar
results, although the exact nature of the non-lineareties and
hysteresis differ. The measurement in fig 1 was made along the
(1,1,1) direction but no significant differences where found
between different crystal directions.

In order to release internal mechanical stress and to cure
lattice defects introduced by the sawing and polishing of the
sample it was annealed for 35 min at $1000^{O}C$ with a slow coo-
ling (~ 5 hours). This treatment had a significant effect.
Although there were still regions with large non-linearetics,
there were also areas of the crystal with much improved line-
arity, fig 2.

A completely linear behaviour was achieved with a bias field
perpendicular to the light beam. This can be explained by the
alignment of the magnetization of the entire sample to a common
direction from which it is then rotated linearly by the longi-
tudinal field. This method of linearization was not further
investigated since it was considered to give a complex sensor
construction. To gain better understanding of the magnetic
behaviour and possibly achieve a better linearity, without
using a bias field, YIG slices (1.4 mm x 1.4 mm x 0.3 mm) were
used for further experiments. Measurements were made along the
(1,1,1) crystal direction, perpendicular to the slice surface.
When the polarization rotation was measured with a 0.2 mm beam
diameter, the result was as in fig 3.

The reason for the better linearity in the measurements with
the thin sample in fig 3 than in those with the cubic sample
can be found in the magnetic domain behaviour. With the cubic
crystal domains are formed in a 3 D structure but with the
thin sample a more well defined 2 D structure with all domains
extending all the way through the sample is achieved. This can
be seen in fig 4 were a measuring light beam, narrow enough (30
μm) to resolve the individual domains, is scanned over the
sample.

With an external magnetic field the area balance between the
domains in the two directions is changed causing the average
rotation as measured with a larger beam diameter to change.
Thus, the size of the measurement area is important. Fig 5
shows the deviation from linearity as measured with 0.2 mm
and 2 mm beam diameters.

Besides the linearity we have investigated the temperature
dependence of the rotation and the sensitivity to fields per-
pendicular to the measured field. According to our measurements
the polarization rotation has a temperature coefficient of +
+ 0.1 %/^{O}C in the range [$20^{O}C$, $120^{O}C$]. Perpendicular fields, up
to 10 mT, influences the relationship between applied longitu-
dinal field and polarization rotation only to a small extent
(< 1% deviation from linearity). Fields above 10 mT causes much
larger deviations with non-linearities of 10% or more.

Sensor design considerations

The primary demand on a useful sensor is of course to give a reproducible and unambigous relationship between polarization rotation and applied field. Linearity is also desireable, though not necessary. From our measurments the following design rules can be concluded.

- The measuring light beam should be expanded to cover the entire crystal surface, to minimize the effects of single domain behaviour.

- The crystal should be annealed after cutting and polishing, to cure and release the mechanically induced lattice defects and tensions. It should be noted that the domain wall movements are obstructed by lattice defects as well as surface defects and both the crystal growth and the polishing should be done with care, to avoid such defects.

- The crystal geometry should be optimized considering the demands on high sensitivity (thicker crystal) and well-defined domain structure (thinner crystal). A way to combine these demands is a multilayer structure, or a light beam configuration utilizing multiple reflections. Other ways to increase sensitivity might be to change garnet composition and/or use light of shorter wavelength.

- The temperature dependence of the rotation can be electronically compensated for, using simultaneously measured temperature values. An alternative is to use another garnet composition [4].

- To reduce the influence of magnetic fields perpendicular to the measuring direction a magnetic circuit surrounding the sensor crystal can be used. It is of course also possible to measure and compensate for the perpendicular field.

Acknowledgement

References

1. A.J. Rogers: Proc. IEE, Vol. 120, No 2 p.261, February 1973
2. A. Papp, H. Harms: Applied Optics, Vol. 19, No 22 p. 3729, November 1980
3. U. Holm, H. Sohlström, T. Brogårdh: "Measurement system for Magneto-optic Sensor Materials", to be published in Journal of Physics E
4. Y. Tsujimoto, O. Kamade, T, Taniuchi, S. Serizawa: "Temperature stabilized fiber-optic magnetic-field sensors using mixed rare-earth garnet crystals", OFC '83.
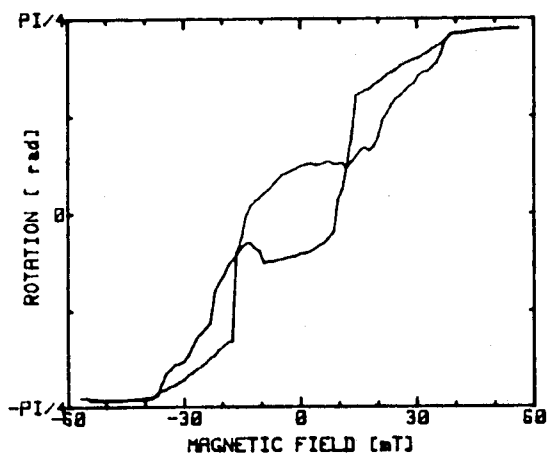
Fig.1 Polarization rotation in 2x2x2mm
       YIG cube
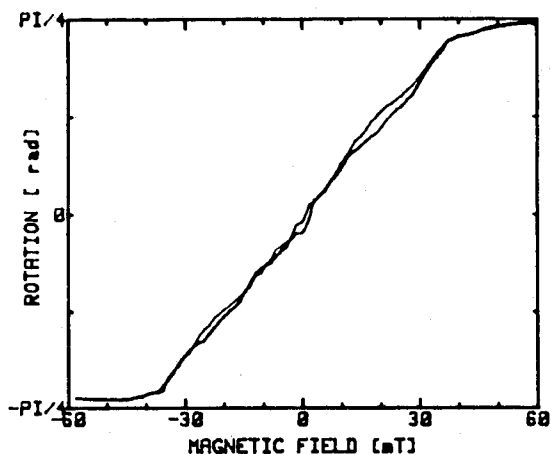
Fig.2 Polarization rotation in 2x2x2mm
       YIG cube, after annealing
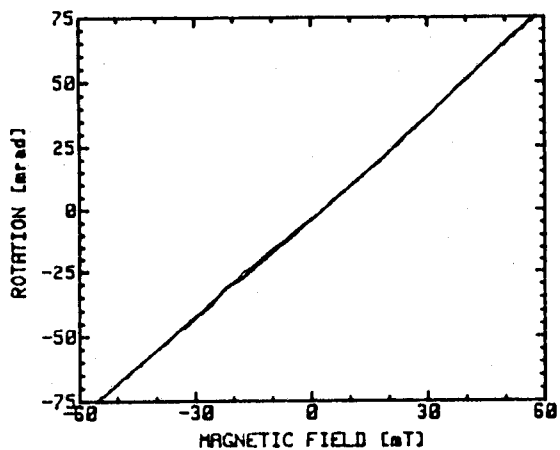
Fig.3 Polarization rotation in
       0.3x1.4x1.4mm YIG slice
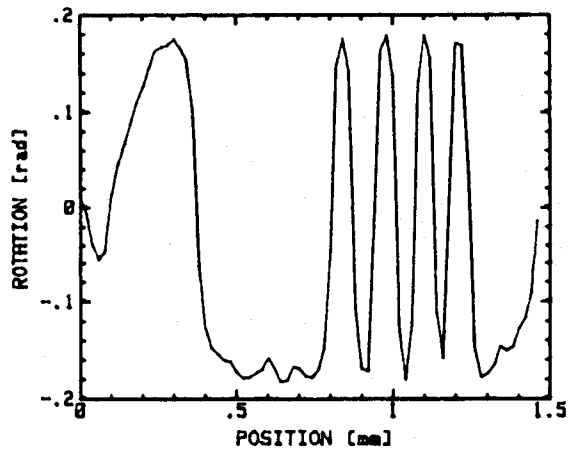
Fig.4 Polarization rotation measured with
       30 micron beam diameter, scanned
       over the YIG slice
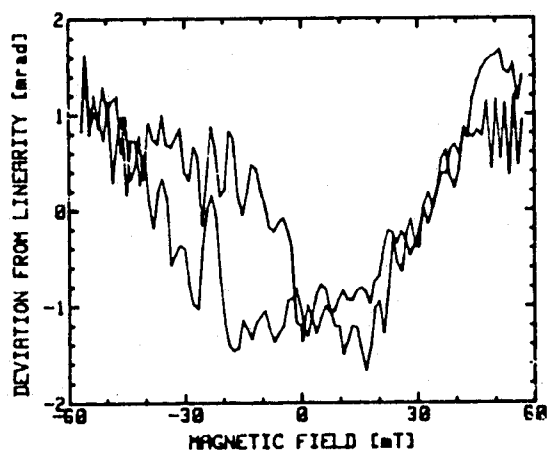
Fig.5a Deviation from linear relationship
        between applied field and polari-
        zation rotation in 0.3x1.4x1.4mm
        YIG slice, measured with 0.2 mm
        light beam diameter
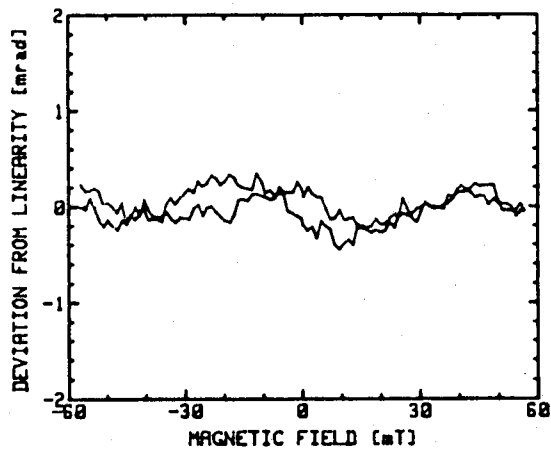
Fig.5b Similar to fig.5a but with
        2mm beam diameter

Paper C

U. Holm and H. Sohlström
Measurement of YIG crystal characteristics
for the design of optical magnetic field sensors
TR 84.01, Instrumentation Laboratory;
Royal Institute of Technology, Stockholm, 1984.

ABSTRACT

Measurements of the magneto-optic properties of YIG crystals, aiming at the design of fiber optic magnetic field sensors are presented. The Faraday polarization in YIG samples of different shapes, in applied fields −60 mT to +60 mT is given. Both measurements with sufficient spatial resolution to study single domains and averaging measurements are included. The effects of temperature, perpendicular fields and sample treatment is studied. With thin, 0.3 mm samples, the linearity of the relationship between applied field and polarization rotation is found to be good with deviations from linearity of less than 1%.

CONTENTS

1. INTRODUCTION

1.1 Fiber optic current measurement using the Faraday effect

Fiber optical sensors to measure various physical parameters have been developed [1]. The motives for this development are the high sensitivity attainable with some sensor types and the inherent insulating properties and immunity to electro-magnetic interference.

Fiber optic measurement of current is of interest in high voltage power transmission applications. It is accomplished through measurement of the magnetic field surrounding the conductor. Two different phenomena can be utilized for fiber optic magnetic field sensing [2], magnetostriction and the Faraday effect. Sensors based on magnetostriction are limited to very low field applications. For power line current sens-ing purposes the Faraday effect is used.

The Faraday effect is the fact that, when a linearly pola-rized light wave passes through a dielectric medium subjected to a longitudinal magnetic field, its plane of polarization is rotated. In dia- and paramagnetic materials, which are magnetically linear, the relation between applied field and rotation can be described by the Verdet constant.

$$\Delta\phi = V \cdot H \cdot l$$

$\Delta\phi$ = polarization rotation
V = Verdet constant
H = magnetic field strength
l = interaction length

The Verdet constant is small, typically Less than 10^{-5} rad/A. Larger polarization rotations can be achieved with ferri- or ferromagnetic materials, as will be discussed below. These materials are, however, not magnetically linear and cannot be described using the Verdet constant.

With a known input polarization plane, the amount of polarization rotation can be detected using a polarization splitting Wollaston prism and two photodetectors.

The first optical current measurement systems were developed as early as in the mid sixties [3]. In these flint glass rods were used as sensing devices. The free air transmission of laser beams used in these systems made them sensitive to, among other things, vibrations and weather conditions.

The development of usable optical fibers gave new possibilities. Monomode optical fibers can, to a limited extent, transmit linearly polarized light without depolarization. Furthermore, silica fibers exhibit Faraday effect. The fiber itself can therefore be used not only to transmit the light to the sensor but also as sensing device. As the Verdet constant is small in the fibers, typically $4 \cdot 10^{-6}$ A/m, the interaction length between magnetic field and light must be long in order to give a significant rotation [4].

An alternative approach is to use a sensor material with large Faraday rotation. Then the sensor can be small, adaptable for a number of applications, not only current measurement.

1.2 YIG

YIG, Yttrium Iron Garnet ($Y_3Fe_5O_{12}$), is a ferrimagnetic synthetic garnet with a significant Faraday effect. However, it has not been useful for fiber optic sensor applications until recently, since no reliable optoelectronic components have earlier been available in the wavelength range where YIG is transparent, above 1.1 μm. However, because of the interest in the 1.2 μm – 1.6 μm region for communications use, such components are now becoming available.

In YIG, just as in iron, magnetic domains are formed. In each domain, the magnetization is aligned in one direction and saturated. The size and form of the domains are determined by

energy relations between the magnetic energy and the energy
needed to form the domain walls.

The major applications for YIG are microwave components and
bubble memories. In bubble memories epitaxially grown YIG
films are used. Recently there has been an interest in the
use of YIG and YIG films in optical isolators and switches
[5].

Optical waveguides can be formed in YIG films. The concept of
a magnetic field sensor in the form of a single mode YIG
waveguide is interesting. Such a sensor can, combined with
polarization preserving monomode fibers, form a polarization
modulating measurement system with interesting properties.

1.3   A project to study YIG and YIG waveguides

YIG waveguide sensors and more conventional bulk YIG sensors
are studied in a joint research project at the Instrumenta-
tion Laboratory of the Royal Institute of Technology, the
Institute of Optical Research and the Microwave Institute,
all in Stockholm. The project is supported by the National
Swedish Board for Technical Development.

For sensor use, the properties of YIG in low applied fields
are of interest, rather than those of YIG, uniformly satura-
ted by large applied fields, which has been the subject of
most reports published [1]. The detailed knowledge of the
behaviour of YIG in low applied fields, needed to evaluate
the idea of, and to design a YIG sensor, made extensive
measurements necessary. The effect of crystal orientation,
sample geometry, sample treatment, temperature and magnetic
fields perpendicular to the measuring direction had to be
investigated. From the first preliminary measurements, made
in cooperation with the Institute of Optical research, it was
clear that the magnetic domain structure of the material was
a key parameter.

A major problem in our studies has been shortage of YIG samples. Long delivery times have caused considerable delay. Our measurements have been made on samples cut from a very limited number of crystals but, as the characteristics of all our samples have been similar, we believe that they are typical. The report describes the studies of the characteristics of YIG crystals, aiming at sensor development, made at the Instrumentation Laboratory of the Royal Institute of Technology. Some sensor design suggestions based on the measurement results are also given.

2.   MEASUREMENTS

2.1   Measurement equipment

A measurement system for magneto-optical sensor characterization has been developed [6]. The features of the system are:

- Arrangement for the determination of the rotation of light polarization in a sample as a function of applied field [-60 mT, 60 mT] and temperature [20°C, 120°C]. Accuracy is better than 0.5 mrad.

- Arrangement for the determination of sample transmission. Accuracy better than 2%.

- Variable measuring light beam diameter and precision sample position control. This makes it possible both to scan the light beam over the sample and to integrate the measurements over a desired area.

- Computer logging and controlling of measurements. This gives both increased number of measurement and increased accuracy due to automatic calibration routines.

In the system, polarised 1152 nm He-Ne laser light is sent through the sample and is split into two orthogonal directions of polarization (±45° to the polarization incident on

the sample.) These two light beams are detected by germanium photodiodes. The signals are transferred to the computer where the polarization rotation is calculated. For the transmission measurements, a small fraction of the light is deflected before the sample, to give a reference level of incident light intensity.

1.2   Measurements

All of the presented measurements were made upon samples cut from a YIG crystal that was supplied by Dr E.A.D. White at the British Telecom Research Lab. in England. Comparative measurements on cubic crystals from other suppliers give similar results. The results of the following measurements will be discussed.

a) Polarization rotation as function of applied magnetic field parallel to the light beam in a 2 mm x 2 mm x 2 mm sample. Beam diameter 200 μm.

b) Same as a) but with the sample saturated by a magnetic field perpendicular to the light beam.

c) Same as a) after annealing of the sample.

d) Polarization rotation on different locations of a sample with the dimensions 0.3 mm x 1.4 mm x 1.4 mm. Beam diameter 30 μm. Light beam perpendicular to the slice.

e) Same as d) at different temperatures.

f) Same as d) at different perpendicular magnetic fields.

g) Polarisation rotation as function of applied magnetic field parallel to the light beam, with different beam diameters. Same sample and orientation as in d).

3.   MEASUREMENT RESULTS AND INTERPRETATIONS

3.1   Sample preparation

From the raw crystal, approximately 1 cm in diameter, grown by slow-cooling technique, a 2 mm thick slice was cut, normal to the (1,1,1) crystal direction. This slice was visually inspected by means of a TV-system (fig. 1).

Fig. 1   2 mm YIG slice cut from crystal. Dark area at the edge is the unpolished outside of the crystal. Dark spots inside the area illuminated from the rear are inclusions.

Several large inclusions and surface defects can be seen. 2 x 2 x 2 mm samples were then cut from the inclusion-free parts and polished to optical quality. Some of these cubes were later cut into 0.35 x 2 x 2 mm and again polished. In the same way 0.3 x 1.4 x 1.4 mm samples were prepared.

3.2   Measurements on 2 x 2 x 2 mm YIG cues

3.2.1 Polarization rotation in cut and polished samples

Our first measurements were made on the YIG cubes with a
measuring beam diameter of 200 μm (fig. 2).
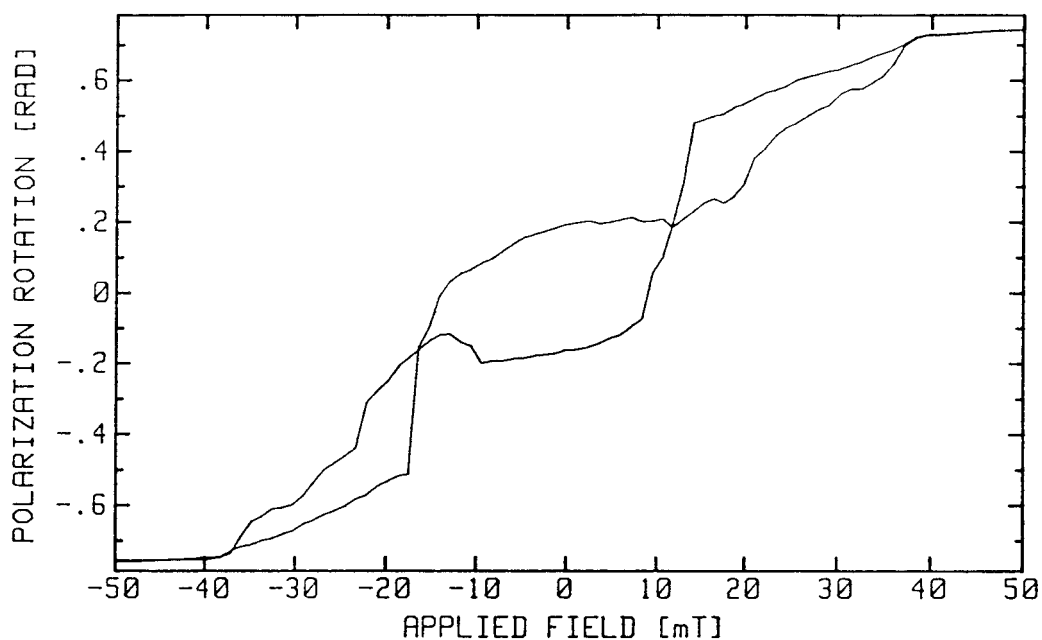
Fig. 2   Polarization rotation as function of applied field in
          2 x 2 x 2 mm cube. Measured parallel with (1.1.1)
          direction. Measurement area diameter 200 μm.

All measurements on cubic samples with this beam diameter
give similar results, even though the exact shape of the
non-linearities and hysteresis differ quite a lot. The shape
of the curves are also quite different when measured on
points close to each other on the same sample. We attribute
these results to the existence of a complicated 3-D magnetic
domain structure. The applied field causes the domain walls
to move, but this movement is somewhat obstructed by defects
and irregularities in the crystal structure, and is thus not
homogeneous throughout the sample. As the light beam only
covers a small fraction of the sample, great non-linearities
will be detected.

3.2.2 Effects of a perpendicular magnetic field

One way to reduce the non-linearities should be to saturate the sample with a magnetic field perpendicular to the measuring direction. This aligns all magnetic dipoles in one direction and the domain structure vanishes. When the measuring field is applied, this causes just a small rotation of the aligned dipoles, not a domain wall movement, and this rotation should be a linear function of the applied field. Our measurements indicate a completely linear relationship, clearly confirming theory. As we do not consider a magnetic bias field desirable in a magnetic field sensor, we tried other ways to linearize the characteristics.

3.2.3 Effects of annealing

To verify the assumption that some of the non-linearities were caused by lattice defects, possibly introduced by the cutting and polishing procedure, one crystal sample was annealed. That is, it was heated to 1000 C for 35 minutes and it was then cooled slowly. The effect of this treatment was a greatly improved linearity and less hysteresis (fig. 3).
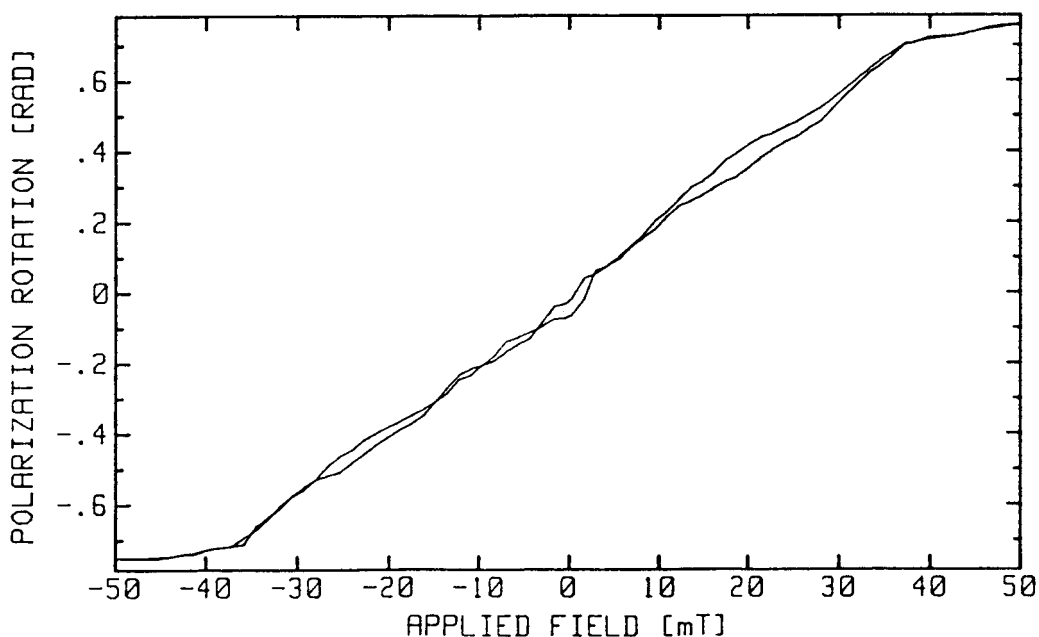
Fig. 2   Polarization rotation in 2 x 2 x 2 mm cube after annealing.

3.3   Measurements on 0.3 x 1.4 x 1.4 mm YIG slice

3.3.1 Effects of sample size

To achieve a more welldefined 2-D domain structure and possibly increased linearity other sample geometries were tried. By decreasing the size of the cubic samples in one dimension, we found that samples with a thickness of about 0.3 mm or less have domains that reaches through the whole sample with domain walls only perpendicular to the slice surface.

Fig.   4 YIG slice viewed through crossed polarizers

Fig. 4 shows a picture of such a sample viewed through crossed polarizers. When a magnetic field is applied perpendicular to this slice, we will get just a change in the area ratio of domains with magnetization parallel and antiparallel to the applied field.

This mechanism was expected to give a more linear relationship. The assumption is clearly confirmed by the curve in fig. 5.
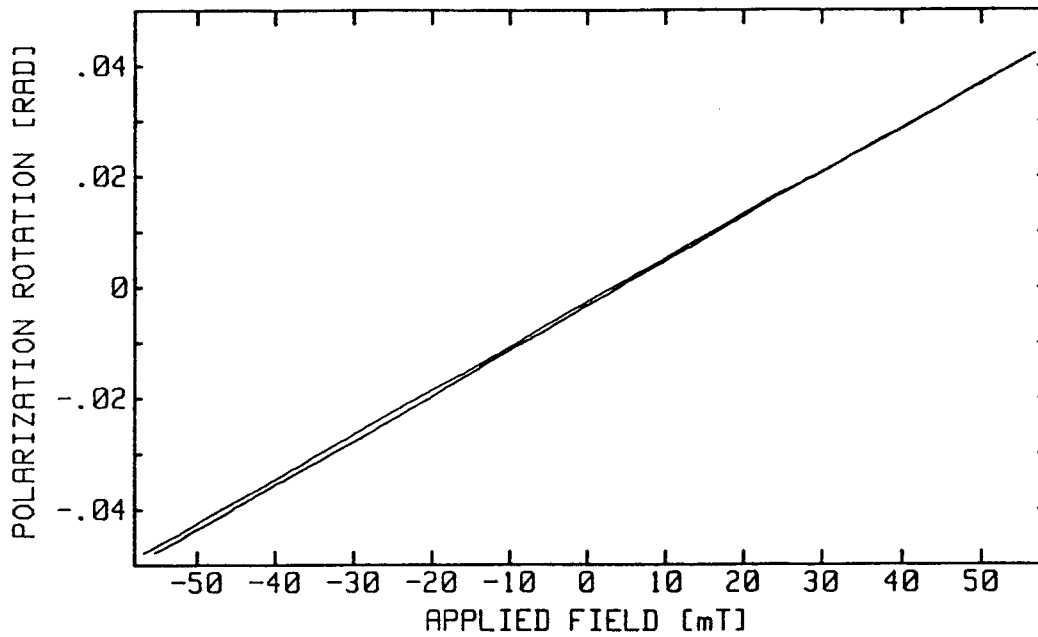
Fig. 5   Polarization rotation in 0.3 x 1.4 x 1.4 mm YIG slice.
          Measured parallel with (1.1.1) direction, perpendicu-
          lar to slice with 300 μm diameter light beam

3.3.2   Measurements of the domain structure

To get a quantitative measure of the domain structure, the
beam was made as small as possible, 30 μm diameter. This beam
was then scanned along a straight line across a sample then
giving the result shown in fig 6. No external field is
applied. The application of such a field will, as predicted,
cause a movement of the domain walls, so as to increase the
area of the parallel domains and decrease the area of the
antiparallel ones (fig. 7).
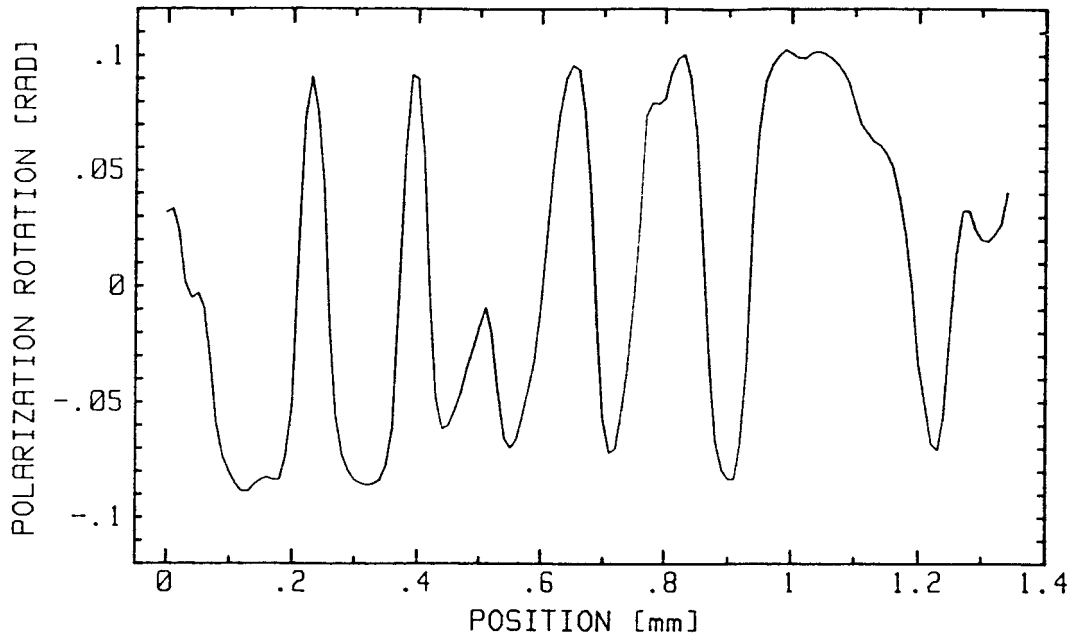
Fig. 6   High resolution measurement of polarization rotation
          in YIG slice
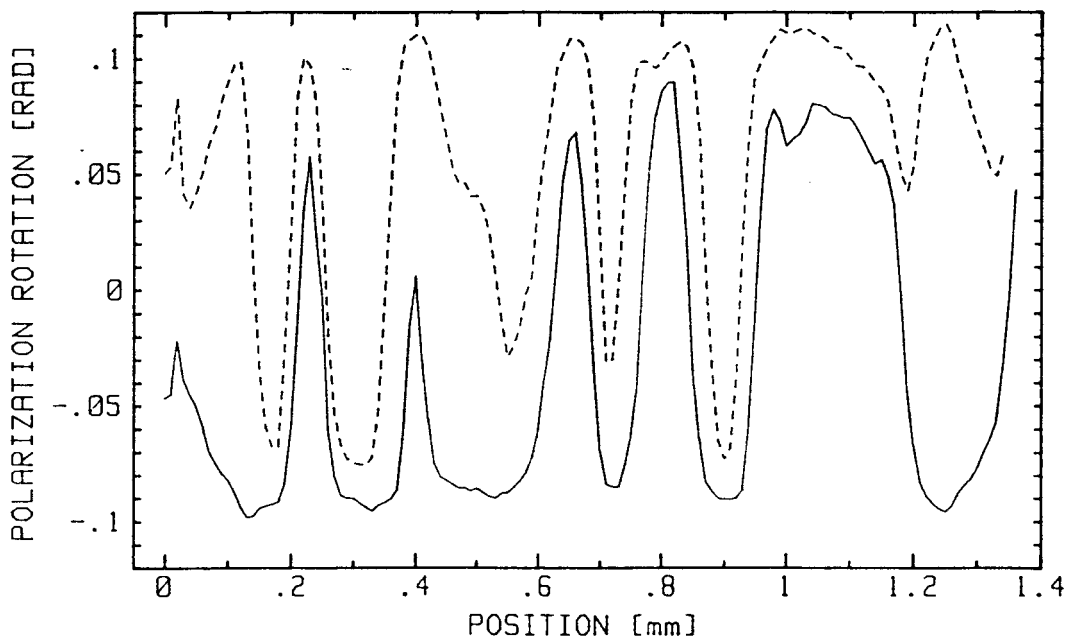
Fig. 7   Domain structure in YIG slice at +50 mT (dotted line)
          and -58 mT (solid line) applied field

Simultaneously one can observe an apparent change of the
rotation within the domains. This is however, we believe,
caused by the fact that not all of the power in the light
beam lies within 30 μm diameter, but only 90%. The rest of
the optical power reaches much further, even covers neigh-
bouring domains. Thus a change of the domain width will
change also the measured rotation in the center of a domain.

3.3.3 Effects of temperature changes on the domain structure
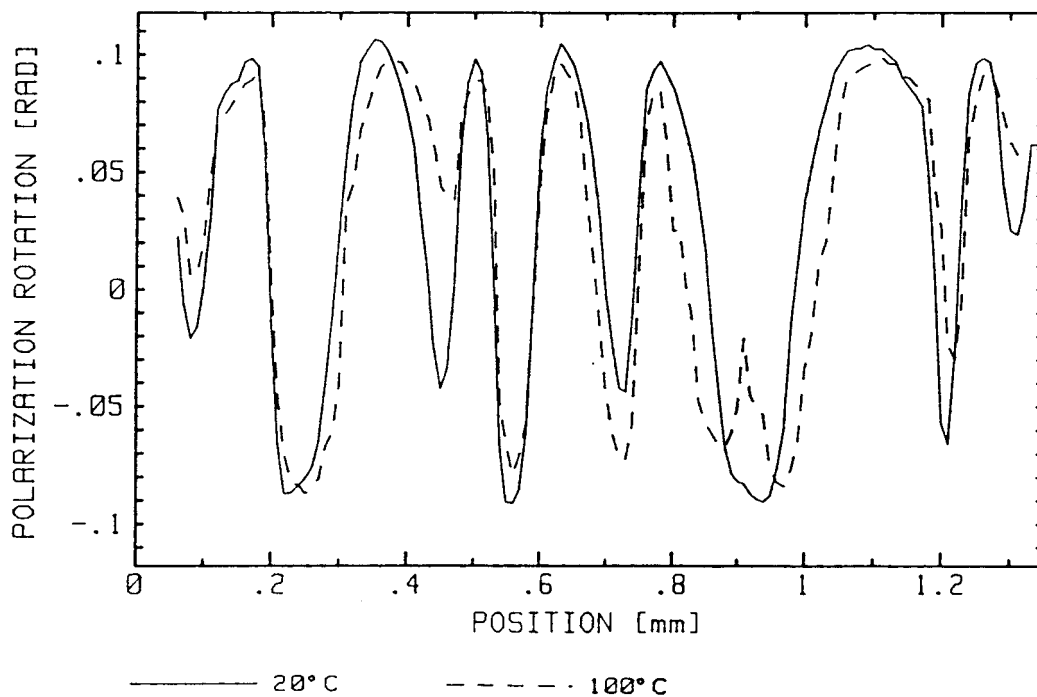
Fig. 8   Domain structure at 20°C and 100°C. Applied field
          33 mT

Fig. 8 shows the domain structure at two different tempera-
tures. It can be seen that both the rotation within the
domains and the domain pattern differs. It is quite clear
that the rotation in each domain is smaller at the higher
temperature. However, measurements of polarization versus
magnetic field shows that the sensitivity $\left(\frac{d\theta_{meas}}{dH}\right)$

increases by typically 0.1%/°C at higher temperatures when a large beam diameter is used, fig. 9. These seemingly contradictory results are in agreement with other published work.
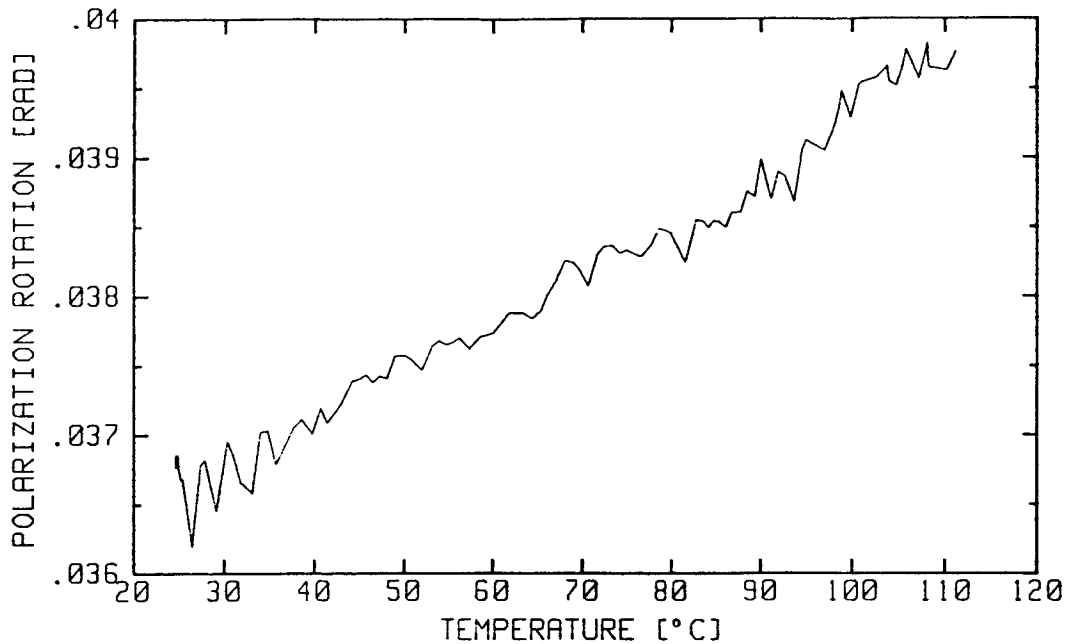
Fig. 9   Temperature dependence of polarization rotation as measured with a 3 mm beam. Applied field 40 mT

In ref [7] the polarization rotation in a saturated sample, corresponding to the rotation in the domains, is shown to decrease with increasing temperature in the interval studied here.

In ref [8] the measured polarization rotation sensitivity to magnetic field is shown to increase at higher temperature. (It is worth noting that his sensitivity in many works are referred to as "the Verdet constant", which is correct only in linear magnetic materials, and not in those in which domains are formed.)

We can at present not explain this increasing sensitivity at increasing temperature. It is worth further studies though, as there must be two mechanisms working in opposite directions, and there might be a way to make these of equal magnitude and in that way yet an internal temperature compensation.

3.3.4   Influence of a perpendicular magnetic field on the
        domain structure

When a perpendicular magnetic field is applied, strong enough
to magnetically saturate the sample, the domain structure
will vanish, as pointed out before. As can be seen in fig.
10, this aligning of the magnetic dipoles is a continuos,
though quite non-linear process, where both domain wall move-
ments and tilting of the dipoles in the domains occur.

PERPENDICULAR FIELD

————————— 0 mT   ——·——·· 14 mT

— — — — · 8 mT   ——··——··· 38 mT

—— ——— · 11 mT
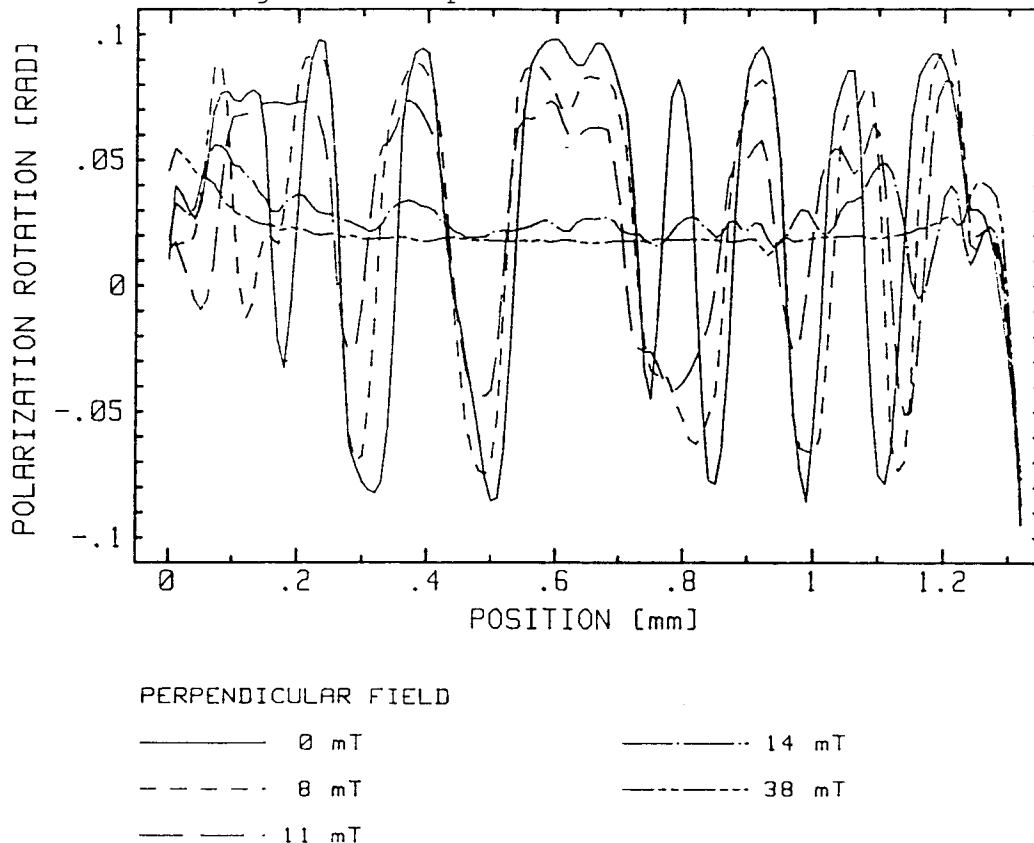
Fig. 10   Domain structure in YIG slice subjected to different
          perpendicular (in the plane of the slice) fields

Fig. 11 might be of help in clarifying the process. Here the
polarization rotation is measured in the plane of a slice
instead of perpendicular to the surface and the applied field
is also in this direction. A slightly bigger sample 0.35 x 2
x 2 mm is used. The non-linear alignment is obvious, small
fields cause very small deviations of the dipoles from the
direction perpendicular to the surface. Then at a certain
level of the field, about 10 mT, a very small increase in the
field causes all the dipoles to lay down in the plane.
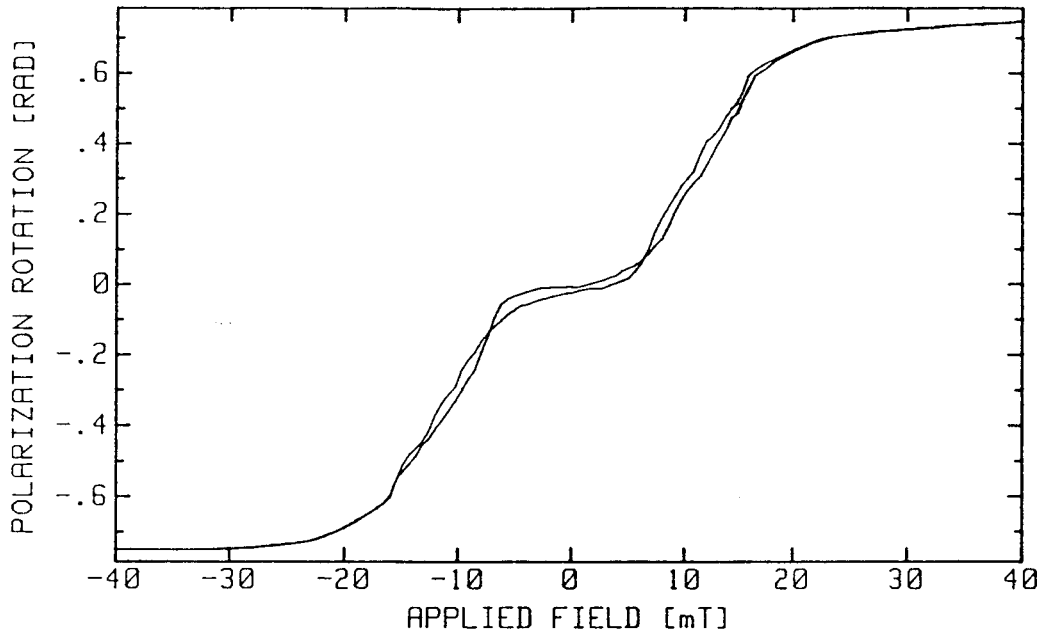
Fig. 11   Polarization rotation measured in the slice plane
           perpendicular to the (1.1.1) direction. Slice dimen-
           sions 0.35 x 2 x 2 mm

3.3.5 Polarization rotation versus magnetic field measured
with different beam diameters

It is quite obvious that also in the 2-D domain structure the
domain wall movements are influenced by defects in the sample
structure. The area change of one domain in an arbitrary
point is therefore not a linear function of the applied
field. Fig. 12 serves as an example. In that measurement a
30 μm diameter beam is centered on a domain wall when no
field is applied. As can be seen, the domain wall movement
in a single point exhibits similar characteristics as those
measured with larger beam diameter in the cubic sample. But
contrary to the cubic samples, the slice gives a quite linear
relationship with beam diameters as small as 200 μm.

Fig. 13 shows deviations from linearity in measurements with
0.2 mm and 2 mm beam diameters.
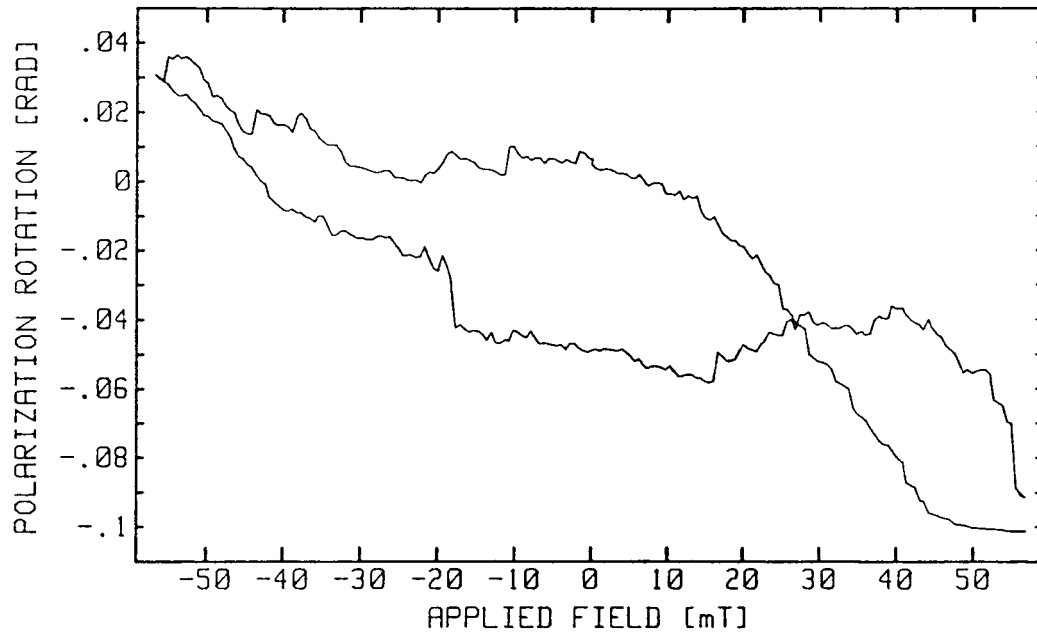
Fig. 12   Polarization rotation measured on small area of
          slice, including a domain wall
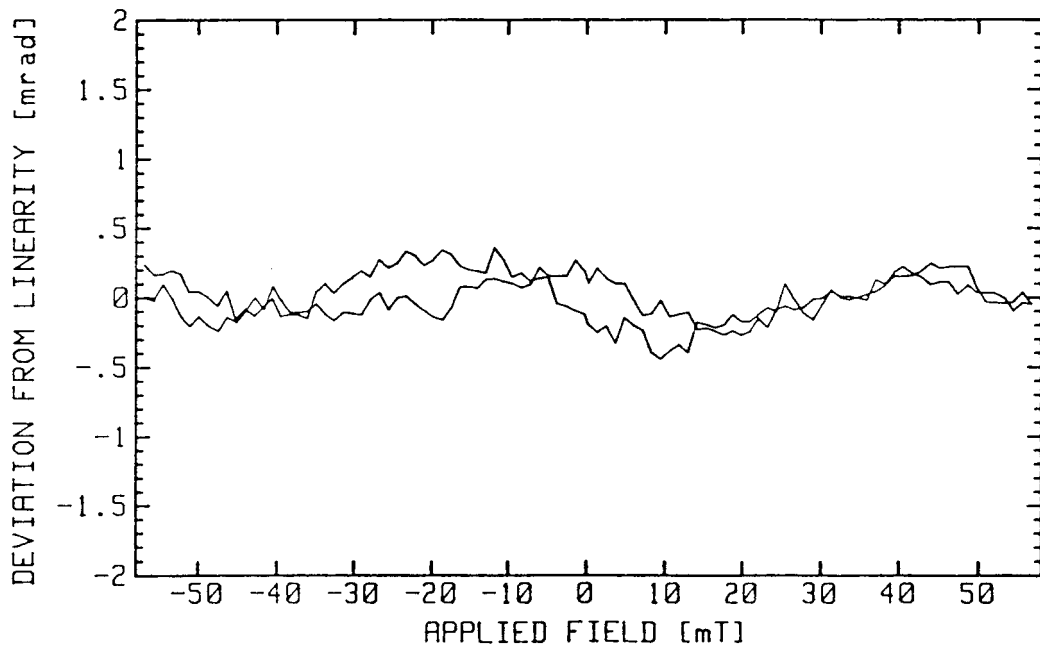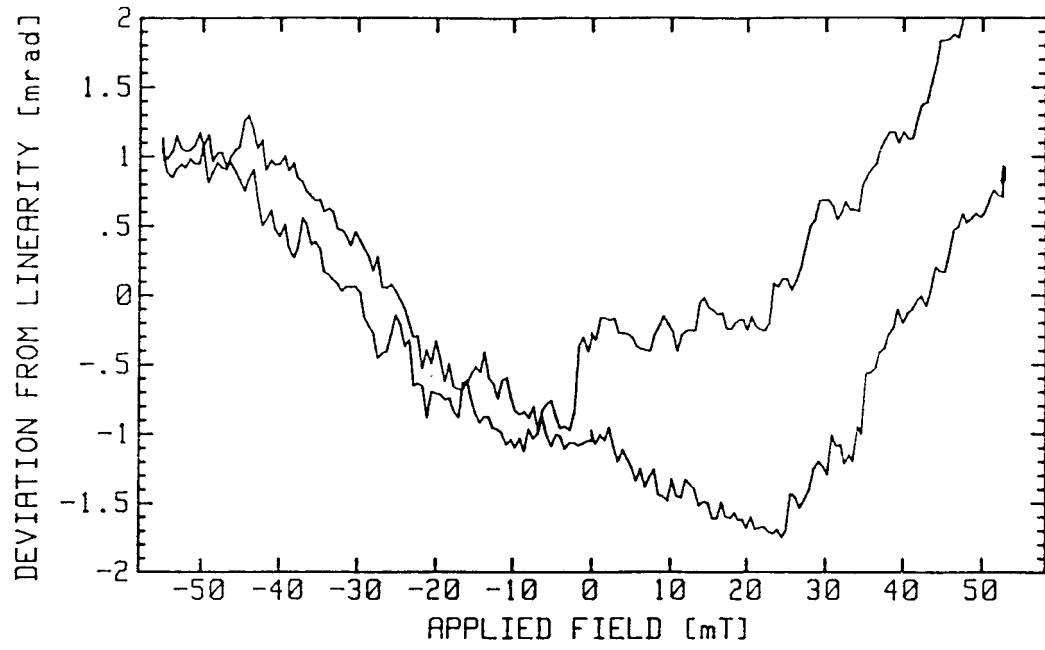
Fig. 13   Deviations from linearity in polarization rotation-
field relationship in 0.3 mm YIG slice, as measured
with 0.2 mm and 2 mm diameter beams

4.   SENSOR DESIGN

4.1   General

Our quantitative and qualitative studies of YIG-crystals give
guidelines for the design of a fiber optic magnetic field
sensor. In the following we will thus discuss how to achieve
a YIG sensor element with as good performance as possible
concerning hysteresis, linearity, temperature, sensitivity and
stray field sensitivity.

Parameters as accuracy and bandwidth are not dealt with since
these are closely related to the performance of the optoelec-
tronic system connected to the YIG-sensor and not to the

4.2   Reproducibility and linearity

The hysteresis in the relation between applied magnetic field
and rotation of polarization must be minimized, as this sets
a limit on the minimum detectable field. Our measurements
indicate the following design rules for this purpose:

• Use crystals grown by a technique that gives as few lat-
  tice defects as possible.

• Perform the cutting and polishing of the crystals with
  care, not to introduce unnecessary stress and defects.

• Anneal the crystals after the mechanical treatment.

• Cut the sensor crystal into a slice, not thicker than 300 μm,
  to get a two-dimensional domain pattern, which in our
  measurements gives least hysteresis.

• Use a light beam for measuring the rotation of polariza-
  tion that covers as much of the slice as possible and that
  certainly not has a diameter less than 300 μm.

The linearity of the relation between polarization rotation
and applied magnetic field is limited in two ways. First by

the irregularities of the same kind as those causing hysteresis as discussed above. These non-linearities are of course diminished in the same way as the hysteresis effects. Secondly, the linearity is also limited by magnetic saturation of the crystal. The value of the saturating magnetic field depends on the geometric shape of the crystal. The slices used in our measurements will saturate when the applied field is about 150 mT. If stronger fields are to be measured, the strength of the field of the crystal may be lessened by a magnetic circuit.

4.3   Temperature dependence

As pointed out previously the temperature dependence seems to consist of two counteracting parts. The rotation within the domains decreases when the temperature increases, which should give a decreasing measured rotation. However, the measured rotation increases when the temperature increases. Though we have not further investigated this yet, there might be ways to change the relative magnitude of these two king them equal and thereby get a temperature independent sensor.

However, as the temperature dependence is quite small, 0.1%/°C in our measurements, it is also possible to make a sensor equipped with a fiber-optic temperature sensor and make an electronic temperature compensation.

4.3   Stray field sensitivity

We have shown that the sensitivity to perpendicular fields is quite non-linear. Perpendicular fields smaller than 10 mT cause small errors <1%, while fields extending 10 mT rapidly cause errors of 10% and more. If the sensor will be exposed to perpendicular fields strong enough to give an unacceptable error, there are two possible ways to handle this. One is to use a magnetic circuit preventing the perpendicular fields from reaching the sensor. Another way is of course to measure

the fields in three directions and electronically compensate
for the influence of the stray fields.

REFERENCES

[1]   T.G. Giallorenzi, J.A. Bucaro, A. Dandridge, G.H.
        Siegel Jr, J.H. Cole, S.C. Rasleigh and R.G. Priest:
        Optical Fiber Sensor Technology.
        IEE Journal of Quanturn Electronics, vol QE-18, no 4,
        p 626, April 1982.

[2]   U. Holm and H. Sohlstrom: Magnetic Field Sensing Using
        Optical Fibers.
        TRITA-ILA 82-04, Instrumentation Laboratory, Royal
        Institute of Technology, Stockholm.

[3]   M.N. Rzewuski and M.Z. Tarnawecky: Unconventional
        Methods of Current Detection and Measurernent in EHV
        and VHV Transmission Systems.
        IEEE Transactions on Instrumentation and Measurement,
        vol IM-24, no 1, p 43, March 1975.

[4]   A. Papp, H. Harms, H. Aulich, W. Beck, N. Douglas and
        H. Schneider: Magnetooptical current transformer.
        Applied Optics, vol 19, no 22, p 3729, November 1980.

[5]   A. Shibukawa and M. Kobayshi: Optical TE-TM mode con-
        version in double epitaxial garnet waveguide.
        Applied Optics, vol 20, no 14, p 2444, July 1981.

[6]   U. Holm, H. Sohlstrom and T. Brogardh: Measurement
        System for Magneto-Optic Sensor amterials.
        To be published in Journal of Physics E.

[7]   E.V. Berdennikova and R.V. Pisarev: Sublattice con-
        tributions to the Faraday effect in rare earth iron
        garnets.
        Sovjet Physics Solid State, vol 18, no 1, p 45,
        January 1976

[8]   Y. Tsujimoto, O. Kamada, T. Taniucli and S. Serizava:
        Temperature stabilized fiber-optic magnetic-field
        sensors using mixed rare earth garnet crystals.
        OFC -83, New Orleans

[8]   Y. Tsujimoto, O. Kamada, T. Taniucli and S. Serizava:
        Temperature stabilized fiber-optic magnetic-field
        sensors using mixed rare earth garnet crystals.
        OFC -83, New Orleans

Paper D

H. Sohlström, U. Holm and K. Svantesson
"A Polarization Based Fibre Optical Sensor System
Using a YIG Optical Waveguide for Magnetic Field Sensing"
Springer proceedings in Physics 44: Optical Fiber Sensors, H. J. Arditty,
J. P. Dakin, and R. Th. Kersten, p. 273–278, Springer-Verlag, Berlin, 1989.

A Polarization-Based Fibre Optical Sensor System Using a YIG Optical Waveguide for Magnetic Field Sensing

H. Sohlström[1], U. Holm[1], and K. Svantesson[2]

[1]Royal Institute of Technology, Instrumentation Laboratory,
P.O. Box 70013, S-10044 Stockholm, Sweden
[2]Swedish Institute of Microelectronics, P.O. Box 1084,
S-16421 Kista, Sweden

A sensor system utilizing a polarization maintaining fibre for the optical signal transmission and a planar optical waveguide for magnetic field measurements is presented. The system is based on polarization modulation originating from the TE to TM mode conversion in a magneto-optical thin film of Gd,Ga substituted YIG (Yttrium Iron Garnet).

Introduction

In a fibre optical sensor system based upon amplitude modulation one generally wants a separate reference channel. By using this reference one may in principle correct for signal transmission perturbations, assuming that such influences are common to both the signal and the reference channel.

In this paper we describe a measurement system where one polarization maintaining fibre alone provides the two transmission channels. The two eigenmodes of the fibre propagate practically independently of each other and are to a great extent equally affected by environmental conditions. Furthermore the sum of the light intensities of the two modes serves as a normalization quantity when evaluating the signal from the sensor element.

Sensing Principle

The magnetic field sensing is based upon the Faraday effect in a garnet thin film, YIG (Yttrium Iron Garnet), epitaxially grown on a GGG (Gadolinium Gallium Garnet) substrate. The waveguiding sensing element can, in contrast to the bulk YIG crystal sensors previously described,[1] efficiently be coupled to a polarization maintaining fibre.

In a waveguide, the Faraday effect can be described as a circular birefringence that is dependent on the magnetic field in the light propagation direction. This birefringence causes a coupling between the TE and TM modes of the same order. The transfer of power follows the expression

$$F = \left[1+\left(\frac{\Delta\beta}{2\theta}\right)^2 \right]^{-1} \sin^2\left\{ \left[\theta^2 + \left(\frac{\Delta\beta}{2}\right)^2 \right]^{\frac{1}{2}} \cdot z \right\} \tag{1}$$

where F is the fraction of power in the mode not excited at the input, $\Delta\beta$ is the linear birefringence, θ is the circular birefringence and z is the travelled distance.

If $\Delta\beta$ is zero the modes propagate synchronously and a complete transfer of power is possible. This is in effect a rotation of the polarization direction just as in the bulk case.

In the systems presented here, light is launched into one of the polarization modes of the planar waveguide. During the propagation there is a transfer of power into the other mode due to the Faraday effect. This gives a power distribution between the modes which is magnetic field dependent. The light is then coupled into the return fibre, which is oriented in such a way that each of the modes of the planar guide is coupled into one of the corresponding fibre polarization modes. At the output end of the fibre, the light from the two fibre modes is separated and detected. The detector outputs P_1 and P_2 are then combined to give the intensity independent signal S which is a measure of the magnetic field:

$$S = \frac{P_2}{P_1+P_2} \qquad (2)$$

Below we present two sensor configurations, one transmissive and one reflective. In the reflective configuration the same fibre is used to carry the light both to and from the sensing element.

To be able to understand the behaviour of the sensor one has to consider the magnetic properties of the garnet materials used in this work. Ferrimagnetic materials such as YIG exhibit a spontaneous magnetization in the form of a magnetic domain structure. In the absence of an external field these domains are oriented in such a way that the total magnetization of the material vanishes. If an external magnetic field is applied, the domains will change their distribution, size and shape. The circular birefringence, which is proportional to the magnetization parallel to the light propagation, will in general not have a useful relation to the applied field.

A sufficiently large external field will align all domains into a single domain. A varying field together with such a bias field gives a uniform change in the orientation of the magnetization and thus in the Faraday rotation. This is the approach used here[2]. A similar result can be achieved without a bias field with materials that have a strong magnetic anisotropy.

System Realization

TRANSMISSIVE SENSOR
The transmissive sensor configuration is shown in fig 1. A polarization maintaining fibre was used to send polarized light to the sensing element. Since the fibre core diameter and the YIG film thickness were approximately the same it was possible to couple a large fraction of the light from the fibre into the zero order TE mode of the film, which allowed 16 modes. For a correctly positioned fibre we could observe less than 3 % of the total power in mode 2, less than 1 % in mode 4 and no significant amount in any other mode.

At the opposite edge of the film, the light from the TE and TM film modes was coupled into the two polarization modes of a second polarization maintaining fibre. As the coupling between the
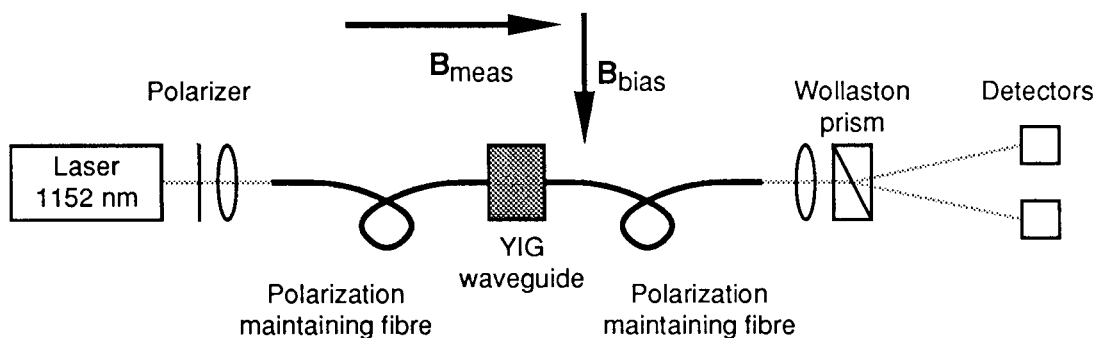
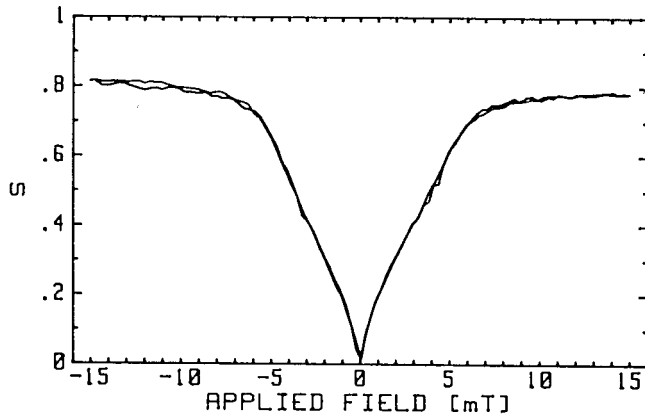Fig 1. The transmission sensor set-up. The waveguide is 4 mm long and 6.7 μm thick.

Fig 2. System output S versus B_{meas} with a sensor according to fig 1 and a bias field of 3 mT.

modes in the fibre is negligible, their power ratio remaind practically unchanged throughout the fibre length. The light from the two fibre modes was geometrically separated by a Wollaston prism and detected by two germanium photodiodes.

As the light was not laterally confined in the waveguide, only a rather small fraction was coupled into the second fibre. Results from measurements with the transmissive sensor are shown in fig 2.

REFLECTIVE SENSOR

To be able to collect a large fraction of the light some kind of focusing optics had to be introduced. Also, from a practical point of view, it would be advantageous if the fibres were attached on the same side of the sensing element, or even better, if only one fibre could be used.

These objectives were met by the one-fibre system in fig 3. The same polarization maintaining fibre was used to carry the light to and from the sensing element, which is shown in greater detail in fig 4. The rear edge of the sensing element, which was polished into a semi-circular shape and gold coated, focused the light back into the fibre. Due to the nonreciprocity of the Faraday effect, the effective interaction distance will be twice the radius.

Power that is reflected from other points in the system than the rear edge of the waveguide may cause interference problems. To reduce some of the critical reflections, the input end of the
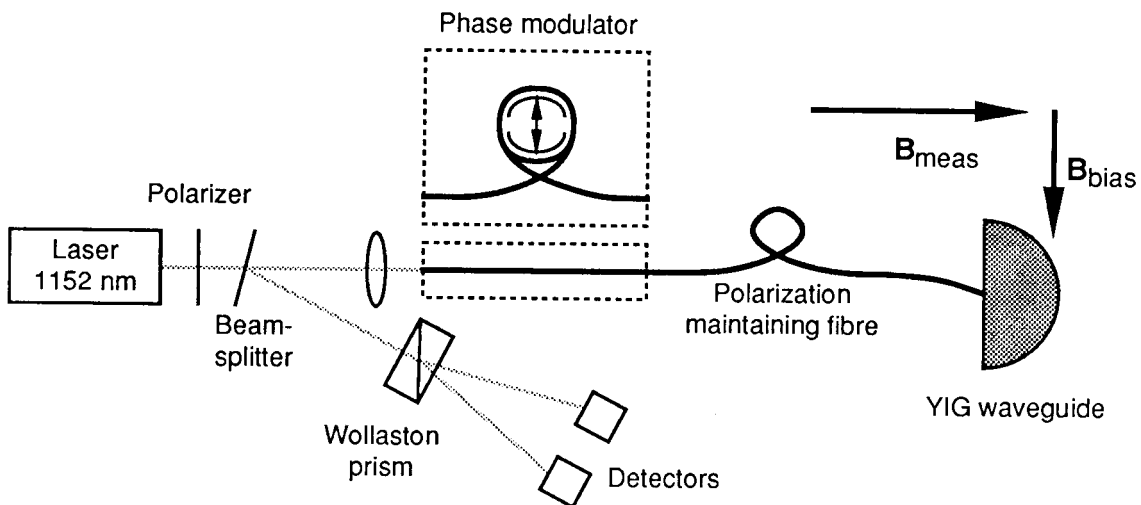
Fig 3. The reflective sensor set-up. For the results presented below, 2 m of Furukawa polarization maintaining fibre for 1.3 µm was used. The use of phase modulation is described in the text.

275
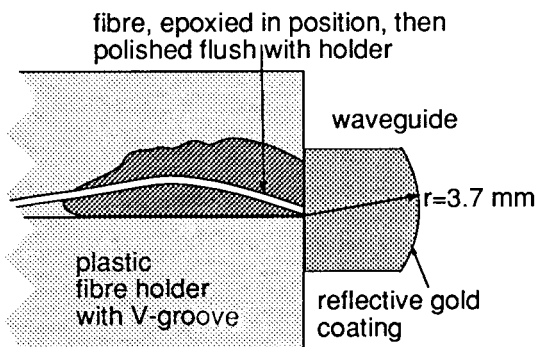
Fig 4. Experimental reflective sensor. Waveguide as in fig 1.
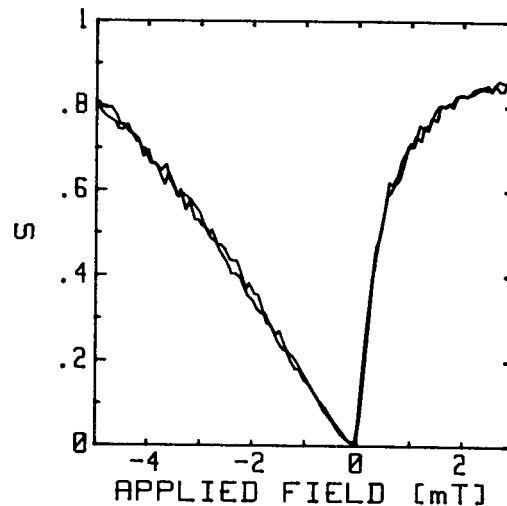
Fig 5. System output when the applied field was varied from -6 mT to +4 mT and back in two cycles. A bias field of 3 mT was applied perpendicular to the measured field. 1.15 μm HeNe laser light and no phase modulation.

fibre was polished with its surface normal 6° off the fibre axis and the fibre was attached to the waveguide at an angle in the waveguide plane.

When the sensor was subjected to a magnetic field varying from -6 mT to +4 mT along the sensor axis the system output S varied as shown in fig 5. A bias of 3 mT was applied perpendicular to the measured field. The nonlinearity of the curve is due to the magnetic properties of the material which strongly depend on the composition. The ripple of the curve is due to interference caused by residual reflections in the system.

We have also made experiments to investigate the sensitivity of the system both with respect to power fluctuations and system loss variations. The results shown in fig 6 verify that the two-channel system presented here is, as assumed, fairly insensitive to such perturbations. The small differences between the curves visible in fig 6a are attributed to detector offsets that were not compensated for in this preliminary experiment.

Although the reflections from the fibre ends were virtually eliminated, other reflections caused disturbing interference in the P_1 channel. Phase modulation was applied in order to reduce the effect of these residual reflections. In this case the fibre was wound several turns around two plexiglass halfcylinders, as schematically indicated in fig 3. A 50 Hz sinusodial force was applied thereby causing the fibre length to be modulated. The modulation was set to such a level that the optical phase difference between the unwanted reflection and the sensor signal swept over more than ten interference fringes for each halfcycle of the modulation signal. With this arrangement, the interference was averaged out to a negligible level with a 100 ms integration time, fig 7.

The reflected power only affects the P_1 quantity which appears in the denominator of (2). As the sum P_1+P_2 is only used as a normalization quantity, a small amount of non-coherent additive power may be tolerated.

Another way to reduce the interference disturbance is to use a light source with a much shorter coherence length than that of the gas laser used in the above measurements. Experiments with a conventional laser diode will be carried out later in order to verify this statement.
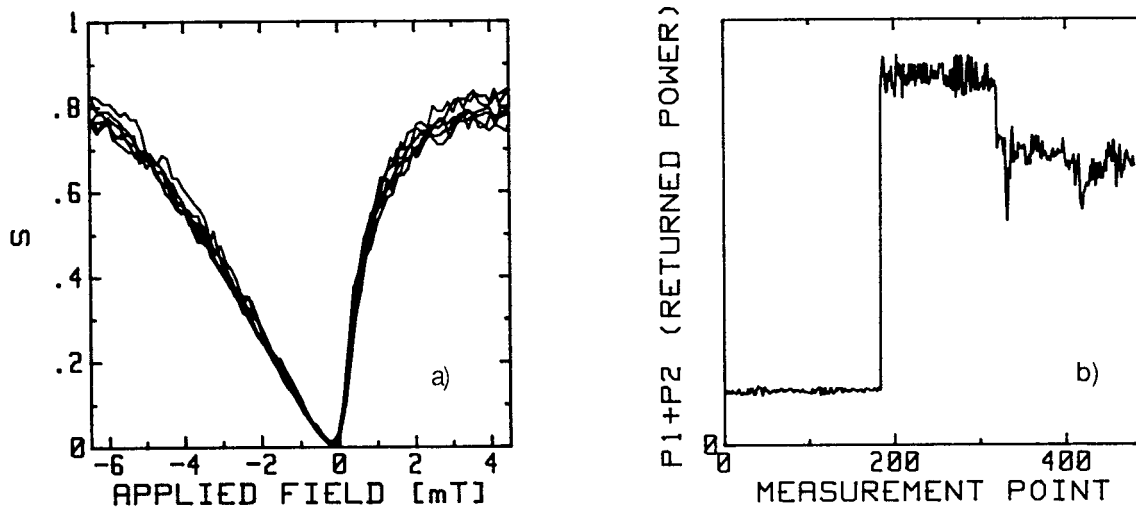
Fig 6. a) System output S during a measurement sequence of -6 mT to + 4 mT and back 3 cycles with a bias field of 3 mT. During the first cycle, the laser power was reduced. During the second cycle, the system was undisturbed and during the last cycle the fibre was perturbed by winding it around a 10 mm diameter rod.

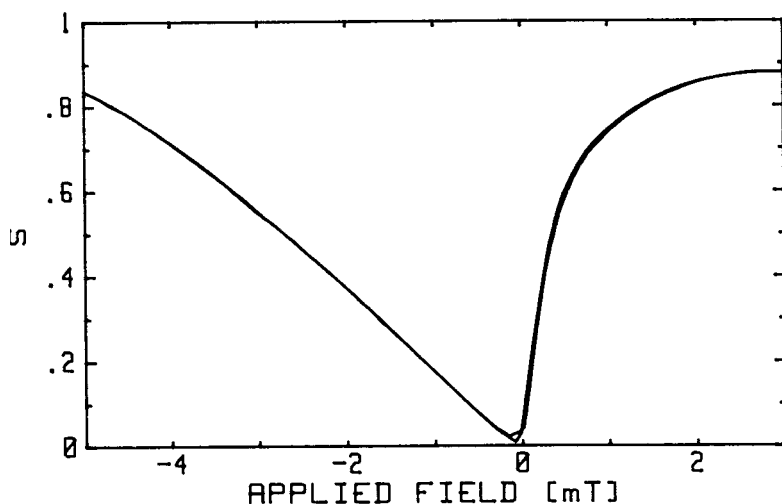b) P_1+P_2 ($\approx$returned power) during the measurement sequence.

Fig 7. Result from measurement similar to the one in fig 5, but with fibre length modulation.

Conclusions

We have presented a sensor system utilizing a polarization maintaining fibre and a planar optical waveguide for magnetic field measurements. The system is based on polarization modulation originating from the TE to TM conversion in a magneto-optical thin film of Gd,Ga substituted YIG. Both a transmissive and a reflective sensor systems have been demonstrated. We have shown that the use of the two polarization modes of a polarization maintaining fibre as measurement and reference channel gives a system which is highly insensitive to power and loss fluctuations. We have also demonstrated that phase modulation further reduces the noise in the system.

277

Acknowledgements

We would like to thank Dr H. LeGall and Dr J. M. Desvignes at CNRS, Meudon, France, who have provided the YIG film samples. We would also like to thank Mr Bengt Molin who has skillfully prepared the sensing elements.

This work was supported by the National Swedish Board for technical development.

References

1 U. Holm, H. Sohlström and T. Brogårdh: YIG-sensor design for fiber optical magnetic field measurement, OFS 84.

2 H. Sohlström, U. Holm and K. G. Svantesson: Characterization of Magnetooptical Thin Films for Sensor Use, ECO 2, Paris 1989, SPIE Proc, 1126.

Paper E

H. Sohlström, U. Holm and K. G. Svantesson
"Characterization of Magnetooptical Thin Films for Sensor Use"
SPIE Proc Electro-Optic and Magneto-Optic Materials and Applications,
J. P. Castera, vol. 1126, p. 77–84, 1989.

Characterization of Magnetooptical Thin Films for Sensor Use

Hans Sohlström, Ulf Holm and Kjell G. Svantesson*

Royal Institute of Technology, Instrumentation Laboratory, P. O. Box 70013, S-100 44 Stockholm, Sweden
* Swedish Institute of Microelectronics, P. O. Box 1084, S-164 21 Kista, Sweden

ABSTRACT

As a part of a fibre optical sensor development project we have made an evaluation of different optical waveguiding techniques to study the properties of thin magnetooptical films. Because of the application the methods are focused on the determination of the Faraday rotation, the linear birefringence and the dynamics and anisotropy of the magnetic properties of the samples. Measurements using holographic grating, prism and edge (end-fire) light coupling to different substituted YIG films are presented. The advantages of the different methods are discussed and it is shown that the launching technique may affect the properties to be measured. Film stress caused by the prism coupling method is found to influence the magnetic anisotropy.

1. INTRODUCTION

Magnetic garnet films have found a number of applications, e.g. in memory devices, optical isolators, modulators and sensors. In some cases, the magnetooptical properties are utilized, either using the film as an optical waveguide or with light propagating perpendicular to the film. In some applications such as in bubble memories the magnetic properties are utilized.

Regardless of the ultimate application, optical waveguiding techniques can be used in the characterization of magnetooptical thin films, particularly when spatial resolution is required. However, depending on the light coupling method the different film parameters could either be affected or not directly determinable.

As a part of a project to develop a fibre optical magnetic field sensor we have studied the magnetic and magnetooptical properties of a number of substituted YIG (Yttrium Iron Garnet) film samples. The sensor has a sensor element made from YIG and the signal is carried by a polarization maintaining fibre. Because of the application it was natural to use optical methods and to focus our interest on the sensor relevant properties of the films.

In this paper we discuss a number of optical waveguiding methods to study the different film properties. The methods differ in the means by which the light is coupled into and out of the film. We report on measurements using holographic grating, prism and end-fire light coupling. The grating method has been used to determine the linear birefringence, $\Delta\beta$, and the Faraday constant, θ_F, while the other two methods have been used to study the magnetic properties of the samples. We do not present the results as such, but rather use them as a demonstration of the different measurement methods. This means that we do not discuss the suitability of the the films as sensor materials.

The thicknesses of the films where in the range of 5-10 µm, allowing them to be butt-coupled to a polarization maintaining fibre. The films typically supported 10 to 20 modes. The measurements have been made using a 1.152 µm HeNe gas laser. In the realization of the sensor system a 1.3 µm laser diode will be used. This work will be reported later.

2. TE TO TM MODE CONVERSION IN A MAGNETOOPTICAL WAVEGUIDE

In a magnetooptical waveguide the magnetic field dependent circular birefringence, i. e. the Faraday effect, can cause a nonreciprocal coupling of energy between the TE and TM modes. In the presence of linear birefringence however, the transfer of power cannot be complete. The coupled fraction of power is described by the expression [1]:

$$F = \left[1+\left(\frac{\Delta\beta}{2\theta_F}\right)^2\right]^{-1} \sin^2\left\{\left[\theta_F^2+\left(\frac{\Delta\beta}{2}\right)^2\right]^{\frac{1}{2}}\cdot z\right\} = A\,\sin^2(\alpha\cdot z) \tag{1}$$

where F is the fraction of power in the mode not excited at the input, $\Delta\beta$ is the linear birefringence, θ_F is the circular birefringence and z is the travelled distance along the guide.

3. MEASUREMENTS AND ANALYSIS USING HOLOGRAPHIC GRATINGS

3.1. Method features

We have previously reported on the method of having a holographic grating as the light coupler on top of the waveguide to be investigated [2]. In this reference a formalism for a thorough analysis of the optical parameters is reported. Therefore, we only discuss the determination of the quantities $\Delta\beta$ and θ_F in this paper.

The grating method, in contrast to the standard prism method using rutile prisms, easily allows both the TE and TM mode of the same order to be coherently excited. This fact makes it possible to study the mode interaction along the waveguide. Therefore θ_F and $\Delta\beta$ can be accurately determined according to the expression (1) without the critical prism positioning that is necessary with the prism method.

3.2. Experimental configuration

The grating is made from Shipley AZ1450 positive photoresist spun on the sample and is formed by exposure of an argon laser two beam interference pattern directly on the sample surface. The grating covers the whole sample and acts as a distributed weak light coupler by which any part of the film can be studied. The grating will not mechanically disturb the sample, but, to some extent, the grating will optically load the waveguide. This effect could be corrected for if necessary. However, in most cases the effect is probably negligible.
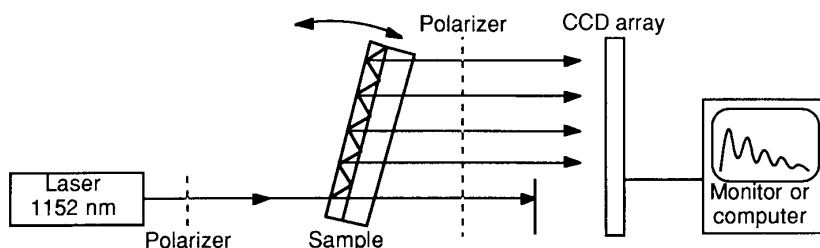
Figure 1. Experimental set-up for the grating measurements.

The measurement set-up is sketched in fig. 1. The point of coupling light into the waveguide is chosen by moving the sample to the desired position. Once the point of light entrance is chosen the sample is turned to the angle corresponding to the mode to be excited. To select the state of polarization of the entered light a polarizer and a retarder can be used. This is possible due to the fact that the grating is isotropic with respect to the state of polarization and that the TE and TM modes of the same order have practically the same coupling angle (within the laser beam divergence). When light of a wavelength in the transparent region of the film is impingent upon the grating it will couple into the film if the condition

$$N = \frac{\lambda}{d} + \sin(\phi)$$ (2)

is met. N is the effective index of the guided mode, d is the grating period, λ is the light wavelength and ϕ is the coupling angle. In fact eq. (2) is a modified way of writing the ordinary grating formula.

Light will be coupled out at the same angle ϕ as above along the whole light path. This means that the light on both sides of the sample propagate in co-linear directions and only the sample has to be turned to choose the different modes. Then, by viewing the sample through a polarizer, the loci of equal states of polarization will easily be recognized in the periodic pattern from the detector.

In the recordings a linear CCD array (Thomson TH7802A(Z)) was used in conjunction with a digital storage oscilloscope (Tektronix 2430). With this equipment the spatial resolution on the film surface amounts to about 75 samples per mm.

Examples of measured signals are displayed in fig. 2. Figure 2a shows the pattern from the first order mode and fig. 2b from the second order mode of a Bi substituted YIG sample [3]. The signals are decreasing due to absorption in the film. They are also affected by varying outcoupling efficiencies and other factors which will manifest themselves as signal noise.
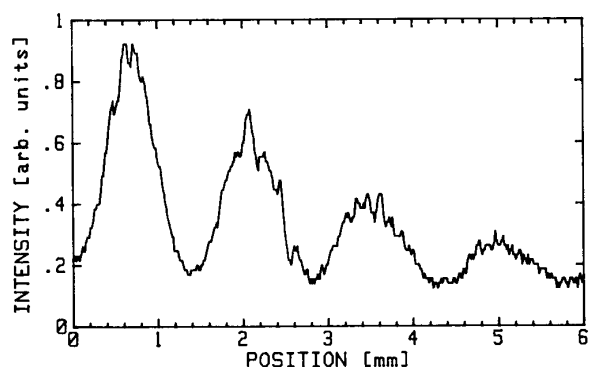
Figure 2a. Signal obtained using a holographic grating on a Bi substituted YIG sample. First order mode.
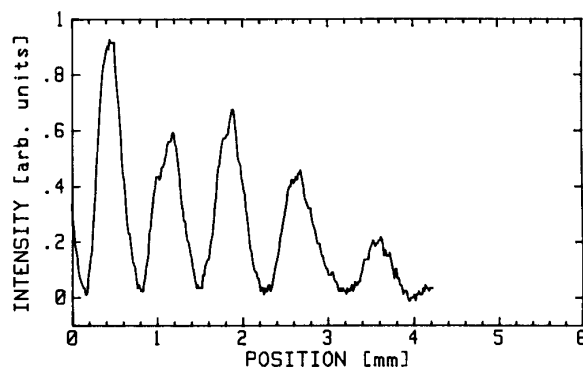
Figure 2b. Signal obtained using a holographic grating on a Bi substituted YIG sample. Second order mode.

3.3. Signal evaluation

It has previously been demonstrated that the variations in the signal, apart from the $sin^2(\alpha \cdot z)$ dependence, cf. eq. (1), can be corrected for [4]. Briefly this can be described as follows: The signal for the chosen mode is recorded twice. In the second recording the second polarizer is oriented orthogonally to the first one. Explicitly this implies that the first recording can be written

$$S_1 = f(z) \, B \, sin^2(\alpha \cdot z) \tag{3}$$

and the second recording

$$S_2 = f(z) \, [1 - B \, sin^2(\alpha \cdot z)] \tag{4}$$

The amplitude B equals A of eq. (1) when only a TE or a TM mode is excited. B equals 1 if the modes are equally excited. By summing these signals we get the unknown variation f(z) along the waveguide. A point by point division of eq. (3) or eq. (4) by f(z) then gives the desired result, i. e.

$$s_1 = S_1/(S_1 + S_2) = B \, sin^2(\alpha \cdot z) \tag{5}$$

$$s_2 = S_2/(S_1 + S_2) = 1 - B \, sin^2(\alpha \cdot z) \tag{6}$$

Curve fits to these functions then give the parameter values.

In the following discussion we assume that only the circular birefringence θ_F is magnetic field dependent whereas the linear birefringence $\Delta\beta$ is not. This greatly simplifies the analysis. However, the case of a magnetic field dependent $\Delta\beta$ could also be handled in a more thorough analysis [2].

In the determination of θ_F and $\Delta\beta$ one can use either of the following two procedures.

The first procedure is similar in the evaluation to measurements when prism couplers are used. The sample is magnetically saturated in a direction parallel to the light propagation. Either the TE or the TM mode is excited and recordings are made with the second polarizer parallel and perpendicular to the excited direction respectively. The calculations are performed according to the discussion above and the result corresponds to eq. (5) and eq. (6). From the modulation of these two functions and their periodicity two equations are obtained from which θ_F and $\Delta\beta$ can be calculated cf. eq. (1).

In the second procedure one takes advantage of the fact that the TE and the TM mode of the same order can be coherently excited. Because of this there can be a conversion of energy between polarization states in the waveguide also without any circular birefringence. In this case the analysis is performed as follows. Light is coupled to the waveguide in a 45° direction to the TE and TM mode of the chosen order. A possible difference in the grating coupling efficiency for the modes can be neglected. Recordings are then taken with the sample magnetically saturated in directions parallel and perpendicular to the light direction respectively. Signal processing is performed according to eqs. (5) and (6) and the periodicity, i. e. the spatial frequency of the patterns are determined. In the parallel case the argument of the sin^2 function contains θ_F and $\Delta\beta$. In the perpendicular case the argument contains only $\Delta\beta$. Thus also θ_F can be calculated.

In samples where θ_F is very high, as in the above illustrations of Bi substituted YIG, either of the two methods could be chosen for a direct determination of θ_F, preferably if a mode is chosen for which $\Delta\beta$ is minimum. This mode easily manifests itself by being the one of lowest periodicity in the 45°-light – perpendicular-field situation.

In view of the spatial resolution capabilities of the measurement system very high θ_F:s could be measured. Fig. 2b shows a rotation of 2400°/cm ($\Delta\beta$ included). A practical limit is judged to be in the vicinity of 15000°/cm. The obtainable accuracy is high because the outcoupled signal from several periods of the polarization state evolution can be used. The accuracy may also be further increased by using results from several modes.

4. MEASUREMENTS USING PRISM COUPLING

4.1. Experimental considerations

In this section we describe measurements where we have used the magnetooptical mode conversion to probe the magnetic properties of the samples. For this purpose we have used the well known prism coupling method, fig. 3. It is easy to apply and does not, in contrast to the other two methods, require any sample preparation. By using birefringent prisms, it is easy to selectively excite and monitor the TE or TM mode of the desired order.

The high input and output coupling efficiencies make high resolution measurements of the conversion possible. The prism method should therefore in principle be well suited for studies of magnetic hysteresis effects etc. However, as will be shown below, it has serious limitations in this application.
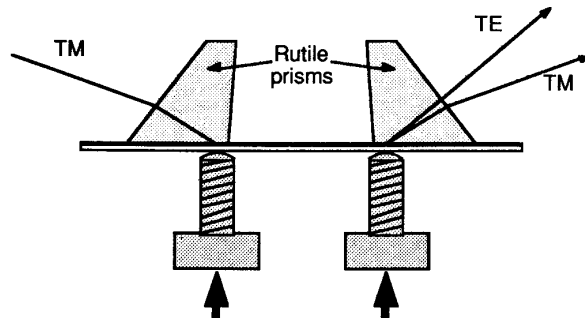
Figure 3. Measurement of TM to TE mode conversion using birefringent prisms.

We have used two ways of magnetic field variation in the prism coupling measurements. In section 4.2. we present results with field variations along one axis only, with and without a supplementary constant perpendicular bias. This configuration is chosen because it most closely resembles the sensor configuration we have had in mind.

In section 4.3. we present results where an applied field of a constant magnitude is rotated in the plane of the film. This method was used in order to further study the anisotropy of the samples. In the measurements, the earth magnetic field of about 50 μT has been compensated for.

4.2. Results with one-dimensional field variations

In this case we have monitored the TE to TM mode conversion versus an applied field. The composition of the film was known to give an in-plane spontaneous magnetization with a low anisotropy [5]. A similar composition has previously been used in a sensor with a detection limit as low as $6 \cdot 10^{-12}$ T/$\sqrt{\text{Hz}}$, [6]. When a small field, varying from a negative to positive value and back again, is applied parallel to the light path, the result looks according to fig. 4.

Close to zero field, there are domains with different directions of magnetization. If easy directions exist, the magnetization directions will be distributed among them in such a way that the average direction is still determined by the direction of the applied field. The averaged magnitude will, however, be less than the magnetization of the individual domains leading to a reduced conversion. Whether the conversion goes to zero or not during any observable field interval depends on the behaviour of the domains in the light path. That their behaviour depend on the magnetic history is evident from the hysteresis of about 20 μT as seen in fig. 4. We can also see that the conversion changes in steps revealing domain wall movements.

When the applied field is increased the domains will align in a direction determined by the applied field and the magnetic anisotropy of the sample and eventually merge into one domain, which covers the whole sample. In the case shown in fig. 4, the interaction length is slightly to short to give the maximum conversion obtainable with this sample.

A sufficiently strong constant bias field, in the plane of the film and perpendicular to the light propagation, will also create a single domain. This domain will then rotate under the influence of the applied field. In general our experiments showed no hysteresis for bias fields above 1 mT, fig. 5. In some cases, however, it remained even for fields of several mT and changed in nature when the prisms were repositioned.
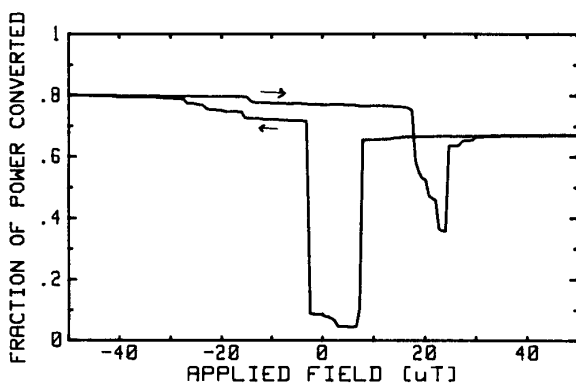
Figure 4. TM to TE mode conversion versus an applied magnetic field in a 6.4 μm thick sample of YIG:Gd,Ga. The interaction length was 4 mm.
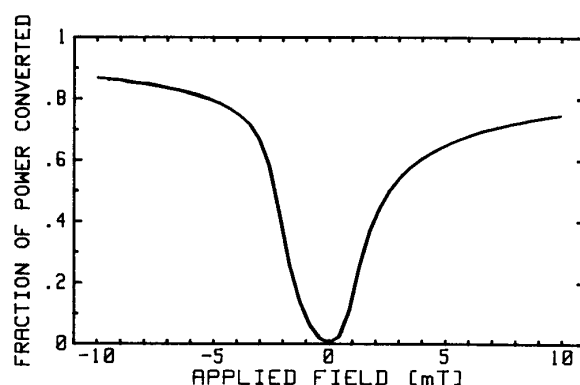
Figure 5. TM to TE mode conversion versus an applied magnetic field. An in plane bias field of 5.2 mT is applied perpendicular to the light propagation direction. Sample and interaction length as in fig. 4.
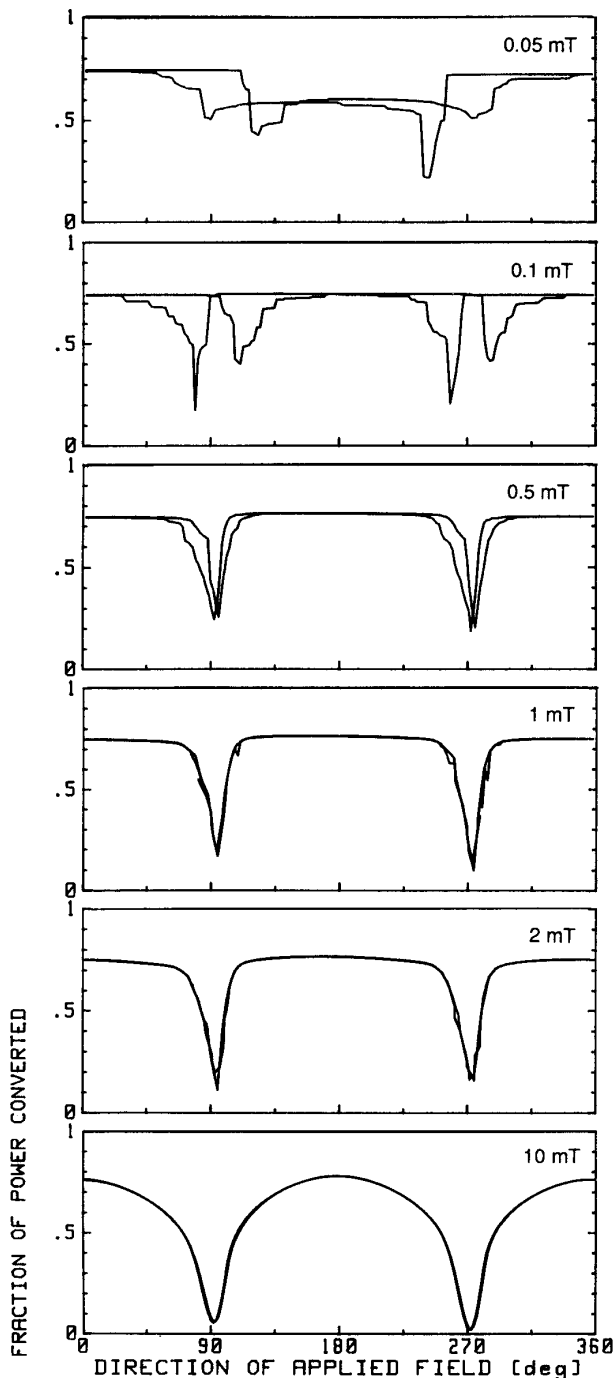
Figure 6. TM to TE mode conversion with rotating fields of magnitudes 0.05 mT, 0.1 mT, 0.5 mT, 1 mT, 2 mT and 10 mT respectively. The curves show bidirectional measurements (0→2π→0). The same sample as used in fig. 4 and 5 with 5 mm interaction length. Field direction 0 is parallel to the [1̄ 1 0] direction.

The nonsymmetry of the curve in fig. 5 originates from the magnetic anisotropy, causing the magnetization direction to differ from the direction of the applied field. If the bias field is further increased, the nonsymmetry is reduced, indicating that the direction of magnetization more closely follows that of the applied field.

4.3. Results with two-dimensional field variations

In the above measurements, where the applied magnetic field consist of a varying field parallel to the light propagation direction and a constant perpendicular bias field, neither the magnitude nor the direction of the field is constant. This complicates the interpretation of the results with respect to the anisotropy of the sample. Instead, it is more convenient to apply a rotating field with a constant magnitude. Fig. 6 shows the results from such a measurement.

For small fields there is a directional hysteresis, which vanishes at about 1 mT, indicating that the many-domain properties now have practically disappeared. The high level of conversion for most directions of applied field indicate that the magnetization remains close to parallel to the light path even when the field is at rather large angles to it. Apparently there is, in contradiction to what was assumed, a strong anisotropy with an easy direction along the light path. However, when the field is increased to 10 mT the anisotropy almost vanishes.

In order to ascertain if the anisotropy was an intrinsic property of the sample or if it was caused by the experimental technique, the sample was turned 45° in the holder. The results were now very similar to the previous ones, which again indicate an easy direction of magnetization along the light path. This suggests that this anisotropy is not a fundamental property of the material, but is caused by the experimental technique. The mechanical stress in the film, caused by the pressure applied to the prisms seemed to be the only plausible explanation.

5. MEASUREMENTS USING EDGE COUPLING

5.1. Method features

Because of the indication that the prism coupling method induces anisotropy in the sample we have introduced edge coupling as the third method in our study. This technique does not cause any additional film stress and is also the only possible one for waveguides with dielectric covers. It can be accomplished either with lens coupling or, for films of suitable thicknesses, with single mode fibre coupling. The main difficulty is then to excite only the mode of interest. Fibre coupling has an advantage here, as the light distribution from the fibre is well defined.

5.2. Experiment

The experiment was set up in such a way that we could use light coupled trough the edge of the sample to monitor the conversion while we at the same time applied a prism to the sample.

The same polarization maintaining optical fibre was used to couple light to and from the sample. To make this configuration possible, the sample was cut and polished in a semicircular form (fig. 7). A reflective gold coating was also deposited on the circular edge. The light from the polarization maintaining fibre was in this way coupled into the film, reflected and focused back into the fibre with no need for any
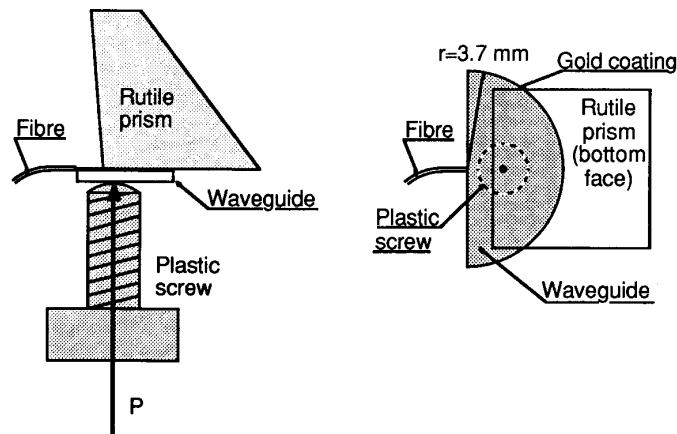
Figure 7. Experiment to show the influence of prism pressure.

external optics. The prism was initially used to monitor the excitation. When the correct excitation was achieved, the fibre was epoxied in place. The coupling pressure, P in fig. 7, could then be adjusted as needed in the measurements.

Only one of the polarization modes of the fibre was excited and the fibre was oriented so that power was launched into the TE mode of the waveguide. The power ratio between the two fibre polarization modes in the reflected light was in this way a measure of the conversion. As the Faraday effect is non-reciprocal in nature, the conversion of the forward and return trip will add, making the effective interaction length twice the radius of the semicircle.

Because of the low numerical aperture of the fibre and the high index of refraction of the film, the light beam propagating in the film will be narrow and can be considered to have a common angle to the magnetization.

A small magnet provided a bias field of about 1 mT perpendicular to the light path in the sample.

5.3. Results

The conversion ratio is plotted versus the applied longitudinal field in fig. 8. As the pressure on the prism was reduced from maximum (100%) to lower pressures (50% and 25% estimated) and finally removed (0%), the results changed. At maximum prism pressure, the magnetization apparently stays parallel to the light path for all fields but those with a very small parallel component, where the total applied field is practically perpendicular to the light path. As the pressure is decreased, the magnetization follows the direction of the applied field more and more closely.

Results from the measurements with a rotating field and with the prism removed are shown in fig. 9. Although the interaction length is slightly different from the one used in fig. 6, it is possible to observe a significant difference in the behaviour. The previous anisotropy with an easy direction of magnetization along the light path has disappeared. The small field directional hysteresis is also reduced.
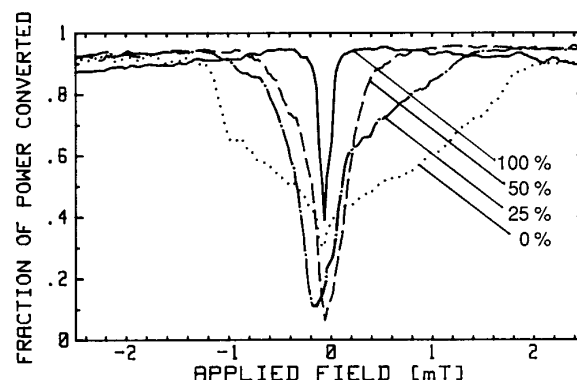
Figure 8. TM to TE mode conversion in experiment according to fig. 7, measured using the light reflected back through the fibre. Prism pressure reduced from the normal (100%) coupling out less than 10% of the the light in the guide, to 50% and 25% and finally removed (0%). The same sample as used in fig. 4-6.
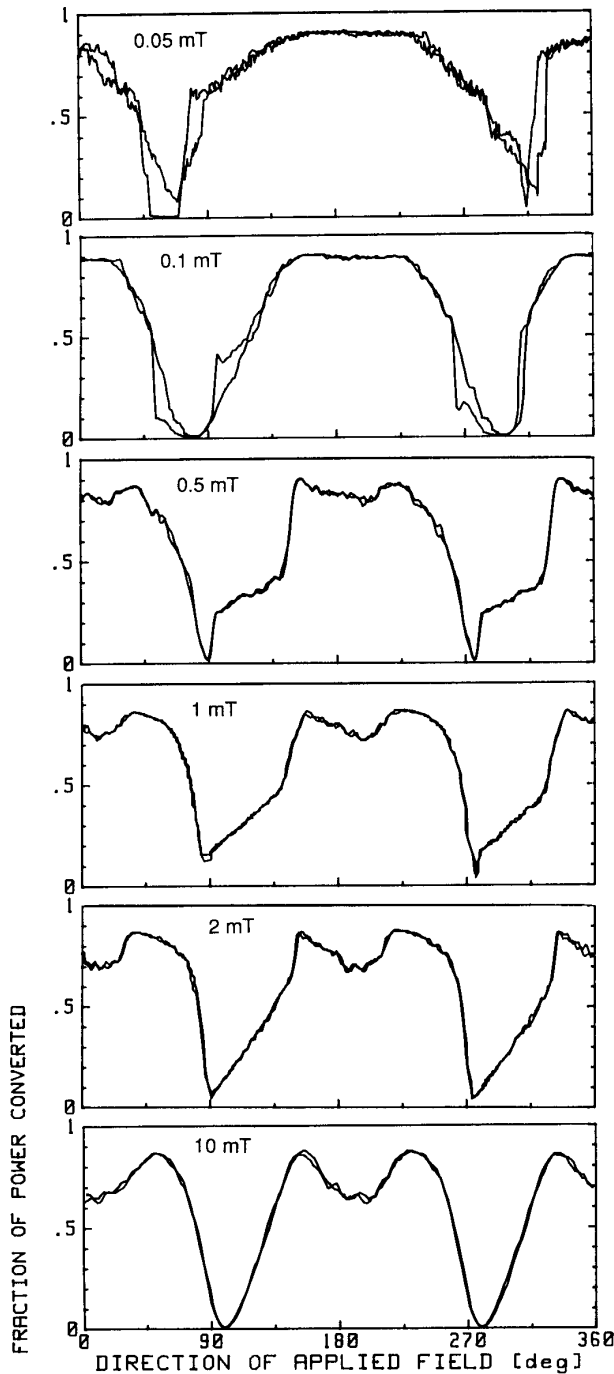
Figure 9. TM to TE mode conversion with rotating fields of
magnitudes 0.05 mT, 0.1 mT, 0.5 mT, 1 mT, 2 mT and
10 mT respectively. Measured using the fibre setup in fig 7.
All curves show bidirectional measurements (0→2π→0). The
noise in the curves is mainly caused by interference due to
unwanted reflections in the optical system.

6. DISCUSSION

In this paper we have presented three complementary
optical waveguiding techniques to qualify magnetooptical
materials to be used in magnetic field sensor applications.
Both optical, magnetooptical and magnetic properties have
been investigated.

The grating method can provide accurate information
about the circular and linear birefringence, the waveguide
thickness and the index of refraction of the film. We have
used this method to select samples with sufficiently small
linear birefringence to allow for a large conversion. The
method provides results that are spatially resolved and gives
an opportunity to map the sample, for example in order to
study localized defects. Thus suitable parts of a wafer could
be chosen for further use. The grating method might also be
used for studies of magnetic properties. However, the
distributed nature of the grating coupler decreases the
amount of light available at each point. This fact may make
it difficult to achieve a high signal resolution.

The prism method provides a more convenient way to
study the magnetic properties as it is fast in application and
does not require any sample preparation such as edge
polishing or grating fabrication. The optical signal was also
high with this method, which simplified the signal
processing.

The results from the prism measurement show the
main drawback of this method; the influence of the pressure
applied to establish optical contact. The pressure inevitably
causes an additional stress in the waveguide material.
When two prisms are used, the stress will be distributed over
the sample, with an axis of symmetry between the contact
points of the prisms. The influence of this stress on the
magnetic behaviour, both with respect to anisotropy and
hysteresis, is evident from fig. 6 (prism coupling), fig. 8 (fibre
coupling and different prism pressures) and fig. 9 (fibre
coupling and rotating field). As observed in fig. 6 it causes a
strong anisotropy with an easy direction of magnetization
parallel to the light path.

The edge coupling method allows stress-free experiments
and was used both as a reference to check the applicability of
the prism method and to test a possible sensor configuration
(A report on the sensor work will be published later).
Because the method requires specially prepared samples
with one or two edges carefully polished it cannot be
considered as a general sample qualification method.

When regarding the results with the prism method the
following fact should be kept in mind. The measurements
were made on samples with a material composition which
give a small inherent in plane anisotropy. Therefore an
induced anisotropy is easily introduced by external forces
such as the prism pressures. It appears from fig. 8 that a
reduction of the prism pressure significantly reduces the
influence on the anisotropy behaviour of the sample. As a
lower pressure results in a smaller optical signal there is an
obvious trade-off here. The use of a liquid in the space
between the sample and the prism will enhance the coupling
efficiency. Up to now we have not made any measurements
down to the practical signal limit, but to our judgement the
prism method should work quite well in many cases.

Although this work has aimed at a special application it
is our belief that our experiences could be useful for material
investigations for other applications as well.

7 ACKNOWLEDGEMENTS

REFERENCES

1. P. K. Tien, "Magneto-optics and motion of the magnetization in a film-waveguide optical switch", J. Appl. Phys. 45, 3059-3068 (1974).
2. K. G. Svantesson, "Measurements on Magnetooptical Waveguides by means of a Distributed Grating Coupler", J. Magn. Soc. Jpn. 11, Supplement, No S1, 405-408 (1987).
3. Sample provided by Dr K. Ando, ETL, Tskuba, Japan
4. U. Holm and K. G. Svantesson, "Measurement of Birefringence in Externally Strained Magnetooptical Waveguides", J. Magn. Soc. Jpn. 11, Supplement, No S1, 377-380 (1987).
5. Samples provided by Dr H. LeGall and Dr J. M. Desvignes, CNRS, Meudon, France
6. G. Doriath, R. Gaudry, and P. Hartemann, "A sensitive and compact magnetometer using Faraday effect in YIG Waveguide", J. Appl. Phys. 53, 8263-8265 (1982)

Paper F

K. Svantesson, H. Sohlström and U. Holm
"Magneto-optical garnet materials in fibre optic
sensor systems for magnetic field sensing"
SPIE Proc Electro-Optic and Magneto-Optic Materials and Applications II,
H. Dammann, vol. 1274, p. 260–269, 1990.

Magneto-Optical Garnet Materials in Fibre Optic Sensor Systems for Magnetic Field Sensing

Kjell Svantesson

Swedish Institute of Microelectronics, P.O. Box 1084, S-164 21 Kista, Sweden. Tel.+46 8 752 10 00, fax +46 8 750 54 30

Hans Sohlström and Ulf Holm

Royal Institute of Technology, Instrumentation Laboratory,
P.O. Box 700 13, S-100 44 Stockholm, Sweden. Tel. +46 8 790 90 41, fax +46 8 10 08 58

ABSTRACT

Magneto-optical garnet materials such as YIG, undoped as well as substituted, exhibit a large Faraday rotation. This fact makes them potentially suitable as sensing elements in fibre optic magnetic field sensor systems.

We describe both an intensity based multimode system using bulk materials and a singlemode polarization based system using waveguiding films. A number of different material compositions, such as undoped YIG, (GdGa)- and different Bi-substituted YIG have been used for the sensor elements. Measurement results are presented and discussed. A detection limit in the μT range and a measurement range exceeding 10^4 have been achieved.

1. INTRODUCTION

Fibre optic based sensor systems offer certain advantages in many measurement applications. This is because of their insensitivity to disturbing electromagnetic interference and the galvanic isolation between the sensing and recording areas due to the use of nonconducting materials for the signal transmission. An application where these properties are particularly advantageous is in the sensing of magnetic fields at high voltage levels, e.g. in the monitoring of the current in high voltage transmission lines or for the measuring of current transients in high voltage distribution plants.

One measurement principle of a fibre optic magnetic field sensor utilizes the Faraday effect. In an all fibre design one then uses a certain length of an optical fibre for the sensor element. However, this solution to the problem implies the disadvantage that the fibre has to be wrapped around the conductor to be measured. Furthermore, the sensor element cannot very easily be miniaturized. In this work we have investigated another approach to the design of the sensor element, viz. the use of a magneto-optical garnet material. In such a sensor type a piece of garnet material is attached to the end of the signal transmission fibre(s).

As a part of a fibre optic sensor project we have investigated a number of different magneto-optical garnet materials for the sensing element in different sensor designs. The performances of these sensors depend on several factors. In our work we have concentrated on the performance depending on the material properties and the geometrical shape of the sensor element. Methods for the characterization of magneto-optical thin films have been reported previously[1] and in this paper we mainly report on the sensor behaviour with respect to geometrical design factors. In many cases geometrical and material composition factors of course cannot be separated.

From a geometrical point of view we distinguish between two principal outlines of the sensor system. One is composed of a multimode optical fibre coupled to a bulk magneto-optical material and the other one is composed of a polarization maintaining singlemode optical fibre coupled to a waveguiding magneto-optical material. We have not been able to perform any optimization of the material properties but have rather had to chose from crystals that were optimized for other purposes. We report on results for the following materials: for the bulk material sensor elements undoped YIG, and Bi-substituted YIG were used, for the waveguiding material sensor element (GdGa)- and Bi-substituted YIG were used.

2. BULK OPTIC SENSOR SYSTEM

2.1. Basic sensor principle and design considerations

The general outline of our multimode-bulkoptic sensor is shown in fig 1a. Light is launched into and returns from the sensor element through a multimode optical fibre. Polarizers are placed on both sides of the crystal. The intensity of the light transmitted through the second polarizer depends on the polarization rotation in the crystal.
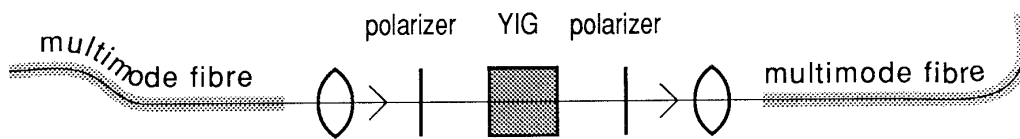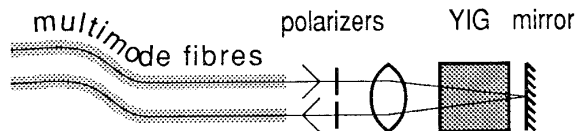

Fig. 1a. Principle outline of the transmission type magnetic field sensor

Fig. 1b. Principle outline of the reflection type magnetic field sensor

In most applications it is inconvenient to have the fibres on opposite sides of the sensor element. Thanks to the non-reciprocity of the Faraday effect it is possible to make a sensor according to fig 1b. In this configuration the two fibres are placed on the same side of the crystal, with a reflector on the opposite side. As the optical path length in the crystal is doubled in this case one gets twice the polarization rotation for a given crystal thickness.

The transmittance of a polarizer follows the Malus $\cos^2$ law. Therefore, different relative orientations of the transmission axes of the two sensor polarizers in fig 1 will produce very different sensor characteristics. We chose the angle 45° between the polarizer axes to achieve the following sensor performance:

• a sensitivity to the direction of the the polarization rotation, and thus to the direction of an applied magnetic field

• a maximum unambiguous range

• a maximum sensitivity to small fields

To get an unambiguous measurement range the polarization rotation in the crystal should not exceed 45°. For the reflection type sensor this puts a limit of 22.5° for a single-pass transmission. The desired crystal thickness is then given by the Faraday rotation per unit length of the material.

The rotation is closely related to the optical absorption which is wavelength dependent. Fortunately, in the wavelength range of 1-1.5 μm, where also suitable opto-electronic components are available, both the absorption is low and the rotation is substantial. The light source used in all the bulk sensor examples was an 1.3 μm LED.

Due to the ferrimagnetic properties of the garnet material, the picture of a pure magnetic field dependent rotation of polarized light is too simplified. The crystals possess an internal magnetization leading to the formation of magnetic domains. When an external magnetic field is applied the size and shape of the domains change, and the measured rotation of polarization will depend on the actual domain distribution along the light path. In the general case this distribution is not reproducible, and will thus not give reproducible measurement result. However, it is still possible to achieve a useful
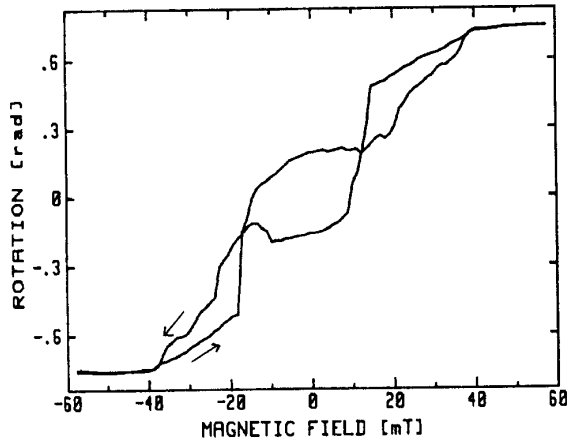
Fig. 2. Polarization versus applied magnetic field in a undoped YIG crystal
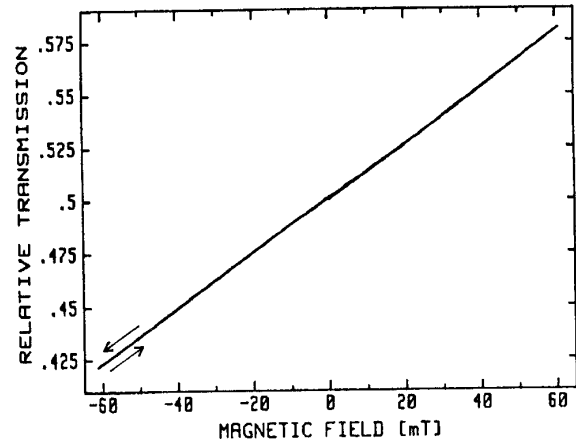
Fig. 3. Sensor performance with a thinned undoped YIG sensor element

sensor performance. By using a large light beam diameter the average rotation of many domains will be measured, making the movement of the individual domain walls less significant.

The sensitivity of a specific sensor depends both on the Faraday rotation within the domains and on how an external field changes the domain distribution. However, a sensor material that is sensitive to small field variations will saturate at low fields. The optimum material characteristics therefore will depend on the requirements of the actual application.

2.2. Sensor performance

2.2.1. Flux-grown undoped YIG sensor element

In our first experiments we used samples from flux-grown single crystal YIG. The samples were cut and polished to the desired shapes. The saturation Faraday rotation of the material was approximately $200°/cm$ at $1.15 \, \mu m$. For a $45°$ rotation in a reflection sensor configuration, this would imply a crystal thickness of 1.1 mm.

In our preliminary measurements a 200 micron wide polarized light beam was passed through a YIG cube with sides of approximately 2 mm. The rotation versus applied magnetic field typically looked like the curve fig 2.

A study of the domains in this crystal reveal a rather complicated three-dimensional structure. A thinning of the crystal in a direction perpendicular to an easy direction of magnetization resulted in a two-dimensional domain structure, i. e., with the domains reaching through the entire crystal. This occurred at a crystal thickness of approximately $300 \, \mu m$. At this thickness the average domain stripe width was about $100 \, \mu m$, [2].

After this treatment, the crystal was placed in a sensor configuration according to fig 1b. The light beam width was now 1.5 mm. The performance is shown in fig 3.

As the total polarization rotation decreases when the crystal becomes thinner, one has to compromise between the reproducibility and the sensitivity of the sensor element. The maximum rotation from a $600 \, \mu m$ path length was approximately $9°$, which only gave a rather small change in relative transmission, as can be seen from fig 3. Another effect of the thinning was that the demagnetization factor reduced the magnetization caused by the external field, leading to a reduction of the sensitivity and an increase of the saturating field.
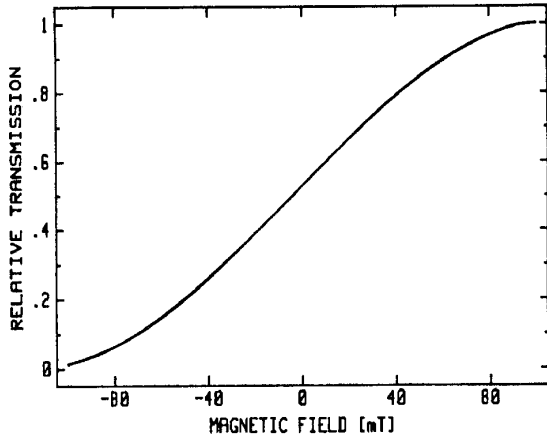
Fig. 4. The sensor characteristics with a (YbTbBi)-YIG sensor element, large field
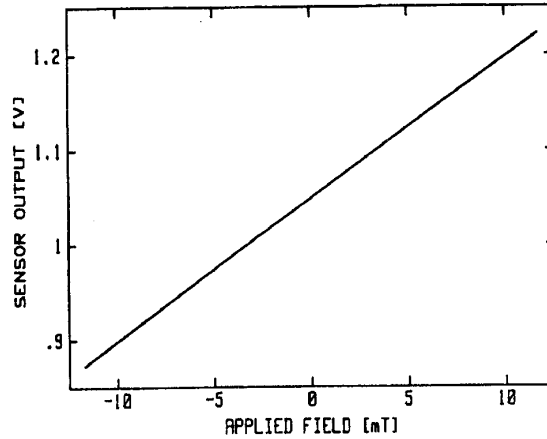
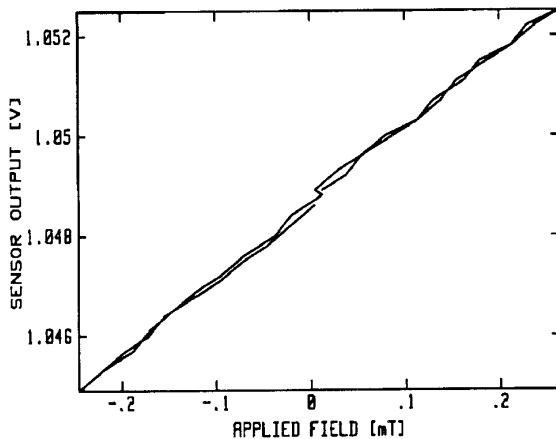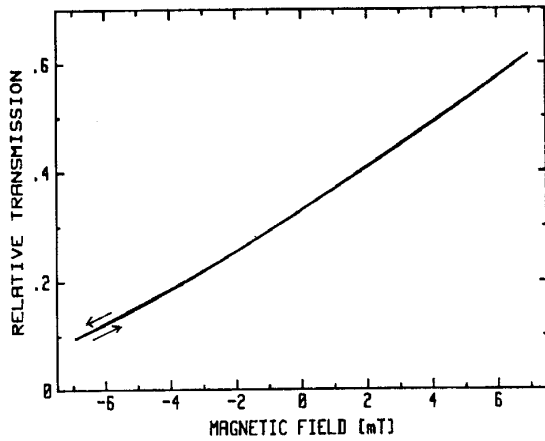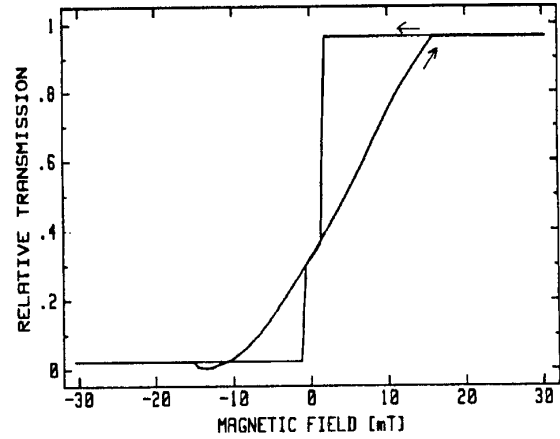Fig. 5. The sensor characteristics with a (YbTbBi)-YIG sensor element, medium field

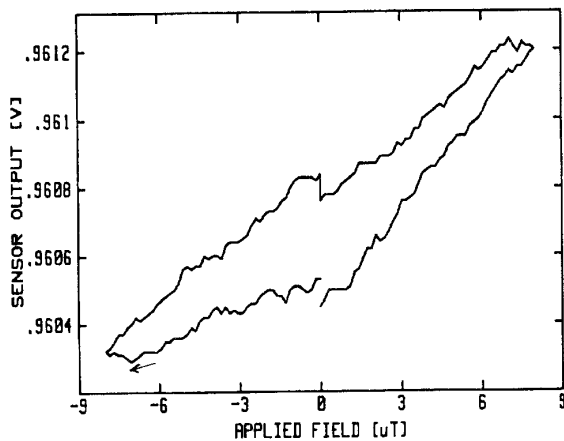Fig. 6. The sensor characteristics with a (YbTbBi)-YIG sensor element, small field

2.2.2. Epitaxially grown Bi-YIG sensor elements

2.2.2.1. Material features

Due to the extensive development work that has been performed on magneto-optical materials for optical isolators during the last years a possibility of getting more suitable materials also for sensors has arisen. These new materials are fabricated by liquid phase epitaxy (LPE) on suitable substrates. By incorporating various substituents that modify the material properties they can be tailored to match several key performances, for example high Faraday rotation as well as low temperature and wavelength dependence of the rotation[3].

2.2.2.2. (YbTbBi)-YIG sensor

This sensor utilized an epitaxially grown (YbTbBi)-YIG crystal in a reflection configuration, fig 1b. The saturation rotation was close to 22.5°, giving a relative transmission range from 0 to 1, as shown in fig 4.

The symmetry of the curve indicates a correct orientation of the polarizers of the sensor, according to the criteria in paragraph 2.1 above. The central part of the sensor characteristics is also very linear, fig 5.

From figs 4 and 6, the detection limit and the relative measurement range of this measurement system is estimated to be 10 μT and 10^4 respectively.

Fig. 7. The sensor characteristics with a (GdBi)-YIG sensor element, medium field

Fig. 8. The sensor characteristics with a (GdBi)-YIG sensor element, large field

Fig. 9. The sensor characteristics with a (GdBi)-YIG sensor element, small field

2.2.2.3. (GdBi)-YIG sensor

The second epitaxially grown isolator material that we used in the reflection sensor configuration, fig 1b, was of the (GdBi)-YIG type. The saturation rotation of this sensor element was similar to that of the previous one, but the saturation field was lower. As expected this gave a higher sensitivity, as is seen in fig 7.

The shape of the curve also shows the consequence of a small deviation from the ideal polarizer orientation.

For a saturating field, this particular material exhibits the effect shown in fig 8. The domains "lock" in the saturated state and remains in this state even when the field is lowered far below saturation. Such a locking was not observed for any field variation below saturation.

The sensor performance at small fields is shown in fig 9. The hysteresis-like behaviour of the characteristics is not related to a magnetic phenomenon, but is an effect of the DC-instability of the electronic system, which limits the small field performance. The detection limit due to the magnetic effects was estimated to be below 1 μT.

The fact that the accuracy of the best sensors was not limited by the magnetic properties of the sensor element, but of the DC-stability of the electronic system indicates a fundamental disadvantage with the light intensity as the information carrier in optical measurement systems. Any change in the received signal will look like a change in the measurand.

3. WAVEGUIDING SENSORS

3.1. Design considerations

To overcome the fundamental disadvantage mentioned in the end of the previous section one can introduce a reference channel. By this arrangement intensity fluctuations may be compensated for. Instead of introducing an extra fibre in the
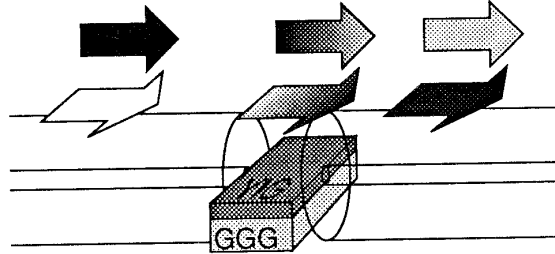
Fig. 10. Basic principle for the waveguiding sensors

systems of fig 1 one may use a singlemode polarization maintaining fibre. Such a fibre can carry two modes of orthogonal polarization independently of each other.

The fibre core dimension of 5–10 μm suggests a wave guiding sensor element in the form of e.g. a YIG film on a GGG substrate. The fibre can then be butt coupled directly to the sensor element. If the fibre is correctly oriented, the two fibre polarization modes will couple to the TE and TM waveguide modes respectively.

In the waveguide, the Faraday effect causes a magnetization dependent circular birefringence that gives a coupling between the TE and TM waveguide modes. The transfer of power follows the expression

$$F = \left[1 + \left(\frac{\Delta\beta}{2\theta}\right)^2\right]^{-1} \sin^2\left\{\left[\theta^2 + \left(\frac{\Delta\beta}{2}\right)^2\right]^{\frac{1}{2}} \cdot z\right\} \qquad (1)$$

where F is the fraction of power in the mode not excited at the input, $\Delta\beta$ is the linear birefringence, θ is the circular birefringence and z is the position along the waveguide. The maximum transfer of power is dependent on the ratio between the circular and the linear birefringence, which is mode dependent.

Planar YIG waveguiding films of suitable thickness for butt coupling to the fibre, i. e. 5–10 μm, will support 10–20 modes. We found that if the fibre end was correctly positioned, power could be coupled to the fundamental mode only. With a suitable film composition it is possible to achieve a small $\Delta\beta$ for this mode. In such a waveguide the Faraday circular birefringence can be considerably larger than the linear birefringence leading to a large magnetic field dependent coupling between the fundamental TE and TM modes. Bi-subsituted YIG films with a very high Faraday rotation reduces the necessity of a low linear birefringence.

In our experiments with waveguiding sensors we used planar waveguides without any lateral light confinement. The absence of such a confinement will lead to light losses. Measures to reduce these losses are discussed below.

The common principle for the sensors described below is as follows, fig 10: Polarized light is coupled from one of the polarization modes of the polarization maintaining fibre into the fundamental TE mode of the planar waveguide. In the waveguide, part of the optical power is transferred to the TM mode. The light is then coupled into the return fibre, which is oriented in such a way that each of the modes of the planar guide match the fibre polarization modes. The power in the two modes, P_1 and P_2, are then separately detected, giving an intensity independent signal S, which is a measure of the magnetic field:

$$S = \frac{P_2}{P_1 + P_2} \qquad (2)$$

In the sensor configuration above, the direction of the magnetic field cannot be determined. As will be demonstrated in section 3.4, the second fibre can be positioned in such a way that the sensor also becomes sensitive to the direction of the magnetic field.
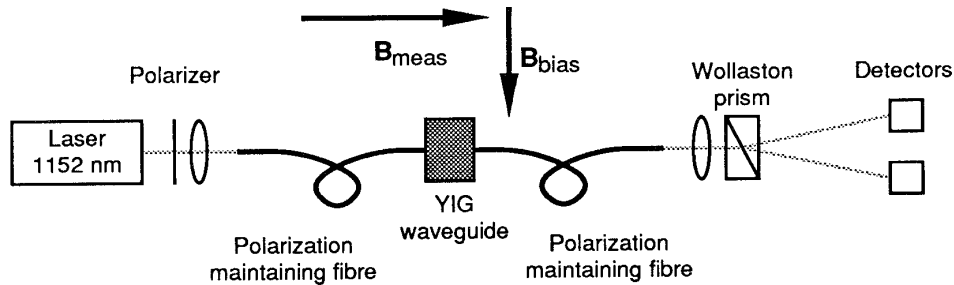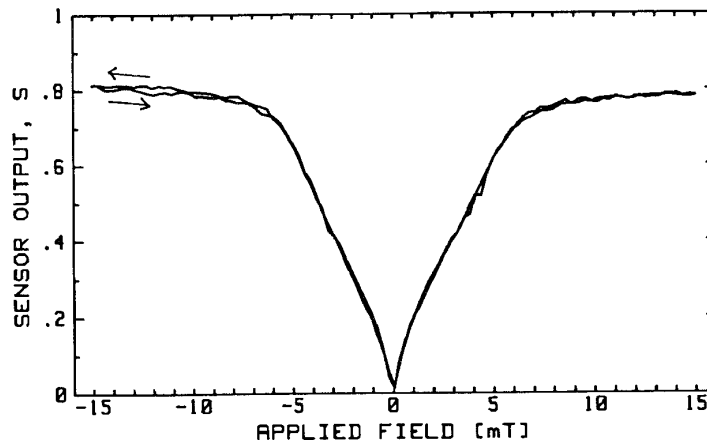
Fig. 11. The transmission sensor set-up.

Fig. 12. Output signal S versus B_{meas} with a sensor according to fig 11 and a B_{bias} of 3 mT.

As in the case of the bulk sensors it is possible to "fold" the optical path and attach the fibres to the same side of the sensor element. Due to the two-channel measurement system it is also possible to use a single fibre to carry the light both to and from the sensor element.

3.2. Transmitting sensor with easy in plane (GdGa)-YIG

The material used for this type of sensor was a 6.7 μm thick (GdGa)-YIG film epitaxially grown on a GGG substrate. The film was known to give an in-plane spontaneous magnetization with a low anisotropy[4]. The magnetization was therefore expected to closely follow the in-plane component of the applied field. A similar composition has previously been used by Doriath, Gaudry, and Hartemann in a magnetometer with a detection limit as low as $6 \cdot 10^{-12}$ T/$\sqrt{Hz}$, [5]. The Faraday rotation of the film was 150°/cm at 1.15 μm. A sensor element in the form of a 4mm long chip was cut and polished. The sensor was assembled according to fig 11.

The bias field in the plane of the film, but perpendicular to the light propagation direction was used to align the domains to a common direction from which they where then rotated by the field to be measured.

Results obtained with this sensor configuration are shown in fig 12.
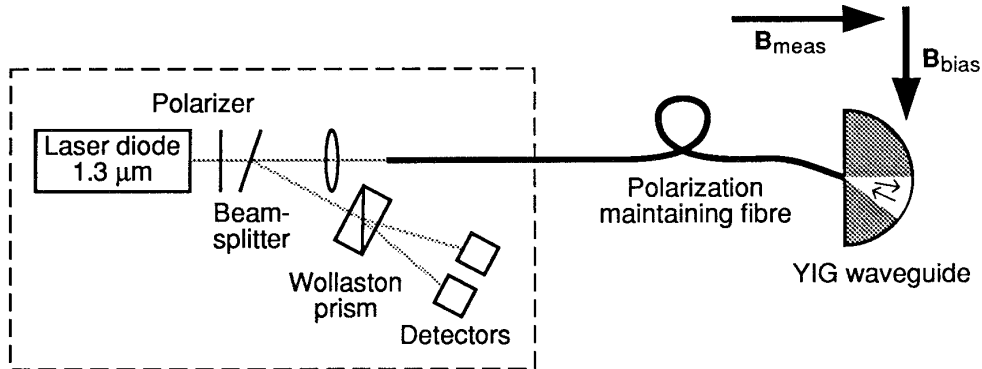
Fig. 13. The reflective sensor set-up.
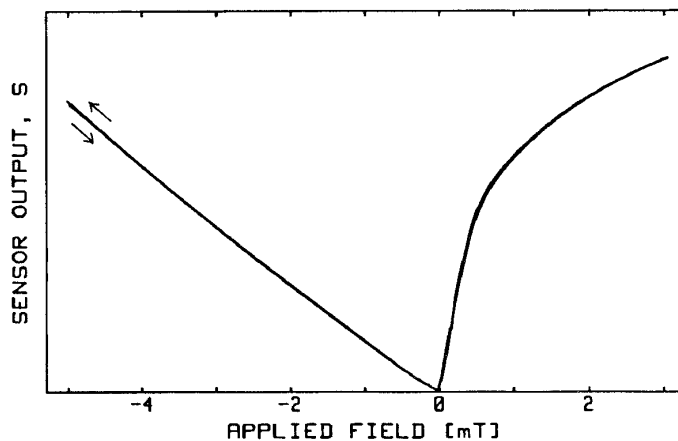
Fig. 14. Output signal S versus B_{meas} with a sensor according to fig 13 with a B_{bias} of 3 mT.

3.3. Reflective sensor with easy in plane (GdGa)-YIG

To be able to collect a large fraction of the light some kind of focusing mechanism must be introduced. Also, from a practical point of view, it would be advantageous to have the fibres attached to the same side of the sensor element, or even better, if only one fibre could be used.

The same material as in the sensor of section 3.2 was used.in a sensor according to fig 13. One polarization maintaining fibre was used to carry the light to and from the sensor element, the rear edge of which was polished into a semi-circular shape and gold coated.

To reduce the unwanted reflections, the input end of the fibre was polished with its surface normal 6° off the fibre axis and the fibre was attached to the waveguide at an angle in the waveguide plane. The short coherence length of the light from the laser diode further reduced the influence of the unwanted reflections[6].

With a bias of 3 mT the sensor gave a response according to fig 14. The nonsymmetry of the curve is attributed to the magnetic anisotropy.
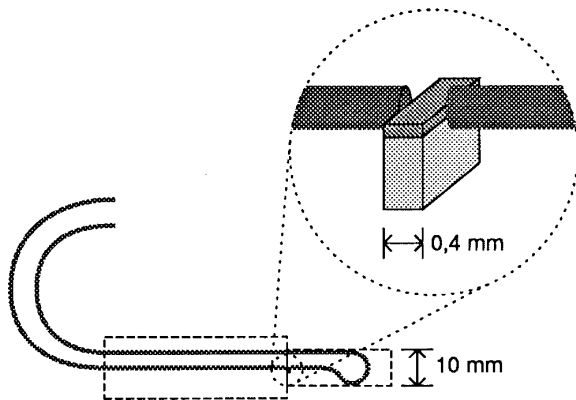
Fig. 15. Sensor geometry with Bi-YIG waveguide
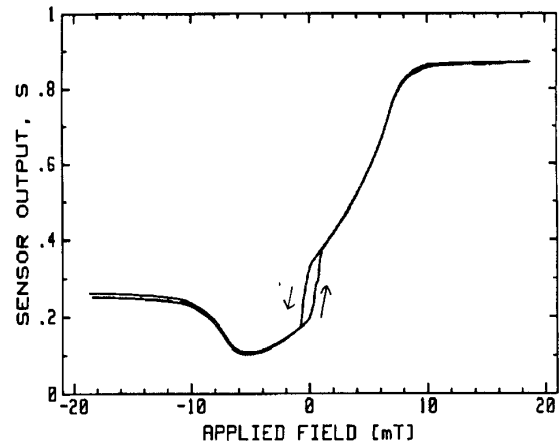
Fig. 16. Output signal S versus B_{meas} with a 3.7 μm Bi-YIG waveguide film.

3.4. Transmission sensor with easy direction perpendicular to plane Bi-YIG

In order to avoid the need for an external bias field we tried a highly anisotropic material with an easy direction of magnetization perpendicular to the film plane. The 3.7 μm thick Bi-substituted film that we used possessed a high Faraday rotation, 1000°/cm at 1.15 μm, [7]. The sensor configuration was similar to the one of fig 11, but with the second fibre rotated 45°. In this way we could achieve a sensor output which was dependent on the direction of the magnetic field. A sensor element in the form of a 0.4 mm long chip was cut and polished. The sensor geometry is shown in fig 15. The light source was a 1.3 μm laser diode.

The sensor output versus the applied field is shown in fig 16. A hysteresis effect appears for field magnitudes less than 1 mT. For such fields the magnetization direction is close to perpendicular to the film plane. For larger fields the performance is as expected, i.e a smooth field versus conversion relationship. It is also evident from the nonsymmetry of the curve that the second fibre was not correctly mounted, but was rotated slightly off the intended angular position.

4. SUMMARY

We have shown that magnetooptical garnet materials can successfully be implemented in fibre optic sensor systems for the sensing of magnetic fields, both with respect to strength and direction. So far the bulk type sensors have given the best performance. The sensor with thick epitaxially grown (YbTbBi)-YIG material had a reproducible measurement range between <10^{-5} T and 10^{-1} T.

The thin film waveguide sensors need further development to be optimized, among other things they are much more difficult to assemble. However, the preliminary results of this work indicates a potential for improvements to fully utilize the two channel measurement technique and possibility of field direction sensitivity.

5. ACKNOWLEDGEMENTS

6. REFERENCES

1. H. Sohlström, U. Holm and K. G. Svantesson, "Characterization of Magnetooptical Thin Films for Sensor Use", *SPIE Proc 1126: "Electro-Optic and Magneto-Optic Materials and Applications"*, J. P. Castera, 77–84, 1989.

2. U. Holm, H. Sohlström and T. Brogårdh, "YIG-sensor design for fibre optical magnetic field measurement", *OFS 84*, R. Th. Kersten and R. Kist, 333–336, VDE-Verlag, Berlin, 1984.

3. Private communication by Dr. K. Machida et al, Sumitomo Metal Mining Co. Ltd, Tokyo Japan.

4. Private communication by Dr. H. LeGall and Dr. J. M. Desvignes, CNRS, Meudon, France.

5. G. Doriath, R. Gaudry, and P. Hartemann, "A sensitive and compact magnetometer using Faraday effect in YIG Waveguide", J. Appl. Phys. Vol. 53, 8263-8265 (1982).

6. H. Sohlström, U. Holm and K. Svantesson, "A Polarization-Based Fibre Optical Sensor System Using a YIG Optical Waveguide for Magnetic Field Sensing", *Springer proceedings in Physics 44: "Optical Fiber Sensors"*, H. J. Arditty, J. P. Dakin, and R. Th. Kersten, 273–278, Springer-Verlag, Berlin, 1989.

7. Private communication by Dr. K. Ando, ETL, Tskuba, Japan.

Paper G

H. Sohlström and K. Svantesson
”A waveguide based fibre optic magnetic field sensor
with directional sensitivity”

A waveguide based fibre optic magnetic field sensor with directional sensitivity.

Hans Sohlström, Kjell Svantesson

Royal Institute of Technology, Instrumentation Laboratory, S-100 44 Stockholm, Sweden

ABSTRACT

In this paper we report on the design and performance of an extrinsic guided wave fibre optic magnetic field sensor. The sensor utilizes a substituted YIG (Yttrium Iron Garnet, $Y_3Fe_5O_{12}$) thin film as the waveguiding sensing element. A polarization maintaining fibre downlead was used to provide insensitivity to both power and loss fluctuations. The design makes it possible to determine both the magnitude and the sign of the magnetic field.

Measurement results indicate a usable measurement range of at least several mT with a noise equivalent magnetic field level of less than 8 $nT/\sqrt{Hz}$.

1. INTRODUCTION

Fibre optic magnetic field sensors based on a number of different principles have been reported previously. A number of them are based on the Faraday effect, i.e. the polarization rotation that is induced by a magnetic field parallel to the light propagation direction in an optic material. Most of the Faraday effect sensors are of the intrinsic type where part of the fibre itself is utilized for the sensing. Because of the small Faraday rotation in the fibre material one has to use a long length of fibre to provide sufficient polarization rotation. This fact makes the intrinsic Faraday sensors unsuitable for applications where one wants a point determination of the magnetic field.

To be able to design a compact all guided wave Faraday sensor for point detection we have instead used a thin film waveguide sensing element made from Gd,Ga-substituted YIG (Yttrium Iron Garnet, $Y_3Fe_5O_{12}$). This kind of material can be grown epitaxially to form low loss optical waveguides that have a large polarization rotation in the transparent region. Furthermore, such a waveguide can be butt coupled with low insertion loss to a polarization maintaining fibre downlead. The two orthogonal modes of the fibre can then be used as two independent transmission channels forming a balanced system that in principle is insensitive to power and loss fluctuations.

2. SENSING PRINCIPLE

We first look at the sensing waveguide itself. Here, the Faraday rotation can be described as a circular birefringence that is dependent on the magnetization parallel to the light propagation direction. This birefringence causes a coupling between the TE and TM modes of the same order. The transfer of power follows the expression

$$F = \left[1+\left(\frac{\Delta\beta}{2\theta}\right)^2\right]^{-1} \sin^2\left\{\left[\theta^2+\left(\frac{\Delta\beta}{2}\right)^2\right]^{\frac{1}{2}}\cdot z\right\} \tag{1}$$

where F is the fraction of power in the mode not excited at the input, $\Delta\beta$ is the linear birefringence, θ is the circular birefringence and z is the travelled distance.

A planar waveguiding film of suitable thickness for butt coupling to the fibre, i. e. 5–10 μm, will support 10–20 modes due to the large step in index of refraction and is by no means a single mode structure. However, we have found that if the fibre end is correctly positioned it is possible to couple the optical power selectively into the fundamental mode of the waveguide.[1] With a suitable film composition it is also possible to achieve a small $\Delta\beta$ for this mode. In such a waveguide the Faraday circular birefringence can be considerably larger than the linear birefringence, giving a strong magnetic field dependent coupling between the fundamental TE and TM modes.

A straight-forward way to utilize such a waveguide is illustrated in fig 1. In this case one of the polarization modes of a polarization maintaining fibre is used to carry linearly polarized light to the sensor element, where it is coupled into the
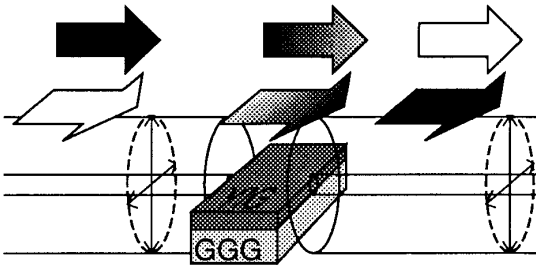
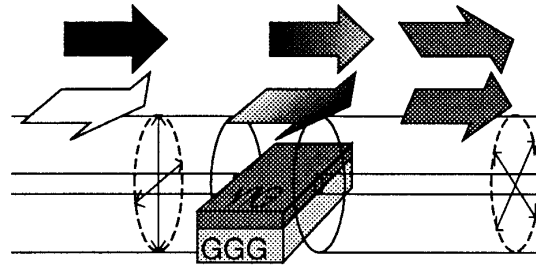Fig 1a. Basic sensing principle   Fig 1 b. Sensing principle with directional sensitivity

fundamental TE mode of the planar waveguide. In the waveguide, part of the optical power is converted to the TM mode according to (1). The light is then coupled into the return fibre, which is oriented in such a way that each of the modes of the planar guide matches one of the fibre polarization modes. At the output end of the fibre, the light from the two fibre modes is separated and detected. The detector outputs are then combined to give an intensity independent signal which is a measure of the magnetic field.

With this configuration it is not possible to detect the sign of the magnetic field. Fields that are parallel to or antiparallel to the light propagation cause TE to TM coupling factors that are equal in magnitude but with opposite signs and consequently they cause equal amounts of light to be coupled into the TM mode. The phases are different for the two cases but as the phase relation between the two fibre modes cannot be maintained in the fibre downlead, this information will be lost.

However, if the return fibre is mounted with its birefringence axes at ±45° to those of the waveguide, each of the planar waveguide polarization modes will couple into both fibre polarisation modes, fig 1b. Each of the fibre modes will then be a linear combination of the TE and TM waveguide mode fields which results in a suitable antisymmetric sensor behaviour. This is in analogy with a conventional bulk optic polarization rotation measurement set-up with the analyzer rotated 45° or –45° from the input polarizer orientation.

To fully understand the behaviour of the sensor one also has to consider the magnetic properties of the sensing element garnet material. Ferrimagnetic materials such as YIG exhibit a spontaneous magnetization that generates a magnetic domain structure. In the absence of an external field these domains are oriented in such a way that the total magnetization of the sample vanishes. In an external magnetic field, the domains will change their distribution, size and shape. Owing to this fact, the circular birefringence, which is proportional to the magnetization parallel to the light propagation, will in general not have an unambiguous relation to the applied field.

A sufficiently large external field will, however, align all the domains to form a single domain. A varying field together with such a bias field also gives a uniform change in the orientation of the magnetization and thus in the resulting Faraday rotation.[2] This is the approach used in this work. A similar result may be achieved without a bias field with a material that possesses a strong magnetic anisotropy.

In our experiments we have used planar waveguides without any lateral light confinement. The absence of such a confinement leads to a light loss when a configuration like the one in fig 1 is used. The loss can be of acceptable size only if the sensor is very short. Consequently there is then a trade-off between polarization rotation and loss, but with materials having a very large Faraday rotation it is possible to find a useful compromise.[3]

In this work we have used another approach that in addition to solving the loss problems also allows the input and output fibres to be mounted side by side instead of in line on opposite edges of the waveguide. The waveguide was made semicircular with the circular edge mirror coated. The fibres were mounted onto the straight edge and the circular edge acted as a focusing
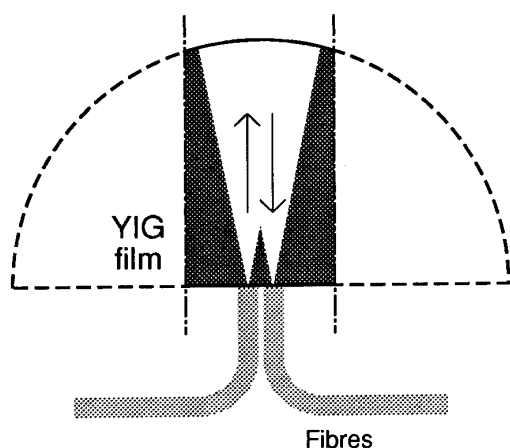
Fig 2. Folded focusing sensor element design. The
broken line indicates part that are not needed for
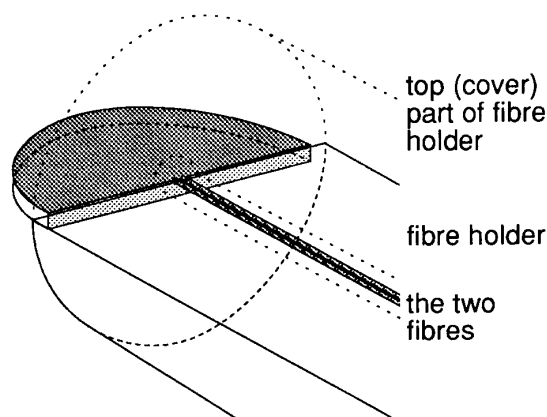the sensing function

Fig 3. The actual sensing element arrangement

reflector, fig 2. As the Faraday effect is nonreciprocal in nature, the mode conversion of the forward and backward trip will add, which makes the effective interaction length twice the sensing element radius.

We have previously reported on a sensor where only one polarization maintaining fibre was used to send the light both to and from the sensor [4], but in such a configuration it is not possible to get the information about the direction of the field.

3. SYSTEM REALIZATION

The material that was used for the sensor element was a 6.7 μm thick (Gd,Ga)-YIG film epitaxially grown on a GGG substrate. The film was known to give an in-plane spontaneous magnetization with a low anisotropy.[5] The Faraday rotation and linear birefringence for films of the same composition had previously been measured at 1.15 μm to be 150°/cm and <75°/cm respectively.[6]

In order to polish the edges to a sufficient quality, two film samples with their film sides pressed against each other were used in the polishing process. When the straight edge had been polished, they were epoxied with the straight edge inward in a slot machined halfway into a 7.6 mm diameter circular steel rod. In this way the samples could be polished to optical quality in a shape defined by the rod. The epoxy was then dissolved and the samples carefully separated. A thin gold film was finally evaporated onto the circular edge of the samples.

The input and output fibres, both York HB 1250, were epoxied onto the flat surface of a halfcylinder plastic fibre holder and with the long axis of the slightly elliptical fibre cores at 90° and 45° with respect to the surface. Another halfcylinder was then epoxied on top of the assembly to protect the fibres, fig 3. When the front face of this fibre holder had been polished flat, the waveguide was positioned for good signal quality in both fibre modes and epoxied in place.

The complete optical set-up is shown in fig 4. As the YIG film is transparent for wavelengths longer than 1.1 μm, a 1.3 μm laser diode was a convenient light source. The detection unit separated and detected the light from the two fibre polarization modes. To get a measurement result that was independent of fluctuations in the laser power and fibre loss we divided the output from one of the detectors with the sum of the two detector outputs.
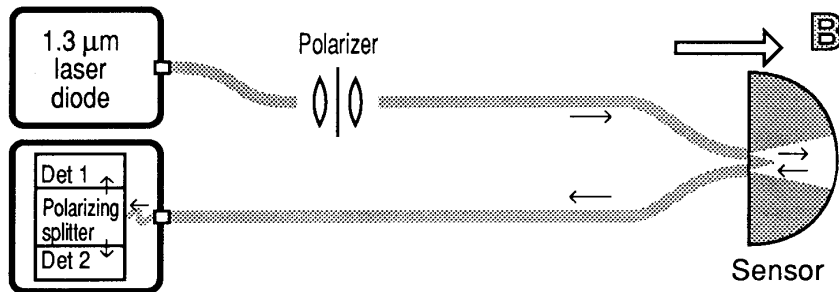
Fig 4. The optical system

To calculate the theoretical sensor output we have used the Poincaré sphere representation.[7] We then find that the pure TE state from the input end of the waveguide as we go along the guide precesses round the total birefringence. From the angular distance to the 45° state on the sphere equator we find the sensor output S to be:

$$S = \frac{1}{2}\left[1+\left(\frac{\Delta\beta}{2\theta}\right)^2\right]^{-\frac{1}{2}}\sin\left\{\left[\theta^2+\left(\frac{\Delta\beta}{2}\right)^2\right]^{\frac{1}{2}}\cdot 2z\right\}; \quad \theta = \theta_{max}M_{parallel} \tag{2}$$

$M_{parallel}$ is the magnetization component along the light propagation direction.

4. EXPERIMENTAL RESULTS

4.1. Bias field selection

The bias field must be large enough to align the domains into a direction from which they can be rotated by the field to be measured. If this is not the case, the domain wall movements will produce an erratic sensor output with jumps and hysteresis. A large enough bias will also reduce the effect of magnetic anisotropy that may be present in the material.

In order to select an appropriate bias field we studied how well the magnetization direction in the sample followed the direction of an external field. In this measurement the sensor output was used as a measure of the magnetization direction. For a very large applied field, the direction of the magnetization should completely follow that of the field and the sensor output versus the field direction would then look like the plot in fig 5. In this fig a calculated sensor output is plotted versus the direction of the magnetization.
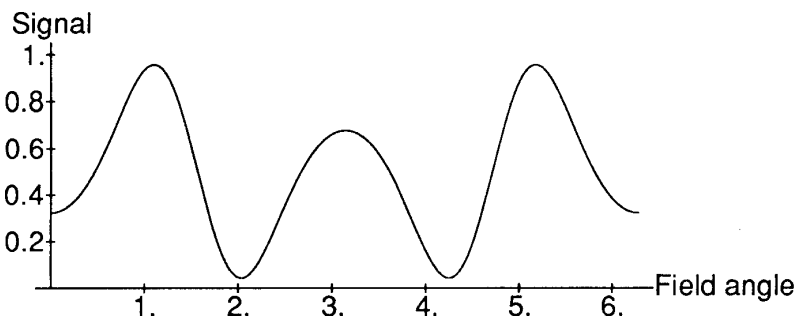

Fig 5. A calculated sensor output signal versus the magnetization direction. $\theta_{max}=130\,°/cm$, $\Delta\beta=50\,°/cm$ and $z=7.6\,mm$. Direction 0 is along the sensor axis, parallel to the light path.

However, for low magnetic field magnitudes, the magnetization does not completely follow the direction of the applied field. Fig 6a shows the experimental result for a field of 100 μT. A field of this magnitude is apparently not large enough to give a uniform magnetization.

When the field was increased to 1 mT the sensor response indicates that the magnetization more closely followed the field, fig 6b, although some kinks remained. These kinks disappeared when the field magnitude was increased to 5 mT, as shown in fig 6c. The measured curve for this case also more closely followed the calculated relationship, indicating that the anisotropy was to a large extent overcome. The calculated function was obtained for $z=7.6$ mm, $\Delta\beta=50°/cm$ and $\theta_{max}=130°/cm$ in good agreement with the previously measured values. In accordance with these results a bias field of 5 mT was selected for the performance measurements.
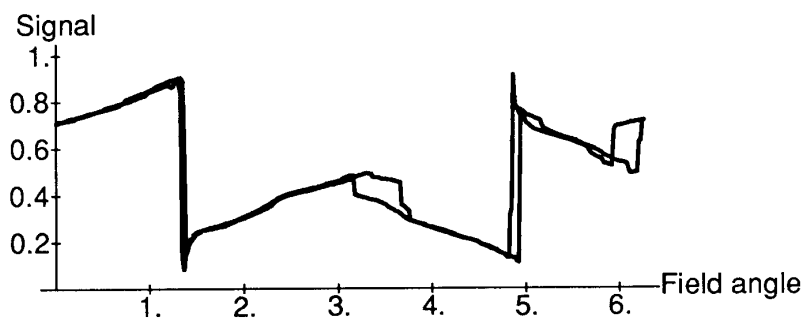
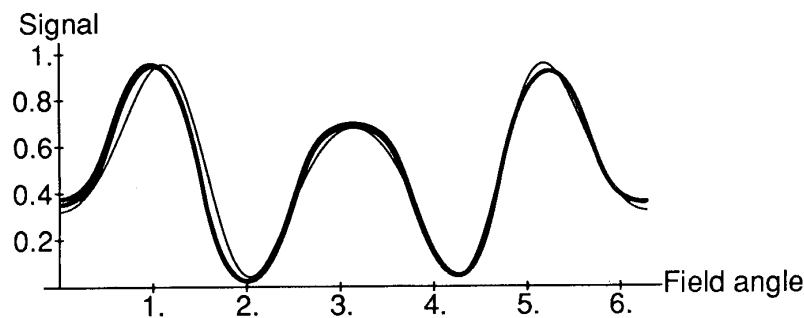*Fig 6. One of the two detector outputs, divided by their sum, versus the direction (0 along axis as in fig 5) of an applied field of*
a) 100 μT
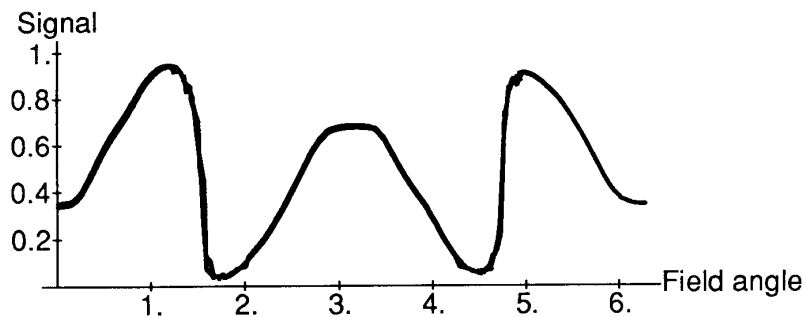
b) 1 mT

c) 5 mT. A theoretical curve similar to the one in fig 5 is also included in fig 6c (thin line).

4.2. Performance measurements

The output signal versus the measurement field, with a bias field of 5 mT, is shown in fig 7. The results show the expected sensor function with a central usable sensing range and a slope reversal at approximately ±2 mT indicating that the optical power couples back into the mode it was originally launched into, equivalent to a polarization rotation of more than 45°. A sensor with a shorter interaction length would give a monotonous relationship, according to fig 8.

A preliminary test made with a HP 3588A spectrum analyzer confirm the distortion free signal and indicate a detector and amplifier noise level equivalent to about 8 nT in a 1 Hz bandwidth with a 5 mT bias field. The detection limit of the sensing element is thus lower than this value. Although this is not the ultimate limit of our sensor, it compares favourably with results obtained by others.[8] By increasing the bias field the measurement range can of course also be scaled to higher values. A more thorough analysis of the sensor behaviour will be reported later.

Signal

1.

0.8

0.6

0.4

0.2

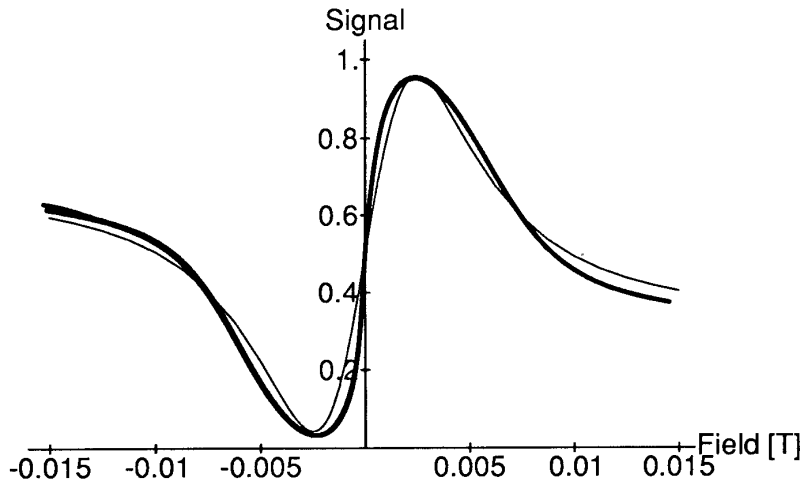-0.015   -0.01   -0.005   0.005   0.01   0.015   Field [T]

Fig 7. The sensor output versus the field applied along the sensor axis with a 5 mT bias field applied perpendicular to this, but in the film plane (thick line) and theoretical curve with sensor data according to the text (thin line).
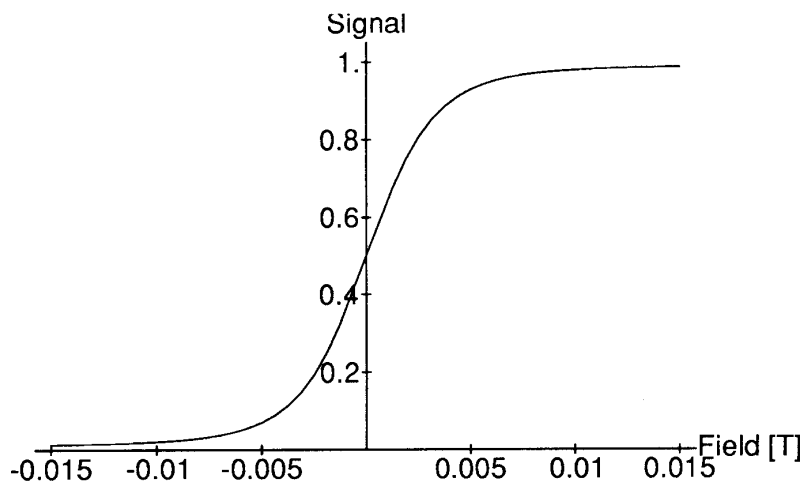
Signal

1.

0.8

0.6

0.4

0.2

-0.015   -0.01   -0.005   0.005   0.01   0.015   Field [T]

Fig 8. A calculated sensor output for a sensor as in fig 7 but with z=3,3 mm, corresponding to a radius of curvature of 1.15 mm for the sensor reflective edge

5. SUMMARY

We have designed an all guided wave magnetic field sensor that utilizes an extrinsic planar waveguide as the sensing element and a polarization maintaining fibre for the downlead. This design allows the sign as well as the magnitude of the applied field to be determined. The sensing element was made from a Gd,Ga-substituted YIG (Yttrium Iron Garnet, $Y_3Fe_5O_{12}$) epitaxially grown thin film.

The two-channel signal transmission through the downlead makes the system insensitive to fluctuations in power and to a great extent also to loss fluctuations. With a suitable bias field it is possible to achieve measurement ranges from about 1 mT and up with a noise equivalent magnetic field level of less than 8 $nT/\sqrt{Hz}$.

6. ACKNOWLEDGEMENTS

REFERENCES

1. To be published.
2. H. Sohlström, U. Holm and K. G. Svantesson, "Characterization of Magnetooptical Thin Films for Sensor Use", *SPIE Proc, vol. 1126: Electro-Optic and Magneto-Optic Materials and Applications*, J. P. Castera, p. 77–84, 1989.
3. K. Svantesson, H. Sohlström and U. Holm, "Magneto-optical garnet materials in fibre optic sensor systems for magnetic field sensing", *SPIE Proc, vol. 1274: Electro-Optic and Magneto-Optic Materials and Applications II*, H. Dammann, p. 260–269, 1990.
4. H. Sohlström, U. Holm and K. Svantesson, "A Polarization-Based Fibre Optical Sensor System Using a YIG Optical Waveguide for Magnetic Field Sensing", *Springer proceedings in Physics 44: Optical Fiber Sensors*, H. J. Arditty, J. P. Dakin, and R. Th. Kersten, p. 273–278, Springer-Verlag, Berlin, 1989.
5. Private communication by Dr. H. LeGall and Dr. J. M. Desvignes, CNRS, Meudon, France.
6. K. G. Svantesson, "Measurements on Magnetooptical Waveguides by Means of a Distributed Grating Coupler", *Advances in Magneto-Optics, Proc. Int. Symp. Magneto-Optics, J. Magn. Soc. Jpn.*, vol. 11, Supplement, no. S1, p. 405–408, 1987.
7. J. F. Dillon jr., "Magneto-Optical Properties of Magnetic Garnets", *Physics of Magnetic Garnets; Proc. of the Int. School of Physics 'Enrico Fermi'; Course LXX*, A. Paoletti, p. 379–416, North-Holland, Amsterdam, 1978.
8. M. N. Deeter, A. H. Rose and G. W. Day, "Fast, Sensitive Magnetic-Field Sensors Based on the Faraday Effect in YIG, *Journal of Lightwave Technology*, vol. 8, no. 12, p. 1838–1842, 1990.

Paper H

H. Sohlström and K. Svantesson
"The performance of a fibre optic magnetic field sensor
utilizing a magneto-optical garnet"

The Performance of a Fiber Optic Magnetic Field Sensor Utilizing a Magneto-Optical Garnet

HANS SOHLSTRÖM
KJELL SVANTESSON

Instrumentation Laboratory
The Royal Institute of Technology
S-100 44 Stockholm, Sweden

Abstract *The design and performance of a multimode fiber optic magnetic field sensor utilizing the Faraday effect in an epitaxially grown thick (YbTbBi)IG film is reported. The sensor is found to be linear over a range of more than 100 dB.*

Introduction

Due to their intrinsically favorable behavior with respect to electromagnetic interference and galvanic isolation, fiber optic sensors are good candidates for current and magnetic field measurements in high-power electric transmission systems. Sensors utilizing the magneto-optic Faraday effect have been investigated for a number of years. When looking for a compact design, magneto-optical garnet materials such as YIG (yttrium-iron-garnet, $Y_3Fe_5O_{12}$) or preferably substituted YIG have shown promising properties [1–4]. One common advantage of these materials is their large Faraday rotation, up to 2000°/cm for Bi-substituted YIG.

The fabrication of pure YIG has a fairly long tradition due to its applications in microwave systems. However, samples resulting from the growth of bulk crystals are not suitable to prepare for optical applications because, among other reasons, they need to be carefully polished. More recently, the liquid phase epitaxy (LPE) technique for fabricating thick magneto-optical garnet layers, mainly for optical isolator applications in optical communication systems, has been developed to a stage where several physical parameters could be handled at will. Furthermore, the LPE technique can yield optical quality wafers of several inches in diameter. To prepare a sensor element from such a wafer only uncritical sawing is needed, which to a large extent facilitates the sensor fabrication.

The sensor reported in this paper utilizes an epitaxially grown (YbTbBi)IG ($(YbTbBi)_3Fe_5O_{12}$) layer on a GGG substrate, with a composition optimized for optical isolator applications, implying low temperature dependence.

Sensing Principle

To utilize the polarization rotation in an intensity-based multimode fiber sensor, polarizers are placed before and after the sensing element. The intensity of the light transmitted

through the second polarizer will then depend on the polarization rotation in the crystal. Thanks to the nonreciprocity of the Faraday effect it is possible to utilize a folded design according to Fig. 1. One then gets twice the polarization rotation for a given crystal thickness. Due to the ferrimagnetic properties of the garnet material, the picture of a homogeneous, magnetic field-dependent rotation of linearly polarized light is too simplified to be useful to predict the sensor behavior.

The internal magnetization of the crystal leads to the presence of magnetic domains that will change their size and shape when an external magnetic field is applied. The resulting polarization state of a narrow ray of light will then depend on the actual domain distribution along its path. This will, in general, not yield reproducible conditions. However, by using a sufficiently wide beam of light the net rotation of a large number of individual domains will be measured, giving a useful sensor performance [5, 6].

In our case we assume that all domains reach through the entire thickness of the layer, with a magnetization direction that is either parallel or antiparallel to the light propagation. In the absence of an external magnetic field, the two types of domains will occupy approximately equal volumes, and with the above assumption, equal areas. However, when a magnetic field is applied, the domains of one kind will grow at the expense of those of the other kind.

In addition to the magnetic properties of the material, the optical conditions will affect the sensor performance. With a spatial coherence of the light, large enough to create interference between light having passed different domains, the sample will act as a phase grating. Sufficiently far behind the sample, the undiffracted light will then have a state of polarization and intensity that depends on the applied field, while the light in the first diffraction order will be polarized perpendicularly to the incident light.

The optical configuration used in our sensor, i.e., with the polarizer far from the sensing element, yields a sensor output that is given by the transmitted intensity of the undiffracted light after the second polarizer. The magnetic field dependence is, in fact, very similar to the one achieved with a material with a homogeneous magnetization.

Our sensor was realized with an epitaxially grown 0.13-mm-thick (YbTbBi)IG layer on a GGG substrate. The domain magnetization was perpendicular to the plane of the layer. The thickness of the layer was chosen to give a single pass maximum rotation of 22.5° at 1.3 μm. The components of the sensor head, i.e., the sensing element, a gradient index lens, and two polarizers, were mounted in a plastic enclosure of 6 mm length and 4 mm diameter. Core fibers of 100 μm with a cladding diameter of 140 μm were used for the signal transmission.

Measurement Results

The dc magnetic field characteristics of the sensor are shown in Fig. 2. The saturation points fall at approximately ± 100 mT. The frequency spectra for different ac field levels were also studied to further investigate the central part of the characteristics. Figure 3 shows the output spectrum for a 1-kHz, 27-mT (peak) applied field. Even with this
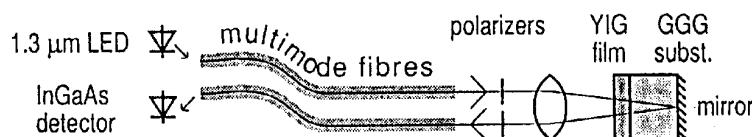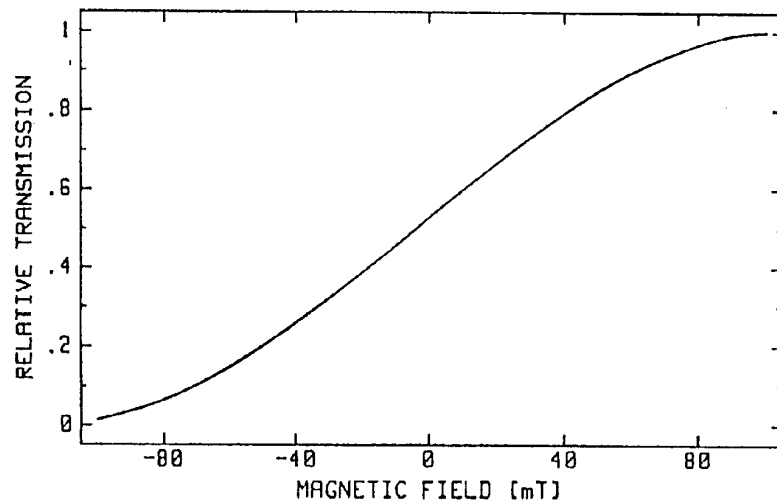

Figure 1. Outline of the folded type magnetic field sensor.

Figure 2. Magnetic field characteristics of the sensor.

relatively large signal amplitude, the distortion was only about 1%. The signal-to-noise ratio for 1-Hz bandwidth was 90 dB. A 20-dB reduction of the signal to 2.7 mT further reduced the distortion to about 0.3% (Fig. 4). The signal was then reduced in steps of 20 dB down to 270 nT. At this signal level, the spectrum analyzer bandwidth was reduced to 88 mHz to separate the signal from the sensor amplifier noise (Fig. 5).

The measurement results are summarized in Fig. 6, where the signal amplitude is plotted versus the applied 1-kHz field amplitude. Apparently the sensor is, within the experimental accuracy, linear over a range of at least 100 dB. In the experimental data presented here, the lowest point is buried in the 1-Hz noise. This noise, however, originates in the detector and its amplifier and is not an inherent property of the sensor
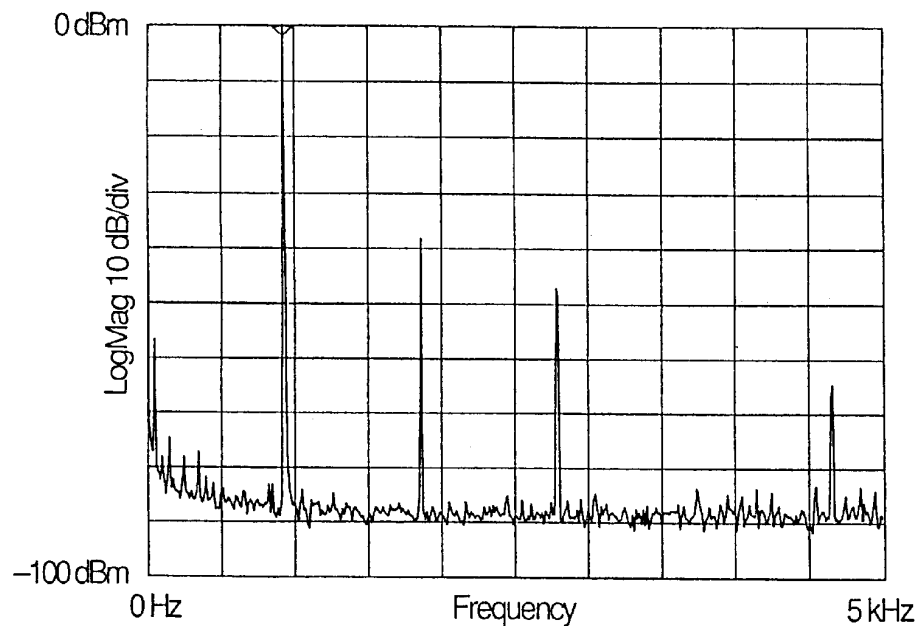
Figure 3. Frequency spectrum (0–5 kHz) of the sensor output for a 27-mT (peak) exitation at 1 kHz. Sensor amplifier 3-dB bandwidth: 5 kHz; analyzer bandwidth: 1.1 Hz.
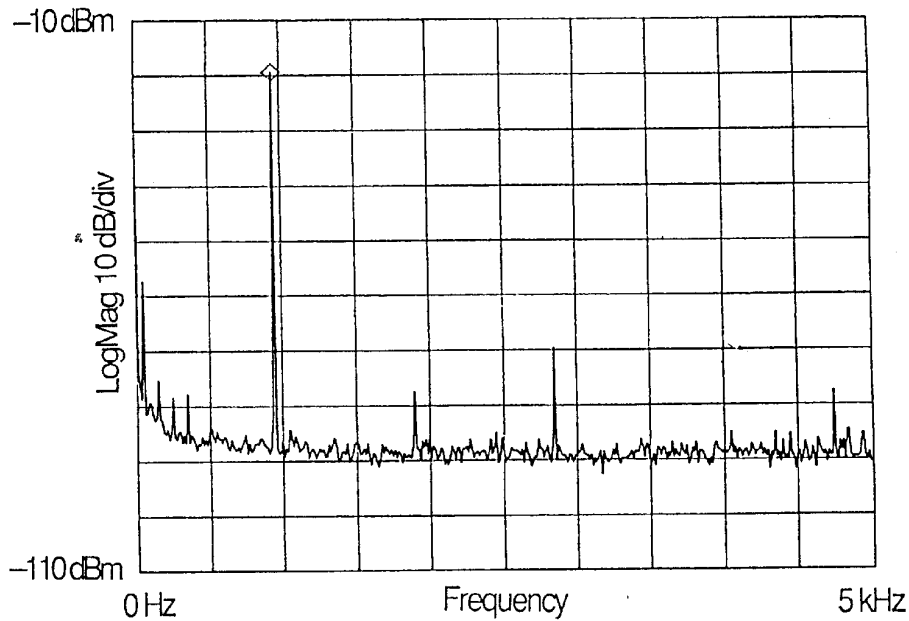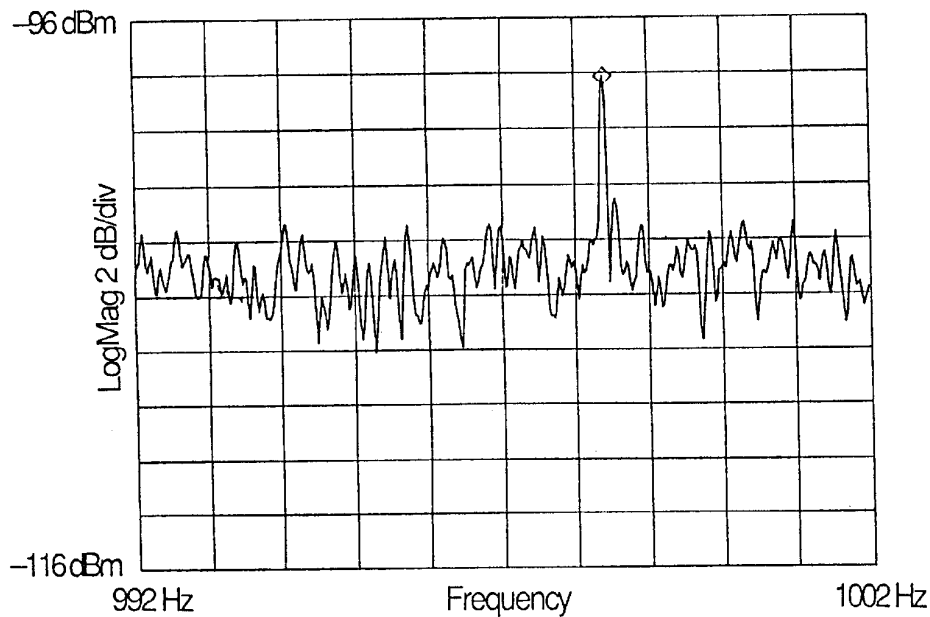
Figure 4. Frequency spectrum (0–5 kHz) of the sensor output for a 2.7-mT (peak) exitation at 1 kHz. Sensor amplifier 3-dB bandwidth: 5 kHz; analyzer bandwidth: 1.1 Hz.

itself. By decreasing the optical loss of the sensor and by improving the amplifier, a 20-dB increase in signal-to-noise ratio should be within reach.

Conclusions

The multimode fiber optic magnetic field sensor that we have reported here is found to be linear over a range of more than 100 dB. The experimental data show a 1-Hz noise

Figure 5. Narrow-band frequency spectrum of the sensor output for a 270-nT (peak) exitation at 1 kHz. Sensor amplifier 3-dB bandwidth: 5 kHz; analyzer bandwidth: 88 mHz.
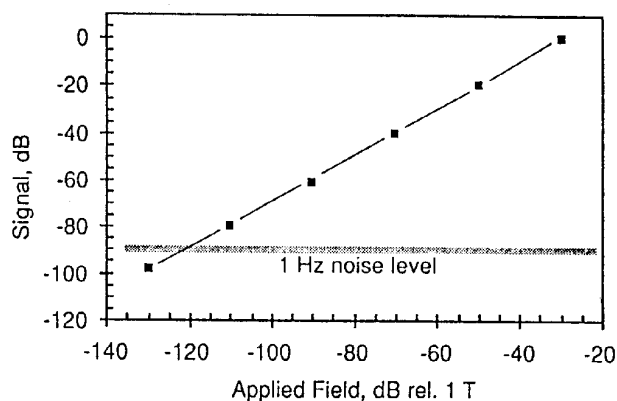
Figure 6. The signal amplitude (dB rel. signal at 27 mT) versus the applied field.

equivalent magnetic field of 1 μT. However, the sensor is linear even below this level. With an optimized design we consider it possible to reduce the noise equivalent field by a factor of 10.

Acknowledgments

References

1. G. Doriath, R. Gaudry, and P. Hartemann, "A Sensitive and Compact Magnetometer Using Faraday Effect in YIG Waveguide," *J. Appl. Phys.* **53**(11), 8263–8265, 1982.
2. K. Svantesson, H. Sohlström, and U. Holm, "Magneto-Optical Garnet Materials in Fibre Optic Sensor Systems for Magnetic Field Sensing," *Electro-Optic and Magneto-Optic Materials II*, H. Dammann (Ed.), *SPIE Proc.* **1274**, 260–269, 1990.
3. H. Sohlström, U. Holm, and K. Svantesson, "A Polarization-Based Fibre Optical Sensor System Using a YIG Optical Waveguide for Magnetic Field Sensing," *Springer Proceeding in Physics 44: Optical Fiber Sensors*, H. J. Arditty, J. P. Dakin, and R. Th. Kersten (Eds.), Springer, Berlin, 1989, pp. 273–278.
4. H. Sohlström and K. Svantesson, "A Waveguide-Based Fibre Optic Magnetic Field Sensor with Directional Sensitivity," *Fiber Optic Sensors: Engineering and Applications, SPIE Proc.* **1511**, pp. 142–148, 1992.
5. U. Holm, H. Sohlström, and T. Brogårdh, "YIG-Sensor Design for Fibre Optical Magnetic Field Measurement," *OFS 84*, R. Th. Kersten and R. Kist (Eds.) VDE, Berlin, 1984, pp. 333–336.
6. M. N. Deeter, A. H. Rose, and G. W. Day, "Fast, Sensitive Magnetic-Field Sensors Based on the Faraday Effect in YIG," *J. Lightwave Technol.* **8**(12), 1838–1842, 1990.